6

Effect of a specific-gene knockout on metabolism

Abstract: The metabolic regulation of the specific gene knockout *Escherichia coli* is explained in terms of ^{13}C-metabolic fluxes, enzyme activities, intracellular metabolite concentrations, and gene expressions. It is shown that the glyoxylate pathway is activated in *pckA* and *ppc* mutants, where the cell yield can be improved as compared to the wild type. In the case of the *gnd* mutant *E. coli*, the ED pathway is activated where Mez is activated for both *zwf* and *gnd* mutants to back up the production of NADPH. The regulation mechanism of the *pykF* mutant *E. coli* is analyzed, where it is shown to be robust against such genes knockout by rerouting the pathways. Moreover, the metabolic regulations of *lpdA*, *sucA*, and *C* mutants as well as *icdA* and *ldhA* mutants are also explained, based on ^{13}C metabolic flux analysis and other information.

Key words: ^{13}C-metabolic flux analysis; *pckA* mutant; *ppc* mutane; metabolic regulation; *gnd* mutant; *pykF* mutant; *lpdA* mutant; *sucA*, *C* mutant; *icdA* mutant; *ldhA* mutant.

6.1 Introduction

In order to understand the role of metabolic pathway genes in metabolism, it is useful to study the effects of a specific gene knockout (or a change in culture environment) on metabolism, based on the metabolic flux distribution obtained by ^{13}C labeling experiments as well as gene expressions, protein expressions (enzyme activities), and intracellular metabolite concentrations (Shimizu, 2004). Here, the change in metabolism due to a single-gene mutation is discussed, focusing on

E. coli metabolism. The different levels of information, such as ^{13}C-metabolic flux analysis, gene expressions by DNA microarray with qRT-PCR, protein expressions by 2D DIGE with shotgun proteomics, metabolite concentrations by CE-TOFMS with LC-MS/MS, have been reported for 24 single-gene knockout *E. coli* mutants, such as *galM*, *glk*, *pgm*, *pgi*, *pfkA*, *pfkB*, *fbp*, *fbaB*, *gapC*, *gpmA*, *gpmB*, *pykA*, *pykF*, *ppsA*, *zwf*, *pgl*, *gnd*, *rpe*, *rpiA*, *rpiB*, *tktA*, *tktB*, *talA*, and *talB* mutants for a continuous culture at a dilution rate of 0.2 h^{-1}, as well as the wild-type *E. coli* BW25113 for a continuous culture at different dilution rates (Ishii et al., 2007). From such data, it is found that while some single-gene knockout mutations in the central metabolism preclude growth on glucose, the majority of such variations seem to be potentially compensated by either using alternative enzymes or by the re-routing of carbon fluxes through alternative pathways, resulting in the robustness of the cell's phenotype such as cell growth (Ishii et al., 2007). This chapter considers how metabolism changes in response to specific pathway gene mutations.

Basically, the regulation of metabolic processes ultimately depends upon the control of protein synthesis and enzyme activity (Martin, 1987). There are three general mechanisms by which the activity of enzymes can be regulated, such as control by reversible binding of effectors, by covalent modification, and by alteration of enzyme concentration. In the first case, the enzyme is activated or inhibited by binding of a signal molecule, which may or may not be the substrate or product of the enzyme reaction, to the specific regulatory site, producing a conformational change. Substrate effect and allosteric control may be the example. In covalent modification, the structure of the enzyme can be altered by the action of other enzymes. For instance, regulation by phosphorylation, i.e. phosphate, is incorporated into the enzyme by a protein kinase using ATP, and is removed by a protein phosphatase. The third mechanism that regulates enzyme activity is the alteration of the concentration of the enzyme protein in the cell. The concentration of a protein in the cell is governed by the rate of the synthesis and the rate of degradation. The rate of synthesis of a particular protein may be controlled at several different levels, such as the rate of transcription of the gene, etc. Other possible sites of control are the processing of the transcript to give mRNA, the transfer of mRNA out of the nucleus, the rate of degradation of mRNA in the cytoplasm, or the rate of translation of mRNA to make the protein on the ribosome. There is strong evidence that the rate of transcription is under rigorous control, which is important in determining the enzyme profile of a particular cell type (Martin, 1987).

Published by Woodhead Publishing Limited, 2013

6.2 Effect of *ppc* and *pck* gene knockout on metabolism

As stated in Chapter 5, if the *pckA* gene, which codes for the gluconeogenic PEP carboxikinase, is knocked out, the formation of OAA is reduced, which activates the glyoxylate pathway. The regulation mechanism is also explained in Chapter 5. The reversible phosphorylation/inactivation of ICDH is catalyzed by the bifunctional enzyme ICDH-kinase/phosphatase, where it is regulated by a number of effectors including OAA, which inhibits the ICDH-kinase and stimulates phosphatase. Thus the decrease in OAA concentrations due to the *pckA* gene knockout gene causes the phosphorylation/inactivation of ICDH, which results in an increase in isocitrate concentration, and the flux through Icl also significantly increases (Yang et al., 2003). Moreover, the *pckA* gene knockout causes accumulation of PEP, which in turn inhibits Pfk activity, and thus reduces the glucose consumption rate. This mutant produces less acetate and CO_2, resulting in higher cell yield with less growth rate than the wild type (Yang et al., 2003). It is shown that *in vivo* regulation of the Pck flux occurs mainly by modulation of enzyme activity and by the changes in PEP and OAA concentrations rather than by the ATP/ADP ratio. This indicates that the reaction catalyzed by Pck can respond flexibly to the availability of PEP and OAA, which may form the metabolic cycle at low glucose concentrations (Fischer and Sauer, 2003). It is known that PEP is an important intermediate in metabolism, since it alone directly regulates the phosphotransferase (PTS) system but also affects Pfk and Pyk activities. Since PEP can be formed gluconeogenetically through Pck from the TCA cycle, Pck serves to maintain the relative balance between OAA and PEP pools and drain off excess carbon of the TCA cycle to supply PEP for cellular requirements (Yang et al., 2003).

In relation to the *pckA* gene knockout, consider the effect of the *ppc* gene knockout on metabolism. Among the central metabolic pathway enzymes of *E. coli*, PEP carboxylase (Ppc) plays an anaplerotic role in replenishing OAA consumed in biosynthetic reactions and keeping the TCA cycle intermediates from starvation. Chang et al. (1999) reported increased D-lactate production by a *ppc* mutant of *E. coli* under anaerobic conditions. Farmer and Liao (1997) over-expressed Ppc and/or induced a glyoxylate shunt by the *fadR* knockout gene, to elevate TCA cycle activity for the reduction of acetate excretion under aerobic conditions, since acetate excretion is a major obstacle in recombinant protein production.

Here, we consider the effects of *ppc* mutation on metabolism based on ^{13}C-labeling experiments, together with enzyme activity and intracellular metabolite concentrations, where *E. coli* BW25113 and its *ppc* mutant (JWK3928) are considered (Peng et al., 2004).

Growth parameters at the exponential growth phase in the aerobic batch culture are shown in Table 6.1. The specific cell growth rate and specific glucose consumption rate of the *ppc* mutant are lower than those of the wild type. The CO_2 evolution rate (CER) is also reduced in the *ppc* mutant. Note that little acetate is excreted in the *ppc* mutant during cultivation, whereas the wild-type *E. coli* produces acetate significantly. As a consequence, an improvement of biomass yield on glucose can be observed in the *ppc* mutant.

Some key enzyme activites of central metabolism, for the cells grown at the exponential growth phase, are shown in Table 6.2. The wild-type *E. coli* shows high Ppc activity, indicating that this anaplerotic pathway plays an important role in metabolism. The activity of Pck, which catalyzes the reverse reaction to Ppc, is considerably lower in the *ppc* mutant. The activities of glycolytic enzymes, such as Hxk, Pgi, Pfk, Fba, and GAPDH and the pentose phosphate (PP) pathway enzymes, such as G6PDH, 6PGDH, and Tal, are all significantly decreased in the *ppc* mutant (Table 6.2). These data correspond to the slower growth and lower glucose utilization rates of the *ppc* mutant (Table 6.1). However, Pyk is an exception, where it is increased 2.4-fold (Table 6.2). The up-regulation of Pyk is expected to channel more carbon flux from PEP to pyruvate due to the blockage of Ppc in the *ppc* mutant. Accordingly,

Table 6.1 **Cell growth parameters of the wild-type *E. coli* and its *ppc* mutant grown on glucose under aerobic conditions**

Parameter	Wild type	*ppc* mutant
μmax (h^{-1})	0.41	0.34
q_{glc} (mmol g^{-1} h^{-1})[a]	5.61	3.16
q_{CO2}(mmol g^{-1} h^{-1})[b]	3.38	2.47
Q_{ace} (mmol g^{-1})[c]	0.22	0.00
$Y_{biomass/glc}$ (g g^{-1})[d]	0.48	0.55

[a]: specific glucose consumption rate
[b]: specific carbon dioxide evolution rate
[c]: specific acetate production rate
[d]: yield of biomass on glucose.

Published by Woodhead Publishing Limited, 2013

Table 6.2 Specific enzyme activities of the wild-type *E. coli* and its *ppc* mutant grown on glucose under aerobic conditions

Enzyme	Wild type	ppc mutant
Hexokinase (Hxk)	0.0752 ± 0.0001	0.0466 ± 0.0001
Glucose phosphate isomerase (Pgi)	2.078 ± 0.004	0.436 ± 0.002
Phosphofructose kinase (Pfk)	0.564 ± 0.003	0.170 ± 0.002
Fructose bisphosphate aldolase (Fba)	0.675 ± 0.003	0.0607 ± 0.0005
Glyceraldehyde-3-phosphate dehydrogenase (GAPDH)	0.692 ± 0.004	0.0899 ± 0.0005
Pyruvate kinase (Pyk)	0.220 ± 0.005	0.534 ± 0.004
Phosphoenolpyruvate carboxylase (Ppc)	0.0448 ± 0.0005	—[a]
Phosphoenolpyruvate carboxykinase (Pck)	0.0427 ± 0.0004	0.0021 ± 0.0004
NADP+-specific malic enzyme (Mae)	0.067 ± 0.002	0.082 ± 0.002
NAD+-specific malic enzyme (Sfc)	0.088 ± 0.005	—[a]
Glucose-6-phosphate dehydrogenase (G6PDH)	0.245 ± 0.002	0.170 ± 0.002
6-Phosphogluconate dehydrogenase (6PGDH)	0.426 ± 0.003	0.00085 ± 0.00004
Citrate synthase (CS)	0.319 ± 0.002	0.369 ± 0.003
Aconitase (Acn)	0.115 ± 0.002	0.179 ± 0.002
Isocitrate lyase (Icl)	0.0361 ± 0.0003	0.113 ± 0.004
Isocitrate dehydrogenase (ICDH)	2.230 ± 0.002	0.971 ± 0.004
Malate dehydrogenase (MDH)	0.121 ± 0.007	0.193 ± 0.006

The unit of the enzyme activity is μmol min^{-1} mg $(protein)^{-1}$
Overall ED pathway activity is represented as mg (pyruvate) min^{-1} mg $(protein)^{-1}$
[a] Not detected.

CS, the first enzyme of the TCA cycle, is up-regulated 1.8-fold in the *ppc* mutant (Table 6.2). This up-regulation is expected to increase the carbon flux from pyruvate into the TCA cycle for the replenishment of OAA in response to Ppc deficiency. The activities of Acn and MDH, but not ICDH, in the TCA cycle, increase in a co-ordinated manner. It is reported that CS and Acn, but not ICDH, are regulated co-ordinately,

which might be due to the fact that citrate is an activator of Acn (Nakano et al., 1998). Note that Icl, encoded by *aceA* involved in the glyoxylate shunt, is significantly induced by about 3.1-fold in the *ppc* mutant (Table 6.2). This regulation pattern clearly demonstrates that the *ppc* mutant utilizes an alternative anaplerotic pathway, the glyoxylate shunt, to replenish OAA in response to the blockage through Ppc.

The concentrations of some key intracellular metabolites are shown in Table 6.3, where the glycolytic intermediates, such as G6P, F6P, F1, 6P, and PEP and the PP pathway intermediate, such as 6PG, accumulate in the *ppc* mutant due to inhibition of enzyme activity in their related pathways. In contrast, the intracellular concentration of AcCoA decreases in the *ppc* mutant, implying higher activity of the TCA cycle (or glyoxylate pathway) relative to glycolysis. OAA is not detected in the *ppc* mutant due to its low abundance, but it is detected in the wild type at low concentrations, implying that intracellular OAA is limited in the *ppc* mutant.

Figures 6.1a and b show metabolic flux distributions in the wild-type *E. coli* and its *ppc* mutant. Three notable differences between the two strains can be observed. First, 50.7% of carbon flux channeled through Ppc, and the backflow through Pck, is also high, accounting for 23.6% of the total glucose consumed in the wild-type strain. The flux from OAA to PEP catalyzed by Pck is significantly decreased to only 0.05% in the *ppc* mutant. These flux results are consistent with those of enzyme activity

Table 6.3 Intracellular metabolite concentrations in the wild-type *E. coli* and its *ppc* mutant grown on glucose under aerobic conditions

Intracellular metabolite (mM)	Wild type	ppc mutant
G6P	0.68 ± 0.09	1.213 ± 0.13
F6P	0.29 ± 0.06	0.48 ± 0.07
F1,6P	1.01 ± 0.1	3.1 ± 0.21
PEP	0.07 ± 0.006	0.2 ± 0.06
6PG	0.38 ± 0.07	0.56 ± 0.09
AcCoA	0.13 ± 0.04	0.077 ± 0.005
OAA	0.03 ± 0.001	—[a]

Cell volume: 2.55 μl mg (DCW)$^{-1}$

[a] Not detected.

Published by Woodhead Publishing Limited, 2013

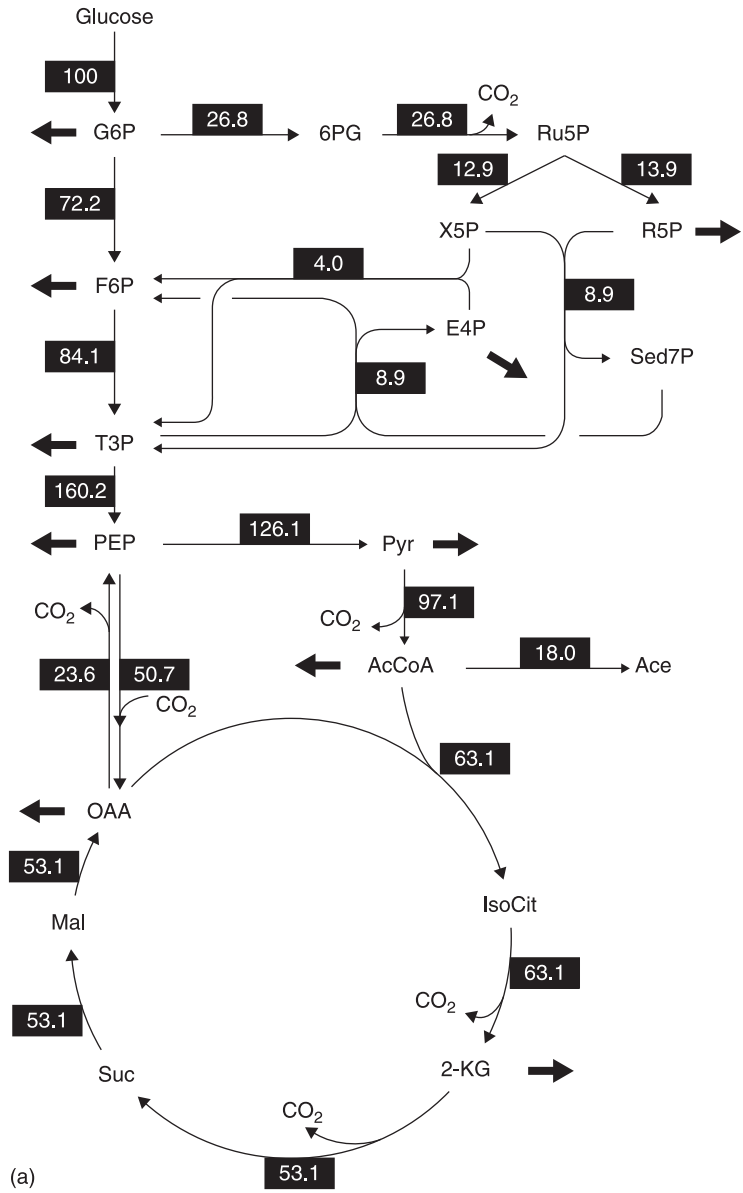

Figure 6.1 **Metabolic flux distribution in the chemostat culture of the wild type *E. coli* (a) and ppc mutant (b).**

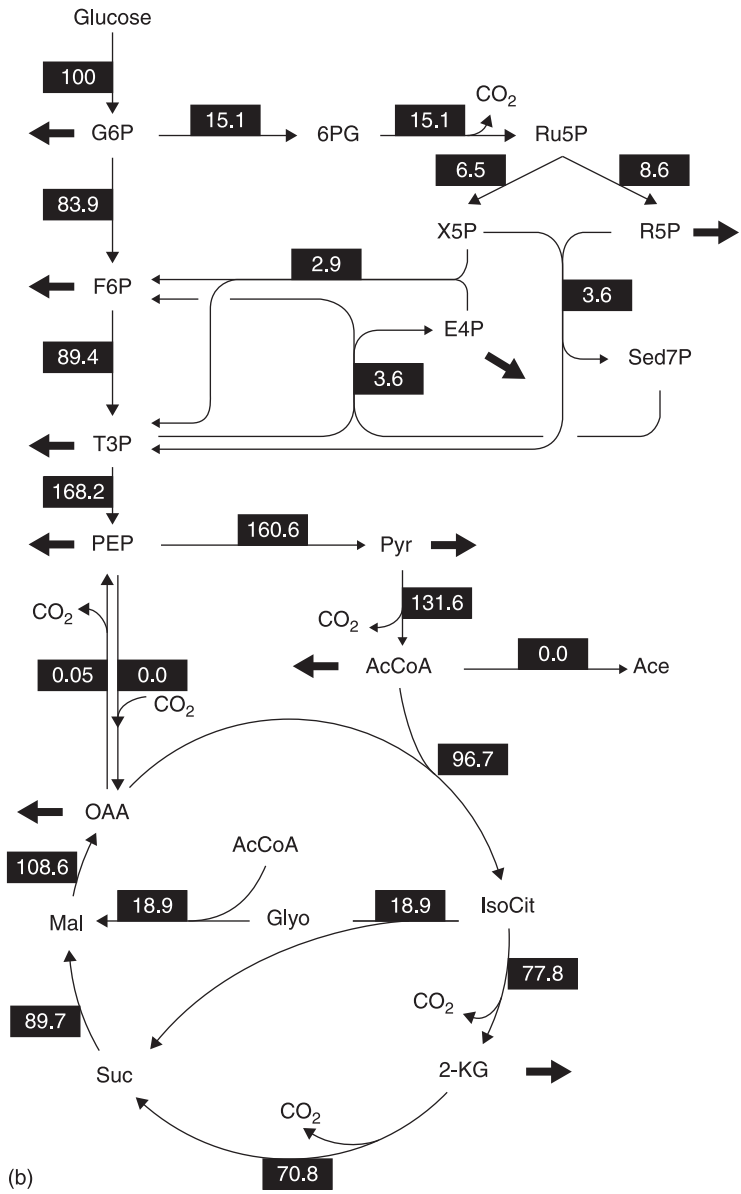

Figure 6.1 (*Continued*) Numbers in black boxes represent the estimated net fluxes at a dilution rate of 0.2 h^{-1}. Flux values are given in parentheses in mmol $gDCW^{-1}$ h^{-1} relative to the specific glucose uptake rate. Arrowheads indicate the primary direction of the determined fluxes. Arrows without destination indicate the withdrawal of the precursors for biosynthesis

Published by Woodhead Publishing Limited, 2013

(Table 6.2), which is also indicated by the visual observation of the ^{13}C–^{13}C scalar coupling multiplet patterns of Asp2 and Phe2 (Table 6.4). The da and dd components in the multiplets of Asp2 relate to the intact C_2–C_3 connectivity of the OAA molecule (the precursor of Asp). Since the intact C_2–C_3 fragments of OAA can be introduced only by the anaplerotic reaction of Ppc, the absence of da and dd components of Asp2 in the *ppc* mutant reflect the lack of *in vivo* activity of Ppc. In addition, the lower abundance of the db component in Phe2 in the *ppc* mutant implies less intact C_1–C_2 fragments of the PEP molecule due to the low activity of Pck. Second, the glyoxylate shunt channels 18.9% of the carbon flux in the *ppc* mutant. Visual inspection of the ^{13}C–^{13}C multiplets of Asp2 reveal a higher abundance of the db component in the *ppc* mutant (Table 6.4), which reflects the contribution of the glyoxylate shunt in excessive intact C_1–C_2 and C_3–C_4 connections (Maaheimo et al., 2001; Yang et al., 2003). Up-regulation of Icl activity in the *ppc* mutant (Table 6.2) is consistent with this flux analysis result. The remaining carbon flux through ICDH via the TCA cycle is still larger than that of the wild type, implying that more NADPH required for biosynthesis can be generated via the TCA cycle in the *ppc* mutant. Third, 26.8% of the carbon flux is channeled through the oxidative PP pathway in the wild type, in contrast to only 15.1% in the *ppc* mutant.

Table 6.4 **The NMR spectra of cellular amino acids in the wild-type *E. coli* and its *ppc* mutant**

Atom	Wild type				*ppc* mutant			
Carbon	s	da	db	dd	s	da	db	dd
Ala2	0.10	0.12	0.06	0.71	0.08	0.09	0.05	0.78
Ala3	0.42	0.58	–	–	0.25	0.75	–	–
Asp2	0.48	0.14	0.29	0.08	0.43	0.00	0.57	0.00
Glu4	0.38	0.01	0.54	0.07	0.28	0.01	0.65	0.06
Gly2	0.37	0.63	–	–	0.23	0.77	–	–
Ile2	0.50	0.01	0.37	0.11	0.39	0.07	0.49	0.04
Ile6	0.44	0.56	–	–	0.29	0.71	–	–
Phe2	0.16	0.16	0.10	0.58	0.13	0.10	0.02	0.75
Thr3	0.47	0.49	–	0.04	0.37	0.57	–	0.06
Thr4	0.55	0.45	–	–	0.59	0.41	–	–
Val2	0.35	0.05	0.51	0.06	0.20	0.05	0.67	0.05

PEP is a critical metabolite in *E. coli*, because of its role not only in the PTS system as a phosphoryl donor, but also in the regulation of many enzymes as an effecter. It accumulates in the *ppc* mutant and allosterically inhibits some of the glycolytic enzymes, such as Pgi and Pfk (Fraenkel, 1999). Inhibition of these enzymes leads to higher intracellular concentrations of their intermediates, such as F6P and F1,6BP (FDP), which in turn affect some other enzymes. For instance, G6PDH is allosterically inhibited by FDP and PRPP and induced by glucose, while 6PGDH is inhibited by FDP, PRPP, GAP, Ru5P, E4P, and NADPH and induced by gluconate (Sugimoto and Shiio, 1987). Apparently, the higher concentrations of intracellular F1,6BP (FDP) in the *ppc* mutant partially cause down-regulation of both enzymes. In addition, the higher flux through the TCA cycle produces more NADPH in the *ppc* mutant, which may also be considered the reason for the down-regulation of 6PGDH. The transcript of the glucose transport gene, *ptsG*, is also associated with accumulation of the glycolytic intermediates, such as G6P and F6P, which degrade the mRNA of *ptsG* by activating the RNaseP enzyme (Morita et al., 2003). Both down-regulation of the glycolytic and PP pathway enzymes results in slower growth rates and lower glucose uptake rates in the *ppc* mutant (Table 6.1). The remarkably reduced Pck activity in the *ppc* mutant may be caused by the higher intracellular concentration of PEP, since Pck is allosterically inhibited by nucleotides ATP and PEP (Krebs and Bridger, 1980). Note that the activation of the glyoxylate shunt contributes to the reduction in CO_2 production in the *ppc* mutant.

6.3 Effect of *zwf* and *gnd* genes knockout on metabolism

The effect of the *zwf* gene knockout on the fluxes is explained in Chapter 5, when compared with *pgi* gene knockout. Although the *zwf* gene knockout shows little influence on central metabolism under glucose-limited continuous culture by flux re-routing via the non-oxidative PP pathway (Zhao et al., 2004a), this mutant shows significant overflow metabolism and extremely low TCA cycle fluxes under ammonia limited conditions (Hua et al., 2003). The effect of the *gnd* gene knockout on metabolism is different from the *zwf* gene knockout mutation. The *gnd* gene knockout activates the ED pathway and causes a decrease in the flux through G6PDH, which reduces NADPH production through

Published by Woodhead Publishing Limited, 2013

the oxidative PP pathway. This decreased NADPH production is backed up by activating Mez using MAL together with transhydrogenase Pnt. The reduced OAA due to the utilization of MAL for Mez, Ppc is up-regulated while Pck is down-regulated. The shortage of R5P, due to the decreased flux through the oxidative PP pathway, is backed up by reversing the non-oxidative PP pathway as compared to the wild type. This back-up system has little effect on the phenotype such as the cell growth rate, while glucose consumption rates are increased (Zhao et al., 2004b). The detailed metabolic regulation analysis is explained in the following.

The batch cultivation results of *zwf* and *gnd* mutants for glucose and pyruvate as carbon sources are given in Table 6.5. As can be seen in Table 6.6, the specific substrate uptake rate and specific CO_2 evolution

Table 6.5 Exponential growth rates of *E. coli* wild-type (*WT*) and mutant cultures on glucose/pyruvate media

Growth rate	Glucose culture			Pyruvate culture		
	WT	*gnd*	*zwf*	WT	*gnd*	*zwf*
(μ)	0.62	0.60	0.56	0.38	0.39	0.36

Table 6.6 Metabolic parameters of *E. coli* continuous cultures at $D = 0.2\ h^{-1}$

Parameter	Glucose culture			Pyruvate culture		
	Wild	*gnd*	*zwf*	Wild	*gnd*	*zwf*
q_S	3.20±0.10	3.75±0.15	3.82±0.07	7.05±0.08	6.68±0.13	6.28±0.10
q_{CO2}	8.17±0.30	9.90±0.50	11.00±0.61	10.82±0.58	9.69±0.51	8.35±0.40
q_{ace}	0.58±0.07	1.31±0.10	1.11±0.07	0.33±0.03	0.37±0.06	0.56±0.05
$Y_{X/S}$	0.35±0.01	0.30±0.02	0.29±0.01	0.26±0.02	0.27±0.03	0.29±0.01
$Y_{CO2/S}$	2.55±0.09	2.64±0.03	2.88±0.12	1.53±0.05	1.45±0.04	1.33±0.07
$Y_{ace/S}$	0.18±0.03	0.35±0.04	0.29±0.02	0.05±0.01	0.06±0.01	0.09±0.02

q_S : Carbon source consumption rate (mmol $g^{-1}\ h^{-1}$)
q_{CO2} : CO_2 evolution rate (mmol $g^{-1}\ h^{-1}$)
q_{ace} : acetate formation rate (mmol $g^{-1}\ h^{-1}$)
$Y_{X/S}$: biomass yield on substrate (g g^{-1})
$Y_{CO2/S}$:CO_2 yield on substrate (mmol $mmol^{-1}$)
$Y_{ace/S}$: acetate yield on substrate (mmol $mmol^{-1}$)

rate (CER) obtained for either mutant grown on glucose are somewhat higher than those obtained for the parent strain. This is contrary to what is observed for mutants grown on pyruvate, where these two rates are markedly decreased. The results also imply the differences in acetate excretion between the parent strain and the mutants. Gene deletion leads to increased acetate production; and this effect is more significant when glucose is used as the sole carbon source.

The enzyme activity in Table 6.7, shows a remarkable increase in Pgi activity for the glucose-grown mutant, as compared to the parent strain. Although a significant increase in the specific activity of Pgi is observed for the glucose-grown *gnd* mutant, the activity of TCA-related enzymes (e.g. ICDH) is only a little higher than that of the parent strain. However, in the case of the *zwf* mutant, a remarkable increase in the activity of ICDH is observed.

The specific activity of Pgi decreases 3.7-fold in the parent strain grown on pyruvate, as compared to that grown on glucose. Moreover, Pgi activity is significantly lower in both mutants than in the parent strain. It is worth noting that a high level of ED pathway enzymes is detected for the *gnd* mutant (398 ± 29 units of activity). Likewise, an active pathway through Mez is observed for both mutants.

Let us now consider metabolic flux analysis. Here, only those that are located at key branch points of the metabolic pathways are shown as the absolute net fluxes with lower and upper bounds (Table 6.8). Others are shown in Figures 6.2 and 6.3 as the best-fit flux distributions relative to the specific uptake rates of substrates (Zhao et al., 2004b).

Table 6.7 **Activities of enzymes located at key branch points and involved in NADPH formation. Activities are given in nmol min^{-1} mg^{-1} protein**

Enzymes	Glucose culture			Pyruvate culture		
	Wild	*gnd*	*zwf*	Wild	*gnd*	*zwf*
6PGDH	381±34	ND	126±10	137±18	ND	114±10
Pgi	1277±89	1675±98	1905±86	343±45	65±9	55±7
ICDH	1205±96	1229±61	1631±98	1390±70	1414±81	1371±69
G6PDH	354±31	248±12	ND	145±10	83±6	ND
Mez	ND	70±6	15±2	<5	19±3	66±5

ND: not determined

Published by Woodhead Publishing Limited, 2013

Table 6.8 Absolute metabolic fluxes at several key branch points in the central metabolic pathways, when glucose or pyruvate were used as sole carbon source. Fluxes are expressed as mmol g^{-1} dry cell weight h^{-1} with 95% confidence limits obtained from statistic analysis. Negative values indicate the reversed pathway direction

Pathway	Wild		*gnd*		*zwf*	
	Optimal estimate	95% confidence limit	Optimal estimate	95% confidence limit	Optimal estimate	95% confidence limit
Glucose culture						
G6P → F6P	2.52	2.32, 2.72	3.33	3.16, 3.56	3.78	3.67, 3.91
G6P → 6PG	0.64	0.57, 0.69	0.33	0.23, 0.41	0.00	–
X5P+E4P → F6P+T3P	0.09	0.08, 0.10	–0.13	–0.12, –0.14	–0.12	–0.11, –0.13
AcA+OAA → CIT	2.34	2.11, 2.55	2.89	2.73, 3.01	3.32	3.03, 3.63
MAL → OAA	2.10	2.01, 2.25	2.31	2.18, 2.46	2.97	2.72, 3.16
Pyruvate culture						
G6P → F6P	0.26	0.24, 0.28	0.04	0.03, 0.06	0.04	0.02, 0.07
G6P → 6PG	0.22	0.19, 0.27	0.00	–	0.00	–
X5P+E4P → F6P+T3P	–0.05	–0.03, –0.07	–0.12	–0.10, –0.13	–0.12	–0.11, –0.15
AcA+OAA → CIT	3.44	3.15, 3.68	3.13	2.94, 3.37	2.63	2.39, 2.88
MAL → OAA	3.12	2.98, 3.32	2.75	2.54, 2.93	1.87	1.63, 2.05

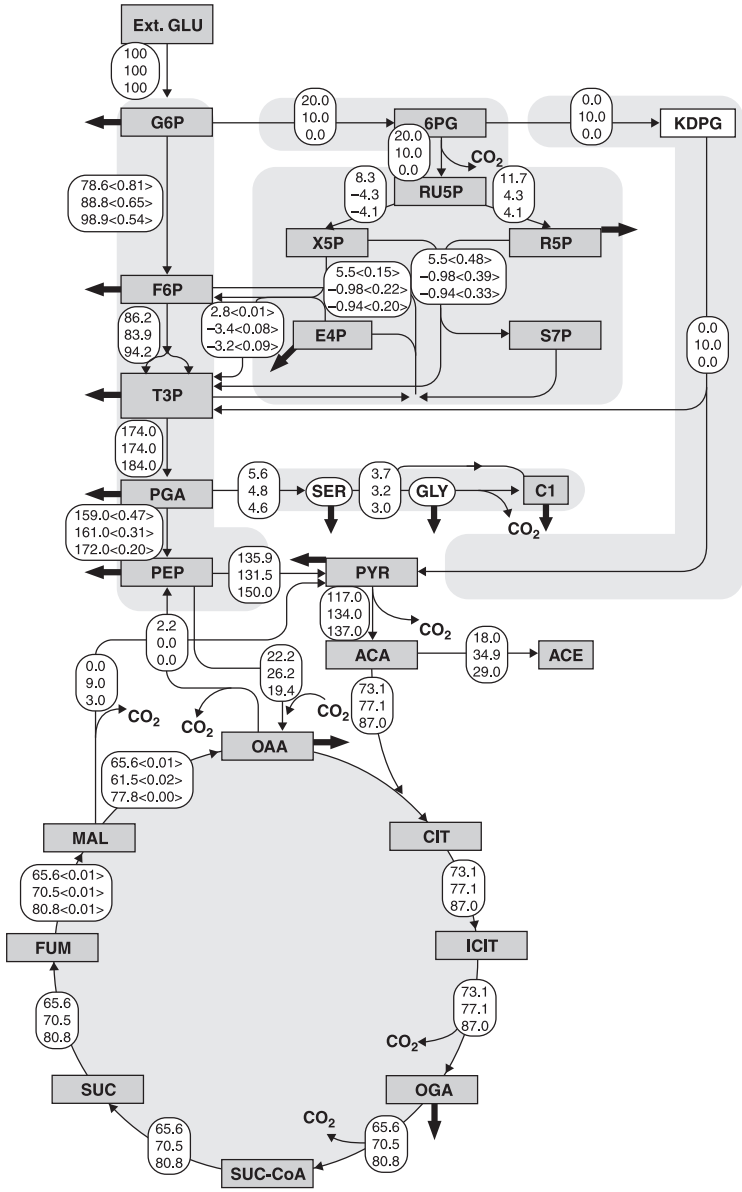

Figure 6.2 Metabolic flux distributions in chemostat culture of glucose-grown *E. coli* parent strain (*upper values*), *gnd* (*middle values*), and *zwf* (*lower values*) mutants at $D = 0.2\ h^{-1}$. Fluxes are given relative to the specific glucose consumption rate and are expressed as the net fluxes. The exchange coefficients are *shown in brackets* for the reactions that were considered reversible. *Negative values* indicate the reversed pathway direction

Published by Woodhead Publishing Limited, 2013

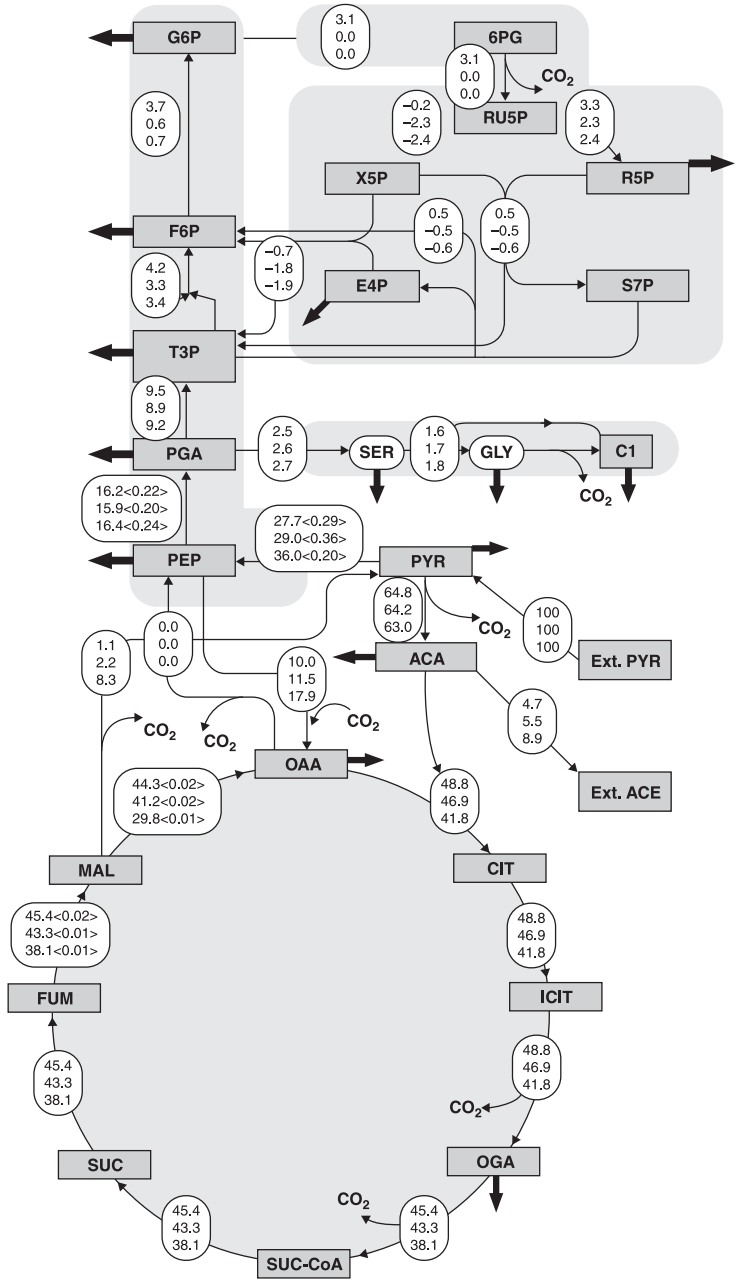

Figure 6.3 Metabolic flux distribution in chemostat culture of pyruvate-grown *E. coli* parent strain (*upper values*), *gnd* (*middle values*), and *zwf* (*lower values*) mutants at D = 0.2 h^{-1}. Fluxes are given relative to the specific pyruvate consumption rate and are expressed as the net fluxes

While the flux through G6PDH is decreased in the *gnd* mutant grown on glucose, this pathway is totally blocked in mutants grown on pyruvate, although the enzyme, G6PDH, remain expressed. Since the flux through the oxidative PP pathway is significantly decreased or totally blocked in the mutants grown on glucose, the metabolic network has to give a higher flux through EMP or ED pathways to the TCA cycle. Opposite relations are seen in the mutants grown on pyruvate, where the deletion of genes causes a reduction in fluxes through the TCA cycle.

Corresponding with observations in the enzymatic study, the metabolic flux redistribution indicates an activation of the ED pathway in the *gnd* mutant grown on glucose and an increase in the flux through Mez in both glucose- and pyruvate-grown mutants. Further inspection of NADPH-generating reactions reveals a negative correlation between the Mez and ICDH pathways in the mutants, i.e. a higher flux of the Mez pathway is always accompanied by a lower flux through the ICDH pathway. Moreover, the conversion of carbon skeletons from the TCA cycle through Mez enables the cells to respond to TCA carbon depletion by regulating the carbon flux through Ppc. This can be shown in the positive correlation between the Mez and Ppc pathways.

Growth characteristics indicate that neither *zwf* nor *gnd* is essential (Fraenkel et al., 1968). However, further inspection of the metabolic parameters indicates a unique alteration in the utilization of the metabolic pathways for optimal growth of the mutants under different culture conditions. This is further supported by the enzymatic study, in which the enzyme activities are strongly dependent on genetic background and environmental conditions.

The carbon can be fed into the ED pathway through two routes in *E. coli* grown on glucose. One route consists of oxidation of D-glucose to D-gluconate by glucose dehydrogenase (GDH) and the phosphorylation of D-gluconate to 6PG by gluconate kinase. The other route is such that glucose is utilized via G6PDH to 6PG. The mechanism for activating GDH in *E. coli* remains intriguing. It is shown (Matsushita et al., 1997) that *E. coli* may not be able to produce gluconate from glucose via GDH, since it cannot synthesize pyrroloquinoline quinone (PQQ), a cofactor of glucose dehydrogenase. Although it may be possible for *E. coli* to scavenge its surroundings for PQQ, the enzyme analysis excludes this possibility when cells are grown in minimal medium.

A negative effect of the *gnd* deletion has been observed for *Saccharomyces cerevisiae* grown on glucose, since intermediates such as 6PG are reported to be toxic in high concentrations (Holger et al., 1996). It is clear that the ED pathway, which is not possessed by *S. cerevisiae*,

Published by Woodhead Publishing Limited, 2013

serves as the route to relieve the toxic level of 6PG in the *E. coli* mutant grown on glucose. Because of the activation of this potential bypass reaction, the flux via G6PDH is reduced but not blocked. The activity of the oxidative PP pathway is therefore partly maintained.

Metabolic flux analysis suggests significant differences in carbon flux distribution over the TCA cycle between glucose- and pyruvate-grown mutants. The deletion of genes causes an enhanced activity of the TCA cycle in the former but a decrease in the latter. Using the flux redistribution and growth parameters presented in Table 6.6, it is reasonable to postulate that although the PP pathway flux is considerably lower during gluconeogenesis, expression of the *zwf* gene may co-ordinate with other genes to control the substrate uptake. The mutant directs a lower carbon flux through the TCA cycle and, therefore, produces CO_2 at relatively low rates, compared to those of the parent strain. This cellular response is necessary because the network has to conserve more carbon for biosynthesis through the reduction in CO_2 production, so that the mutant can grow at the same rate as the parent strain when the carbon source uptake rate decreases.

In *E. coli*, the oxidative PP pathway plays a major role in the generation of NADPH. ICDH is also important in producing NADPH (Choi et al., 2003). Although the shortage of NADPH due to disruption of the oxidative PP pathway can be partially compensated for by an increased flux through ICDH, it appears that the flux via ICDH alone cannot enable the apparent shortage of NADPH to be met under certain circumstances. For this, malate is deviated out of the TCA cycle through Mez to function as the route in which an adequate supply of NADPH is generated to meet the biosynthesis requirements. This postulation can explain the negative correlation between the fluxes through Mez and ICDH, as occurring in the mutants. When glucose is used as a sole carbon source, a higher flux through ICDH is observed for the *zwf* mutant. This can generate more NADPH than in the *gnd* mutant, thus rendering the pathway via Mez less active. However, in the case of using pyruvate as a carbon source, *zwf* gene deletion leads to a lower flux through ICDH, as compared to the case of *gnd* gene deletion. Therefore, the flux via Mez significantly increases to complement the shortage of NADPH. Activation of the Mez pathway changes the flux distribution around the OAA node. The drain of carbon skeletons from the TCA cycle through Mez enables the cells to replenish the OAA pool by regulating the carbon flux through Ppc. To increase the synthesis of OAA from PEP, Ppc is therefore up-regulated in accordance with the activity of the Mez pathway.

In the mutants grown on glucose, all directions of the fluxes through non-oxidative PP pathways are reversed, indicating that the mutant tries to compensate for the lack of E4P and R5P through the glycolytic metabolites GAP and F6P. In mutants grown on pyruvate, an increased flux through Tkt (F6P + T3P → X5P + E4P) is found, suggesting a similar function for the non-oxidative PP pathway as in the glucose-grown mutants. In this way, the non-oxidative branch can function as an important metabolic route without the participation of the oxidative PP pathway.

One of the goals of a gene-knockout study is the engineering of metabolic pathways for enhanced production of industrial chemicals. However, genetically altering metabolic pathways often cause undesirable changes, such as reduced growth, decreased glycolytic flux, and the creation of futile cycles, which may limit its utility (Holger et al., 1996). The results indicate that *E. coli* grown on glucose with genetic disruption in the oxidative PP pathway can serve as a good candidate for industrial production, since the mutations have little effect on cell growth, and the increased activities of EMP and TCA cycle may benefit the production of useful chemicals that are synthesized from precursors involved in these two branches. The genetic alteration of *zwf* is preferred, since mutation in the other gene, *gnd*, activates the ED pathway from which only one molecule of ATP is produced. In view of energy metabolism, the ED pathway is less efficient than EMP, with a net gain of two molecules of ATP for each molecule of glucose.

The problem in utilizing the *zwf* mutant in industrial production is that gene deletion causes an enhanced production of acetate. Acetate accumulation should be avoided in industrial-scale production, since a high acetate concentration in the culture medium has been found to decrease the yield of recombinant protein. This type of overflow metabolism usually occurs when high fluxes from the pyruvate pool exceed the capacity for respiratory metabolism and the balance is therefore excreted as acetate. This can be manifested in the *zwf* mutant, where the flux entering the pyruvate pool is extremely high due to the high activity of EMP. Note that the reason for acetate excretion in the *gnd* mutant is somewhat different from the *zwf* mutant when glucose is used as a sole carbon source. The flux profile of the former demonstrates that the increase in the flux through the early step of EMP is actually counteracted later by enhanced fluxes entering into the non-oxidative PP pathway through GAP and F6P. The increase in the flux through PDHc is mainly due to the supply from the ED pathway and Mez pathway. Thereafter, the increased flux is partly channeled toward acetate excretion as a result of overflow metabolism.

Published by Woodhead Publishing Limited, 2013

6.4 Effect of *pyk* gene knockout on metabolism

Let us consider how the cell regulates the *pyk* gene knockout (Siddiquee et al., 2004a,b; Toya et al., 2010). The growth rate of the *pykF* mutant is a little lower compared to that of the wild type. During exponential growth, acetic acid is also produced but its formation rate is lower compared to that of the wild type, and the CO_2 evolution rate (CER) is lower for the *pykF* mutant, where the decrease in CO_2 evolution rate in the *pykF* mutant may be partly due to an increase in CO_2 fixation through the Ppc reaction. Another possibility may be decreased glucose consumption rate.

The GC-MS and NMR data for the *E. coli pykF* mutant are shown in Tables 6.9 and 6.10. Figure 6.4 shows the metabolic flux distributions of the wild type (upper figure) and for the *pykF* mutant (lower figure). The flux distribution in the *pykF* mutant reveals a high flux from PEP to OAA. The flux through the anaplerotic reaction catalyzed by Ppc in the *pykF* mutant is also high (44%) in the *pykF* mutant as compared to 17% for the wild-type strain. It should be noted that the flux value in brackets for Ppc is also high, which indicates that the flux through Pck is also high. The flux from PEP to PYR for the *pykF* mutant is significantly lower compared to the wild type and is consistent with enzyme activity measurements. It can also be seen that the flux through Mez is high, about 21% for the *pykF* mutant, while it is very low for wild type. Moreover, the glycolytic flux from G6P to F6P is 20% for the *pykF* mutant, while it is 65% in the wild-type strain. However, the flux through the oxidative PP pathway is 79% for the *pykF* mutant, while it is 34% in the wild type. The flux from AcCoA to acetate reduces to 0.82% in the *pykF* mutant, as compared to 20% in the wild type.

The enzyme activity for glycolytic pathway enzymes, such as Pgi, and Tpi, decreases by about 2.65-, 2.45-, and 2.08-fold at high D (0.5 h^{-1}) compared to those at low D (0.1 h^{-1}). Figure 6.5 shows that the enzyme activity of Pfk decreases slightly as D increases, which may be due to the increase in the intracellular concentration of PEP (Figure 6.6). The decreased activity of Pfk at high D increases the concentrations of G6P and F6P, which in turn increase the enzyme activity of G6PDH and 6 PGDH, by about 3- and 9-fold, respectively. The enzyme activity of Pyk at both D values is very low. The enzyme activity of Mez decreases by about 3.5-fold at high D. In accordance with this phenomenon, Pck activity decreases at high D. The enzyme activity of the TCA cycle

Table 6.9 Fragment mass distribution of t-butyldimethylsilyl (TBDMS)-derived amino acids from the *pykF* mutant. Considering standard deviation in the range 0.002 to 0.006 for mass distribution, only mass signals of *m*, *m*+1, and *m*+2 were compared

Amino acids	Fragments	*m*	*m*+1	*m*+2
Ala	$[M-57]^+$	0.699[a]	0.181	0.099
		0.693[b]	0.180	0.097
Asx	$[M-57]^+$	0.650[a]	0.250	0.078
		0.666[b]	0.043	0.031
Gly	$[M-57]^+$	0.744[a]	0.160	0.096
		0.735[b]	0.156	0.093
Glx	$[M-57]^+$	0.540[a]	0.170	0.162
		0.539[b]	0.167	0.153
Ile	$[M-57]^+$	0.685[a]	0.079	0.085
		0.681[b]	0.075	0.080
Ile	$[M-159]^+$	0.641[a]	0.079	0.071
		0.639[b]	0.077	0.084
Leu	$[M-57]^+$	0.677[a]	0.129	0.084
		0.671[b]	0.126	0.081
Leu	$[M-57]^+$	0.614[a]	0.112	0.112
		0.610[b]	0.102	0.106
Phe	$[M-57]^+$	0.629[a]	0.116	0.110
		0.627[b]	0.113	0.097
Phe	$[M-159]^+$	0.568[a]	0.112	0.077
		0.565[b]	0.110	0.075
Met	$[M-57]^+$	0.608[a]	0.041	0.029
		0.606[b]	0.039	0.028
Thr	$[M-57]^+$	0.587[a]	0.242	0.133
		0.586[b]	0.238	0.127
Tyr	$[M-57]^+$	0.617[a]	0.115	0.099
		0.616[b]	0.111	0.095
Tyr	$[M-159]^+$	0.544[a]	0.108	0.076
		0.543[b]	0.106	0.072
Val	$[M-57]^+$	0.640[a]	0.081	0.067
		0.642[b]	0.078	0.063

[a] Experimentally determined
[b] Calculated

Published by Woodhead Publishing Limited, 2013

Table 6.10 Measured and simulated values of the NMR spectra of cellular amino acids. s – Singlet; d_1 – doublet with larger scalar coupling; d_2 – doublet with smaller scalar coupling; *dd* – doublet of doublets

Atom	Measured				Simulated			
	s	d_1	d_2	dd	s	d_1	d_2	dd
Arg γ	0.39	0.61	–	–	0.35	0.63	–	–
Asx α	0.39	0.61	–	–	0.38	0.52	–	–
Gly α	0.34	0.66	–	–	0.32	0.60		
Ile α	0.19	0.11	0.61	0.09	0.17	0.01	0.62	0.02
Ile δ	0.35	0.65	–	–	0.30	0.56	–	–
Leu α	0.17	0.08	0.66	0.09	0.12	0.01	0.63	0.02
Leu β	0.43	0.57	–	0.00	0.42	0.56	–	0.00
Lys ε	0.32	0.68	–	–	0.34	0.63	–	–
Pro α	0.11	0.15	0.19	0.55	0.08	0.12	0.14	0.55

enzyme CS is lower at high *D*, while that of MDH changes little at both *D* values. The enzyme activity of the ED pathway is higher at high *D*. This corresponds to the increase in carbon flow in the oxidative PP pathway. The enzyme activities of Ack and ICDH change little.

Acetate production is substantially lower for the *pykF* mutant compared to the wild type (Ponce et al., 1998; Zhu et al., 2001). The enzyme activities of glycolytic enzymes, such as Pgi, Pfk, Tpi, and Ppc, are higher during 2–4 h of fermentation. Oh et al. (2002) found that Mez and Pck enzymes correlated when acetate was utilized. They explain that the mutation of *mez* and *pck*A genes prevents growth on acetate. As the glucose is consumed and acetate accumulates, cells switch smoothly to co-metabolism, utilizing both glucose and acetate. This switch involves induction of the TCA cycle enzymes and glyoxylate bypass enzymes required to provide energy and to replenish intermediates used for amino acid biosynthesis (Clark and Cronan, 1996). Icl also becomes more active under acetate conditions. TCA cycle genes are known to be under the control of cAMP and Crp, which mediate catabolic repression (Cronan and LaPorte, 1999).

In the case of the *pykF* mutant, the enzyme activities of glycolytic pathway enzymes decreases compared to those of the wild type, while the enzyme activity of oxidative PP pathway enzymes increases for the

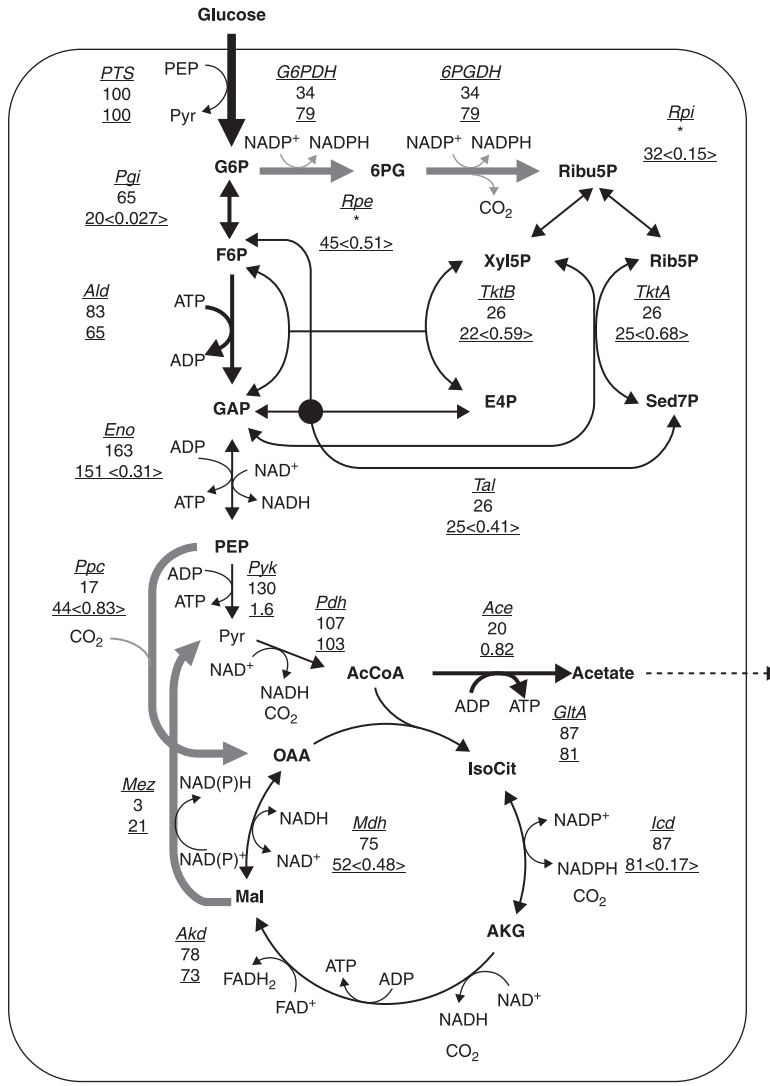

Figure 6.4 Metabolic flux distribution of wild type (upper value) and *pykF*$^-$ mutant (lower value) at dilution rate (*D*) of 0.1 h^{-1}. Values in < > indicate exchange coefficient

Published by Woodhead Publishing Limited, 2013

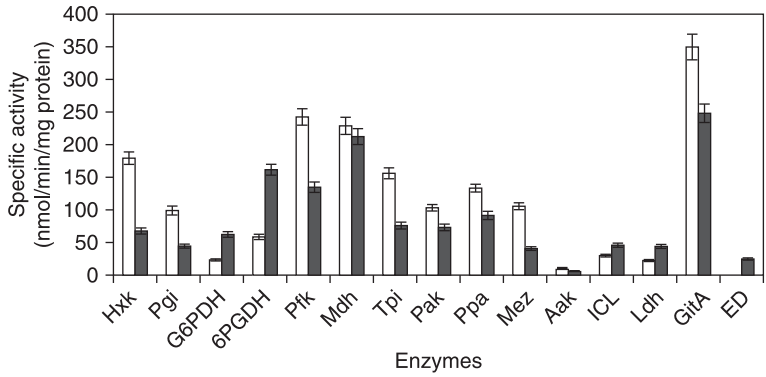

Figure 6.5 Enzyme activities for the *pyk F* mutant at two dilution rates (*D* values): □ = 0.1 h^{-1}, ■ = 0.5 h^{-1}

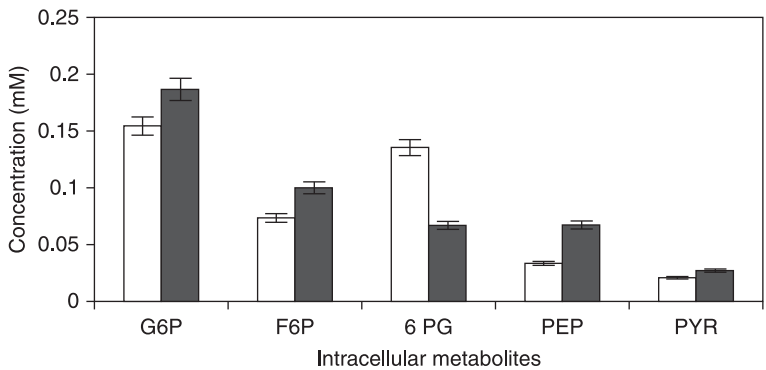

Figure 6.6 Comparison of concentrations of intracellular metabolites in the *pykF* mutant at two *D* values: □ = 0.1 h^{-1}, ■ = 0.5 h^{-1}

former. Ponce et al. (1998) also reported increased activity of the oxidative PP pathway enzymes in the *pykF* mutant. The most significant differences between the wild type and the *pyk F* mutant are observed in Ppc and Mez activities. In the presence of glucose, these two enzyme activities are significantly increased in the *pykF* mutant. This can be explained by blockage of PEP to the PYR pathway activating both Ppc and Mez to supply PYR by forming an alternative pathway. It can be seen that blockage of PEP to PYR will increase the PEP pool in the mutant, which might inhibit Pfk enzyme activity in the glycolytic pathway. The

accumulation of PEP and the activation of the PP pathway (or increased E4P concentration) may activate the aromatic amino acids synthetic pathways (Kedar et al., 2007). The decreased activity of Pfk in turn increases the G6P and F6P concentrations. Increased activity of the oxidative PP pathway is observed in the *pykF* mutant. This might be due to the increased G6P concentration.

Although futile cycling could be induced by simultaneous overexpression of *Ppc* and *Pck* in *E. coli* (Chao and Laio, 1994), it is generally maintained at a low level (Chambost and Fraenkel, 1980; Dalal and Fraenkel, 1983; Chao and Laio, 1994). The enzyme activity results for Ppc and Pck support the futile cycle results obtained by flux calculation.

6.5 Effect of *lpdA* gene knockout on metabolism

The lipoamide dehydrogenase (LPD) encoded by the *lpdA* gene is a component of PDHc, KGDH, and glicine cleavage multi-enzyme (GCV) system. This *lpdA* gene knockout produces more pyruvate and L-glutamate under aerobic conditions than the wild-type strain. It is shown that AcCoA is considered to be formed by the combined rerouting pathways through PoxB, Acs, Ack, and Pta in the *lpdA* mutant. Metabolic flux analysis of the *lpdA* knockout gene mutant indicates that the ED pathway and glyoxylate pathway are activated, while the glycolysis and the oxidative PP pathway, as well as the TCA cycle, are down-regulated (Li et al., 2006a). If only KGDH was blocked by the *sucA* gene knockout, metabolism turns out to be a little different from the *lpdA* gene knockout mutant (Li et al., 2006b). The regulation of the anaplerotic pathway, such as the glyoxylate shunt, plays a role in these mutants. Let us now consider the detailed metabolic regulation analysis.

Figure 6.7 shows the aerobic batch cultivation results using an LB medium containing glucose, where the results indicate that the cell growth of the mutant is slow compared to its parent strain, and it indicates that a fair amount of pyruvate is produced during exponential growth phase of *lpdA* mutant, while little pyruvate is produced in the parent strain. Moreover, 1 g/l of D-lactate and 0.5 g/l of succinate accumulate in the culture of the mutant by the time of complete glucose utilization. The concentration of acetate is almost undetectable in the cultivation of the mutant when glucose is utilized. The accumulated pyruvate begins to decrease rapidly at 6 h after glucose exhaustion. Then the cell starts to

Published by Woodhead Publishing Limited, 2013

grow again using pyruvate as another carbon source, and produces acetate, which is subsequently utilized after the pyruvate is consumed. Although cell growth is depressed in the mutant, the final cell concentrations are higher than that in the parent strain (Figure 6.7).

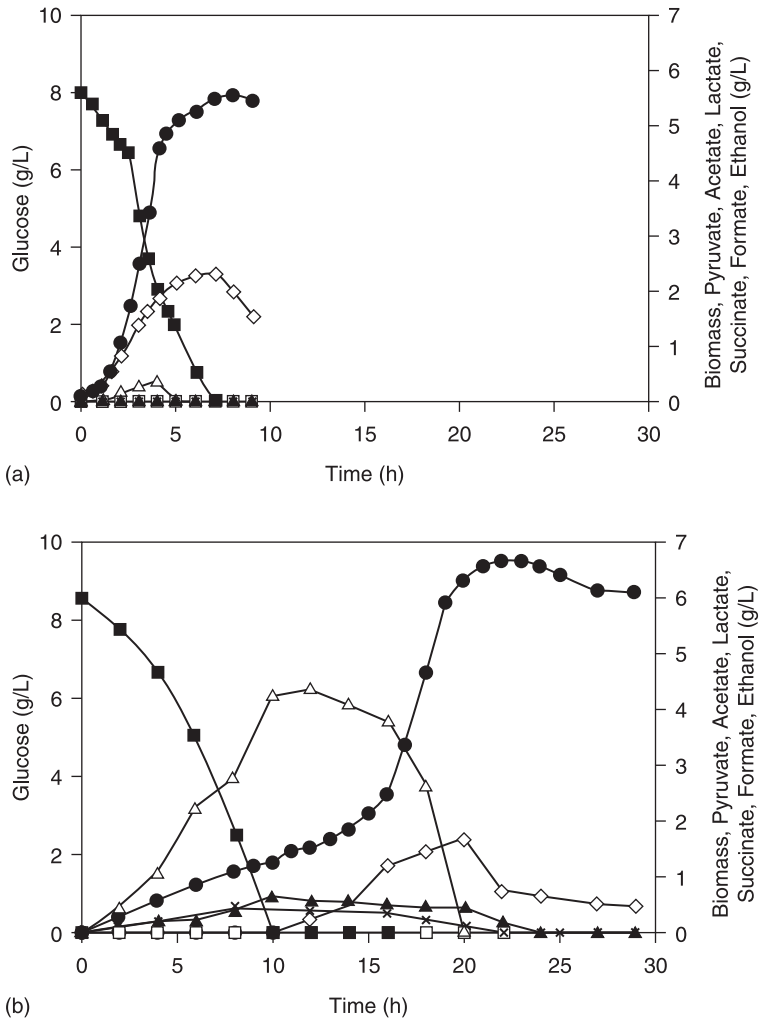

Figure 6.7 Aerobic batch cultivation of (a) *E. coli* BW25113 and (b) *E. coli lpdA* mutant using glucose as carbon source in LB medium: (■) glucose; (●) biomass; (△) pyruvate; (◊) acetate; (▲) D-lactate; (×) succinate; (○) formate; (□) ethanol

Another two cultivations were conducted to investigate the PoxB function in the *lpdA* mutant. Sodium pyrophosphate (10 mM), one of the inhibitors of PoxB, was added to the medium 2 h after the glucose was depleted in the batch culture. It is found that addition of sodium pyrophosphate inhibits PYR assimilation in the *lpdA* mutant and the cell growth almost ceases, while the pattern of the assimilation of acetate is little affected in the parent strain with the addition of this inhibitor. These phenomena indicate that PoxB is essential for the *lpdA* mutant, while it is not so for the wild type.

Figure 6.8 shows that the activity of KGDH in the *lpdA* mutant is negligible compared to the parent strain. Since the *lpdA* gene encodes for the subunit of both KGDH and PDHc, and this subunit plays the similar role in both enzymes, the enzyme activity of PDHc is considered to be small. Figure 6.8 shows that the enzyme activity of some of the glycolytic enzymes, such as Pyk, are up-regulated in the *lpdA* mutant. As for TCA cycle enzymes, the CS activity is down-regulated in the *lpdA* mutant, while the activity of MDH and Fum is up-regulated in this mutant as compared to those of the parent strain. The activity of the oxidative PP pathway enzyme, such as G6PDH, is up-regulated in the mutant and also the activity of the ED pathway enzymes and the glyoxylate shunt enzyme

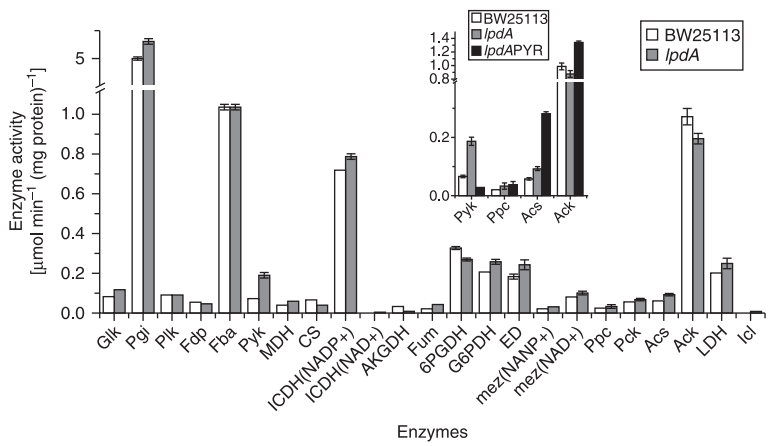

Figure 6.8 **Enzyme activities of *E. coli* BW25113 and *E. coli lpdA* mutant under aerobic conditions in LB medium. The upper smaller graph shows some key enzyme activities of *lpdA* mutant when produced pyruvate was reconsumed**

Published by Woodhead Publishing Limited, 2013

Icl is higher in the *lpdA* mutant. It can be seen that the activities of the anaplerotic pathway enzyme Ppc and $NADP^+$ (NAD^+)-specific Mez are all activated in the *lpdA* mutant. The activity of the fermentative pathway enzymes, such as Acs and LDH, increase in the *lpdA* mutant, while Ack activity decreases in the *lpdA* mutant.

Some of the intracellular metabolite concentrations are compared between the parent and the mutant (Figure 6.9). PYR concentrations are about 10-fold higher in the *lpdA* mutant as compared to that in the parent strain, which may be due to the blockage of PDHc. In addition, accumulation of L-Glu is 20 times higher than in the parent strain. The concentrations of αKG also increase in the mutant. The concentrations of G6P and F6P are slightly higher in the *lpdA* mutant as compared to those of the parent strain, whereas AcCoA is almost undetectable in the mutant.

Table 6.11 shows the growth parameters of the *lpdA* mutant and the parent strain in continuous cultures. It is found that the biomass yield of the *lpdA* mutant is higher than that of the parent strain, while glucose uptake rates are lower for the mutant and the specific CO_2 evolution rate is much reduced in the mutant.

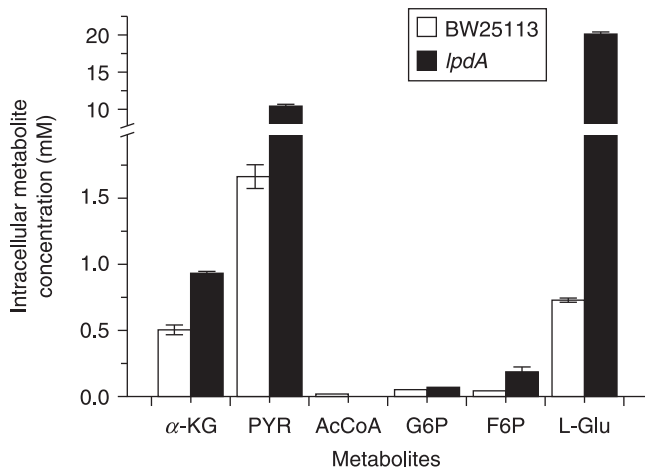

Figure 6.9 **Comparison of the intracellular metabolite concentrations of *E. coli* BW25113 and *E. coli lpdA* mutant in the batch cultivation. (The intracellular concentrations were calculated assuming the cellular volume to be 2.15 ml (g dry cell weight)/l.)**

Table 6.11 Growth characteristics of *E. coli* BW25113 at the dilution rate of 0.2 h^{-1} and its *lpdA* mutant at the dilution rate of 0.22 h^{-1} in continuous culture

Variables	BW25113	*lpdA* mutant
Biomass yield (g g^{-1})	0.40	0.49
Glucose uptake rate (mmol g^{-1} h^{-1})	3.04	2.48
Specific CO_2 evolution rate (mmol g^{-1} h^{-1})	8.17	4.08

Figure 6.10 shows the comparison of the metabolic flux distributions between the *lpdA* mutant (lower values underlined) and the parent strain (Li et al., 2006a). All the flux values are normalized with respect to glucose uptake rates. Figure 6.10 shows that with the blockage of the flux through the reactions of PDHc and KGDH, the mutant exhibits a slight reduction in the flux values of glycolysis and PP pathways, except for a slight increase in the flux through G6PDH. However, the ED pathway is activated in the mutant strain with a flux value of 13.0%. The blockage of the PDHc reaction has also induced the PEP synthase (Pps), which catalyzes the reversed reaction from PYR to PEP, where the exchange coefficient is relatively high at 0.75. Since the *lpdA* mutant cannot utilize the pathway through PDHc to produce AcCoA, the alternative pathway through PoxB is activated. In the TCA cycle, all the net flux values are reduced when compared to the parent strain. With the blockage of the pathway between α-KG and SUC, the flux through ICDH is limited, and this flux value is determined by the biomass formation through α-KG. The glyoxylate shunt is also activated in order to replenish OAA for biomass synthesis. For the reactions through Fum and MDH, both forward and backward fluxes are high in the case of the mutant. The fluxes through anaplerotic reactions increase drastically in the case of the mutant strain, i.e. the flux through Pck increases from 2.2% to 37.3%, the flux through Ppc increases from 22.2% to 64.9%, and the flux through Mez increases to 47.8%.

Since PoxB is known to produce acetate *in vivo* (Lemaster and Cronan, 1982; Grabau and Cronan, 1984), the *poxB* knockout mutant is also cultivated using minimal medium. The *poxB* mutant shows almost the same fermentative properties as those of the parent strain, except that the glucose-uptake rate is slightly lower for the mutant. The enzyme activity of the *poxB* knockout mutant indicates that the activities of glycolytic enzymes, such as Pfk, Fdp, and Fba, decrease in the *poxB* mutant, and the TCA cycle enzymes are also slightly down-regulated in the mutant

Published by Woodhead Publishing Limited, 2013

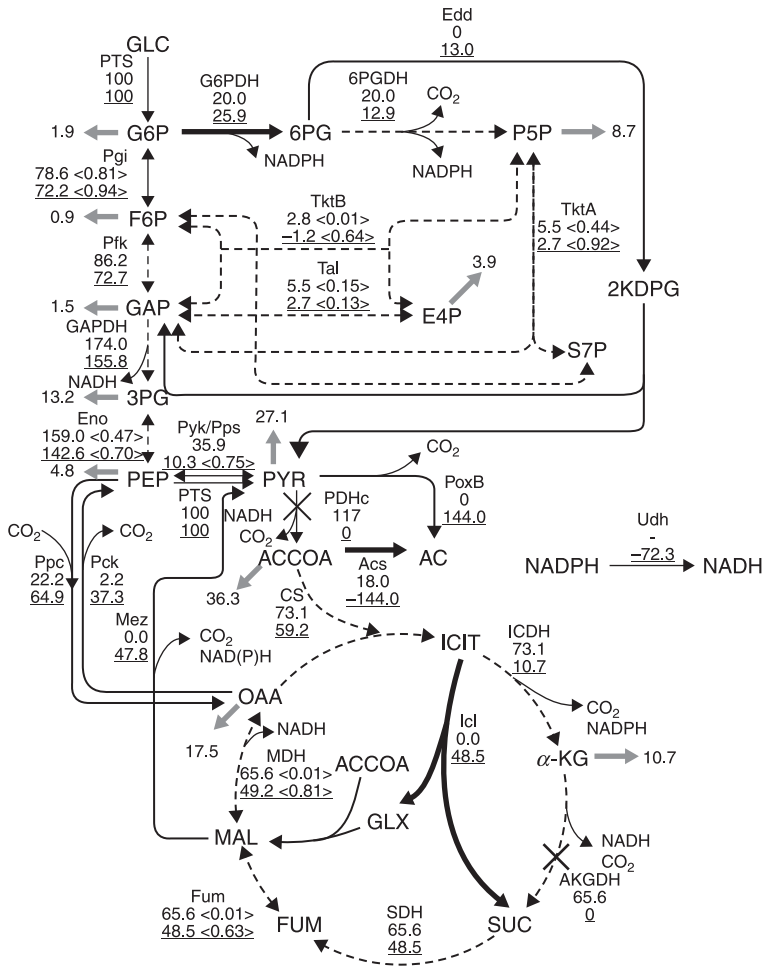

Figure 6.10 Metabolic flux distributions of wild type (upper values) at dilution rate of 0.2 h^{-1} and *lpdA* mutant (lower values, underlined) at dilution rate of 0.22 h^{-1}. Bold solid lines indicate increased fluxes while dash lines indicate reduced flux. Values in ⟨·⟩ indicate exchange coefficient. Gray arrows indicate biomass formation, but only the biomass formation flux for *lpdA* mutant is shown

(Figure 6.11). Interestingly, Ppc, NAD(P)+-specific Mez, Acs, LDH, and the oxidative PP pathway enzyme in the *poxB* mutant, show a similar pattern to that in the *lpdA* mutant.

The knockout of *lpdA* gene causes deactivation of the PDHc, which is the main enzyme catalyzing the reaction from PYR to produce AcCoA. The accumulation of PYR in the *lpdA* mutant may be due to a defect in PDHc activity. To maintain growth, the cell can generate AcCoA from PYR using another less efficient route by first converting PYR to acetate using PoxB, and then convert acetate to AcCoA via Acs and Pta–Ack. The activation of PoxB can be detected in the PDHc-deficient mutant by *in vitro* PoxB enzyme assay (Abdel-Hamid et al., 2001).

Figure 6.7 shows that the *lpdA* mutant has diauxic growth. It has been shown that both *poxB* gene transcription and PoxB activity depend on the *rpoS* gene product, σ^{38} (Chang et al., 1994). Furthermore, bacteria increase RpoS protein levels and RpoS-dependent protective functions during the stationary phase, when the glucose concentration drops below about 10^{-7} M (Notley and Ferenci, 1996). PoxB in the *lpdA* mutant might be activated due to the increased level of σ^{38} factor after the glucose is depleted. Also, during pyruvate assimilation, the Ppc activity increases and Pyk activity is much decreased in the *lpdA* mutant (Figure 6.8). It is assumed that the PYR assimilation in the *lpdA* mutant might be done via PoxB and Ppc. It has been reported that the double mutants lacking the

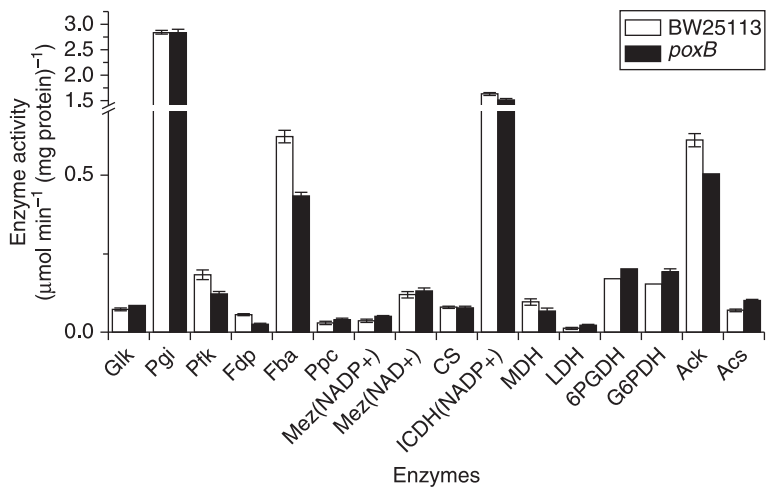

Figure 6.11 **Comparison of enzyme activities of *E. coli* BW25113 and *E. coli poxB* mutant under aerobic conditions using synthetic medium**

Published by Woodhead Publishing Limited, 2013

PDHc and Pps, or the PDHc and Ppc, could not metabolize PYR accumulated during growth on glucose (Dietrich and Henning, 1970). Thus, the direct utilization of PYR accumulated by this mutant is made by the combining reactions catalyzed by PoxB and Pps–Ppc.

As mentioned above, D-lactate is also detected in the culture medium. Normally, D-lactate is produced under anaerobiosis. The LDH in *E. coli* is an allosteric enzyme with PYR acting as an activator at the site distinct from the catalytic site, and the activity of this enzyme appears to be controlled by the cellular concentrations of PYR (Tarmy and Kaplan, 1968a,b). However, it has been reported that the addition of PYR results in a 2- to 4-fold increase in the expression of *ldhA–lacZ* fusions (Jiang et al., 2001). Thus, the increase in the PYR concentrations enhances the production of lactate via gene expression as well as enzyme activity. The inactivation of KGDH in the *lpdA* mutant causes the TCA cycle to be interrupted, which may activate the glyoxylate shunt to supply the precursor for cell growth.

E. coli converts acetate to AcCoA by two distinct pathways, one catalyzed by Acs, mainly functioning under low acetate concentrations, and the other catalyzed by Pta and Ack, which functions under higher acetate concentrations (Kumari et al., 1995). In the *lpdA* mutant, the activity of Acs is higher when glucose is depleted. Furthermore, its activity significantly increases when the pyruvate is assimilated through PoxB. Ack activity is higher only in the second period in Figure 6.8, where pyruvate is used as a carbon source. To supply the AcCoA needed for cell growth, both enzymes for acetate utilization are activated in the *lpdA* mutant. Acs functions both under glucose utilization and pyruvate assimilation, while Pta–Ack functions mainly for growth under pyruvate assimilation.

The low concentration of AcCoA causes down-regulation of CS in the TCA cycle. Another important phenomenon is that the deficiency of KGDH causes the accumulation of α-KG, which is a precursor of Glu. The synthesis of Glu needs NADPH, which may be supplied by the over-production of NADPH in the PP pathway due to the up-regulated activity of the oxidative PP pathway enzymes.

6.6 Effect of *sucA* and *sucC* gene knockout on metabolism

In *E. coli*, *sucA* and *sucC* genes are located in the same operon *sucABCD*. Park et al. (1997) studied how the *sucABCD* genes are expressed in

response to the changes of oxygen and carbon source availability in *E. coli*, and found that *sucABCD* gene expressions are repressed by *arcA* and *fnr* gene products under anaerobic conditions. The *sucA* gene encodes E1 subunit for the KGDH, while *sucC* gene encodes α subunit for the succinyl-CoA synthetase (SCS). KGDH catalyzes the oxidative decarboxylation of α-ketoglutarate (2-oxoglutarate) (αKG) to generate SucCoA and CO_2 along with the production of NADH (Park et al., 1997). SCS catalyzes the substrate-level phosphorylation step of the TCA cycle to convert succinyl-CoA into succinate, accompanying the production of ATP (Wolodko and Bridger, 1987). Both enzymes participate in the generation of the cellular biosynthetic intermediates and the energy generation in the TCA cycle. The TCA cycle is critical for the oxidation of AcCoA and for the production of reducing equivalents that are used by respiratory chains to produce ATP. To understand the role of the TCA cycle in the yeast cell, McCammon et al. (2003) studied some gene expressions in response to the disruption of the TCA cycle, caused by the defects in each of 15 genes encoding subunits of the 8 TCA cycle enzymes, by using a DNA microarray.

Here, consider the effect of *sucA* or *sucC* genes knockout on metabolism in *E. coli*, based on batch and continuous cultivations with gene expressions, enzyme activity, intracellular metabolite concentrations, and metabolic flux distributions based on ^{13}C-labeling experiments. To determine how *sucA* or *sucC* gene knockout affect cell growth characteristics, *sucA* and *sucC* genes knockout mutants are, respectively, grown in a minimal medium with glucose as a carbon source under aerobic conditions (Figure 6.12). The maximum specific growth rates of the wild type strain, *sucA* mutant, and *sucC* mutant, are 0.83, 0.66 and 0.84 h^{-1}, respectively. Acetate production is significantly higher in the *sucC* mutant, as compared to that in the parent strain (Figure 6.12). The produced acetate is not assimilated in the *sucC* mutant. Unlike the parent strain, a little accumulation of L-glutamate is detected in the *sucA* mutant.

Table 6.12 shows the fermentation characteristics of the continuous culture at the dilution rate of 0.2 h^{-1}, where glucose concentrations in the reactor are less than the detectable level for all the cultivations of the parent stain and the *sucA* mutant, while the glucose concentrations in the cultivation of *sucC* mutant are detectable but significantly low (0.03 mM). As shown in Table 6.12, the biomass yields of both mutants are lower than that of the parent strain. The absence of KGDH or SCS activity significantly increases the specific oxygen consumption rate, and

Published by Woodhead Publishing Limited, 2013

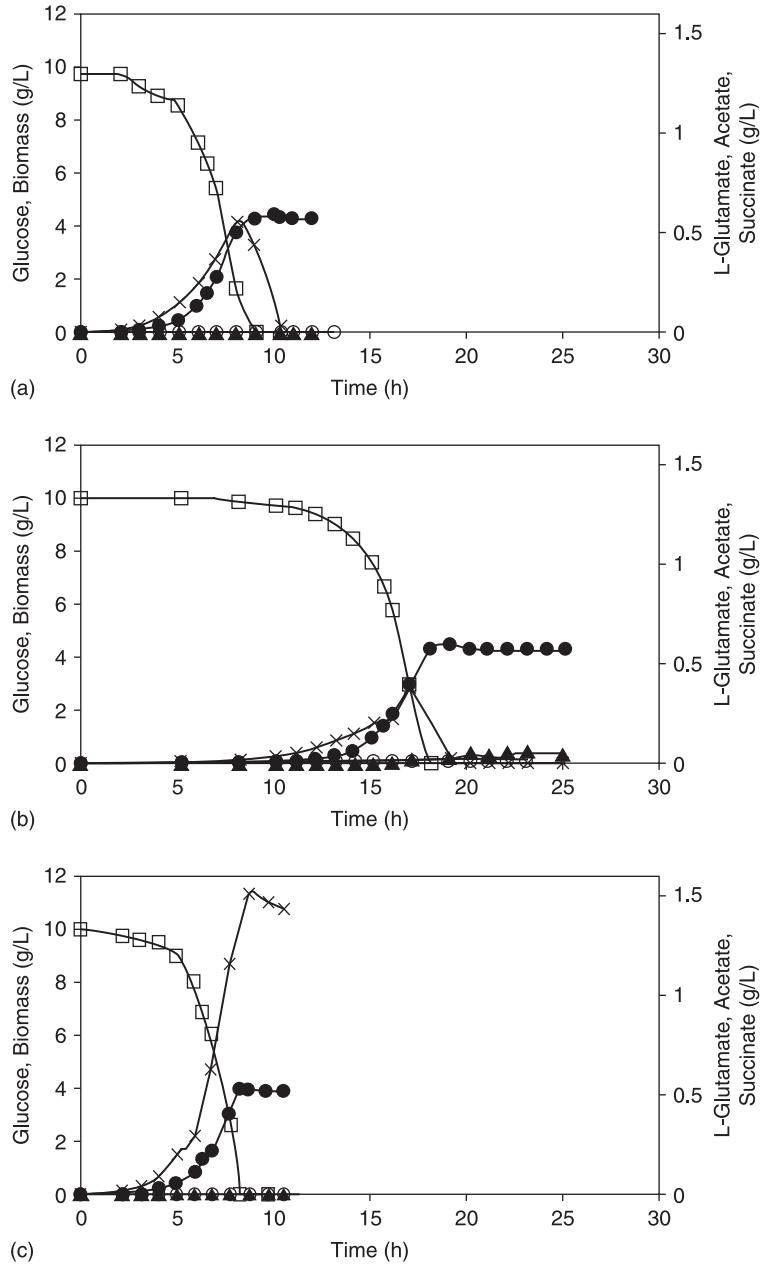

Figure 6.12 Aerobic batch cultivation of: (a) *E. coli* BW25113; (b) *E. coli sucA* mutant; and (c) *E. coli sucC* mutant using glucose as carbon source. Symbols: (□) glucose; (•) biomass; (×) acetate; (▲) l-glutamate; (◊) succinate

Table 6.12 Growth characteristics of parent strain *E. coli* BW25113 and its *sucA*, *sucC* mutants in the continuous culture at the dilution rate of 0.2 h^{-1}

Variables	BW25113	*sucA* mutant	*sucC* mutant
Biomass yield (g g^{-1})	0.45	0.42	0.40
Glucose uptake rate (mmol g^{-1} h^{-1})	2.48	2.65	2.77
Specific CO2 evolution rate (mmol g^{-1} h^{-1})	6.20	6.80	5.45
Specific O2 consumption rate (mmol g^{-1} h^{-1})	9.11	16.29	17.42
Acetate production rate (mmol g^{-1} h^{-1})	–	–	0.35

the specific CO_2 evolution rate (CER) is increased in the *sucA* mutant, while it is reduced in the *sucC* mutant.

Figure 6.13 shows comparison of the enzyme activity at a dilution rate of 0.2 h^{-1}. The enzyme activity of glycolytic enzymes, such as Pgi, Tpi, GAPDH, and Pyk, increase in *sucA* and *sucC* mutants, while the activity of Pfk, the rate-limiting enzyme in glycolysis, is down-regulated in these two mutants. The glycolytic enzyme, such as Pgk, and the PP pathway enzymes, such as G6PDH and 6PGDH, are up-regulated in the *sucA* mutant. The glyoxylate shunt enzymes, such as Icl and MS, are significantly up-regulated for the *sucA* mutant, while this is not the case for the *sucC* mutant. As for the TCA cycle enzymes, the CS, Fum, and MDH are up-regulated in both mutants, while the activity of ICDH is down-regulated in the *sucA* mutant but up-regulated in the *sucC* mutant. It can be seen that fermentative pathway enzyme Ack activity increases, and LDH activity decreases in both mutants.

Figure 6.14 compares intracellular metabolite concentrations between the parent and the mutants in continuous cultivations. The intracellular concentration of G6P is considerably higher in *sucA* and *sucC* mutants, and the concentration of FDP is also higher in *sucA* and *sucC* mutants, as compared to that in the parent strain. PEP concentrations tend to increase, while PYR concentrations decrease in both mutants. The concentration of AcCoA is higher in the mutants, especially in the *sucC* mutant. ATP concentrations are significantly higher in both mutants.

As shown in Figure 6.15, the transcript levels of *arcA* and *fnr* genes are down-regulated in the mutants, and the *rpoS* gene is up-regulated in the mutants. The expressions of *iclR* and *fadR* are down-regulated in the *sucA* mutant but not in the *sucC* mutant, and also the transcript level

Published by Woodhead Publishing Limited, 2013

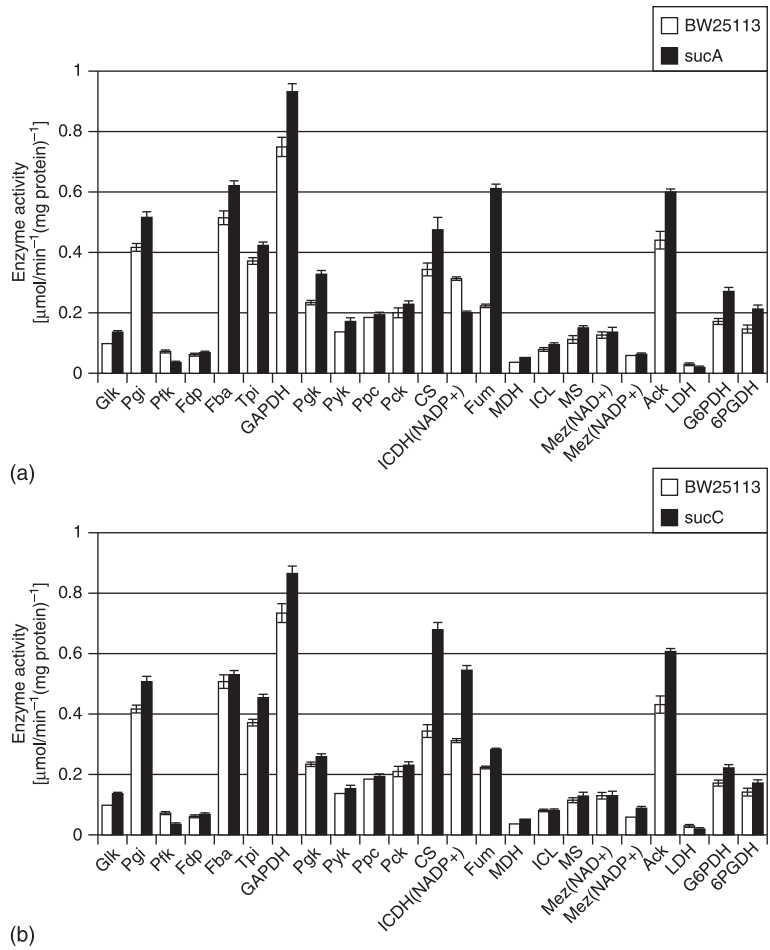

Figure 6.13 **Comparison of enzyme activities at a dilution rate of 0.2 h^{-1} in a continuous culture: (a) *E. coli* BW25113 and *E. coli sucA* mutant; and (b) *E. coli* BW25113 and *E. coli sucC* mutant. (Pgi, ICDH (NADP+) × 5; Pgk × 2; Tpi × 20)**

of the *aceA* gene shows the same trend as the enzyme activity in the mutants.

Figure 6.16 compares metabolic flux distributions of the parent strain and its *sucA* mutant (Li et al., 2005). The flux analysis results indicate that the *sucA* mutant exhibits reduction in glycolysis flux. In the TCA cycle, all the net flux values of the *sucA* mutant are significantly reduced when compared to the parent strain. With the blockage of

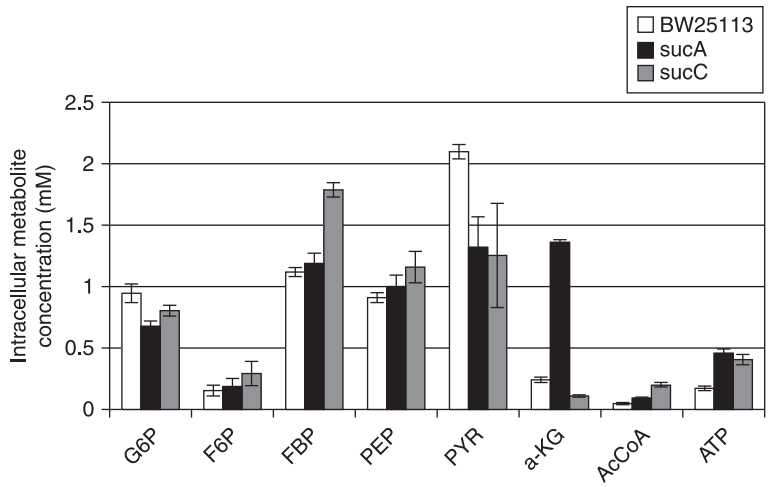

Figure 6.14 **Intracellular metabolite concentrations of *E. coli* BW25113, *sucA* and *sucC* gene knockout mutants at 0.2 h^{-1} specific growth rate in chemostat cultures**

the pathway between α-KG and SUC in the *sucA* mutant, the flux through ICDH is limited. The glyoxylate shunt is activated in order to replenish OAA for biomass synthesis in the *sucA* mutant. Figure 6.16 also shows that the PP pathway fluxes are significantly up-regulated, which is consistent with the enzyme activity results, and the anaplerotic pathways, such as Ppc-Pck and Mez, are also up-regulated in the *sucA* mutant.

In batch cultivations, acetate production patterns show significantly different trends in *sucA* and *sucC* mutants. Acetate production in *E. coli* is generally attributed to the 'overflow metabolism' (El-Mansi and Holms, 1989), which is believed to be the consequence of an imbalance between glucose uptake and demand for energy and biosynthesis (Han et al., 1992; Kleman and Strohl, 1994; Aristidou et al., 1995; Farmer and Liao, 1997; van de Walle and Shiloach, 1998). Acetate formation in *E. coli* can be reduced either by decreasing the specific glucose uptake rate or by enhancing the maximum capacity of the oxidative metabolism (Han et al., 1992). The maximum glucose uptake rate for *sucA* mutant is lower than that of the parent strain, which causes a decrease in the acetate production of the *sucA* mutant in batch cultivation. Although TCA cycle activity is reduced in the *sucA* mutant, acetate production does not increase due to the activation of the

Published by Woodhead Publishing Limited, 2013

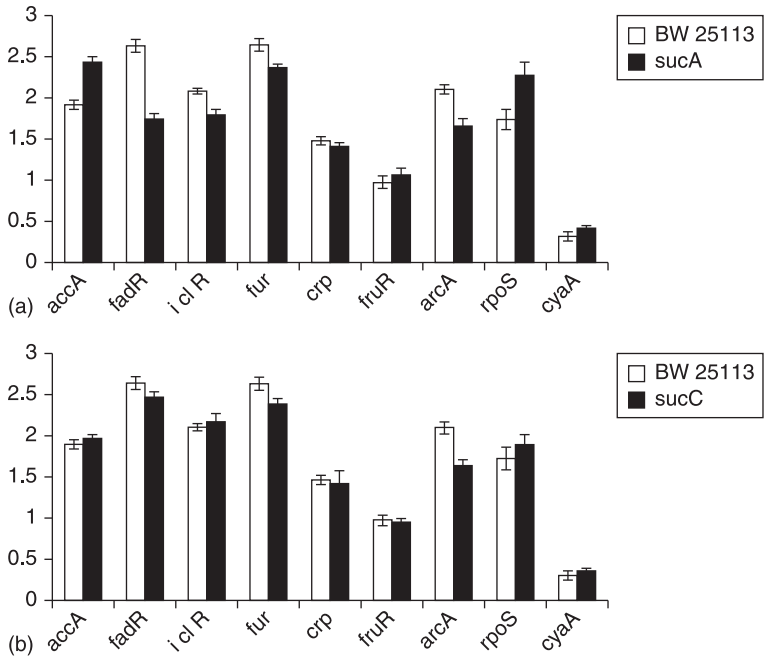

Figure 6.15 **Comparison of some gene expression at a dilution rate of 0.2 h^{-1} in a continuous culture: (a) *E. coli* BW25113 and *E. coli sucA* mutant; and (b) *E. coli* BW25113 and *E. coli sucC* mutant**

glyoxylate shunt in the *sucA* mutant. However, the *sucC* mutant shows high acetate production rates, caused by low TCA cycle activity without glyoxylate shunt activity. Acetate production reduces cell yield in the *sucC* mutant. The *sucC* mutant cannot utilize acetate, which is consistent with other investigation (Mat-Jan et al., 1989). Mat-Jans et al. (1989) shows that the deficiency in SCS prevents aerobic growth on acetate and αKG, but it can grow on TCA cycle intermediates, such as succinate, malate, and fumarate. It may be considered that the SCS mutant makes SucCoA from αKG via KGDH, and makes succinate from fumarate by reversing the succinate dehydrogenase reaction, as under anaerobic conditions. This may explain the decreased CO_2 evolution rate (CER) in the *sucC* mutant. As such, all the TCA cycle intermediates can be fully generated in the *sucC* mutant, which shows a similar growth rate to the parent strain. The activity of Pfk, a rate-limiting enzyme in glycolysis, is down-regulated in both mutants, which are responsible for the decreased

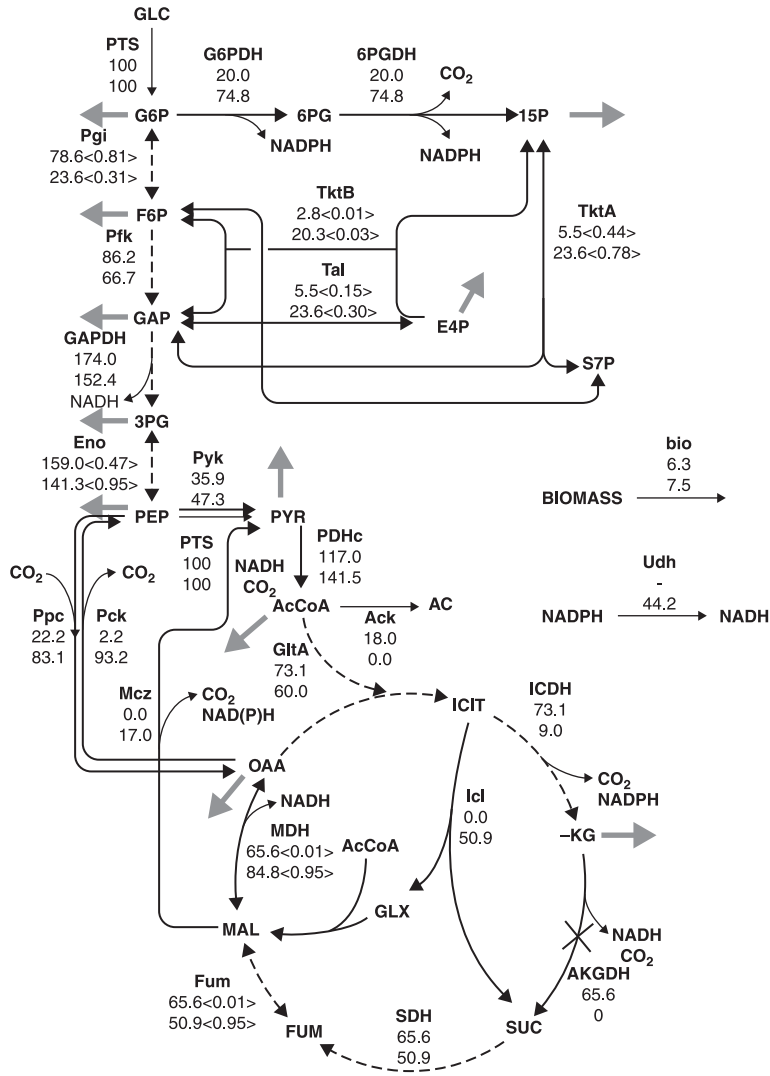

Figure 6.16 Metabolic flux distributions of wild-type (upper values), *sucA* mutant (lower values) at dilution rate of 0.2 h^{-1}. Solid lines indicate increased fluxes, while dash lines indicate reduced flux. Values in '⟨·⟩' indicate exchange coefficient. Gray arrows indicate biomass formation

Published by Woodhead Publishing Limited, 2013

glycolytic flux (Chassagnole et al., 2002). Since it has been demonstrated that Pfk is allosterically inhibited by PEP and ATP, the increase in PEP and ATP concentrations in the mutants cause decreased Pfk activity, though not significantly (Niedhardt, 1996; Chassagnole et al., 2002; Siddiquee et al., 2004a,b).

The accumulation of AcCoA leads to up-regulation of CS in both mutants. Figure 6.14 shows that AcCoA is more accumulated in the *sucC* mutant, and CS is more activated (Figure 6.13). Down-regulation of the global regulatory genes, such as *arcA* and *fnr* (Figure 6.15), also implies the activation of TCA cycle enzymes (Park et al., 1994, 1995a; Perrenoud and Sauer, 2005), such as CS, Fum, and MDH. It is known that the $NADP^+$-specific ICDH is responsible for partitioning isocitrate between the TCA cycle and the glyoxylate shunt, by reversible phosphorylation catalyzed by a bifunctional kinase/phosphatase (Hoyt and Reeves, 1988; Laporte et al., 1985; Nimmo et al., 1987). Figures 6.13 and 6.15 show that the increase in enzyme activity of Icl and MS and the increase in gene expression levels of *aceA* indicate activation of the glyoxylate shunt in the *sucA* mutant but not in the *sucC* mutant. The expression of this *aceBAK* operon is negatively controlled by an adjacent regulatory gene, IclR (Brice and Kornberg, 1968; Maloy and Nunn, 1981), as well as FadR (Maloy et al., 1981). Figure 6.15 shows a slight decrease in the expression of *iclR* and *fadR* in the *sucA* mutant, but not in the *sucC* mutant. It is reported that the expression of *fumAC-lacZ* is up-regulated about 3-fold when acetate is used as a carbon source instead of glucose (Park et al., 1995b). Figure 6.13 shows the activity of Fum as almost 2-fold higher in the *sucA* mutant as compared to that of the parent strain, which also indicates that the *sucA* mutant utilizes acetate through the glyoxylate shunt. Similar to *fumAC* genes, it is reported that *mdh-lacZ* expression is enhanced more than 2-fold when acetate is used as a carbon source instead of glucose (Park et al., 1995b). Figure 6.13 shows that MDH activity is higher in the *sucA* mutant as compared to the parent strain, while the activities of Fum and MDH change very little in the *sucC* mutant.

In both mutants, the reduction of TCA cycle activity also affects the redox balance in the cell, where the reductive NAD^+ and $NADP^+$ are significantly increased. The glyoxylate shunt combining with Pck operates as a cycle, which catalyzes complete oxidation of carbohydrates to CO_2 (Fischer and Sauer, 2003). Figure 6.16 indicates the activation of this cycle in the *sucA* mutant, and the enzyme results also confirm this. This causes CER to increase a little in the *sucA* mutant in the continuous culture. The oxidative PP pathway is enhanced in both mutants, especially

in the *sucA* mutant. The activation of this pathway over-supplies NADPH to the cell, and the NADPH can be interconverted between NADH by the transhydrogenation reaction. Figure 6.16 implies that the *sucA* mutant converts NADPH to NADH by this reaction. Lower pyruvate concentrations in *sucA* and *sucC* mutants cause decreased LDH activity in both mutants (Tamy et al., 1968; Jiang et al., 2001; Li et al., 2006b).

6.7 Effect of *icdA* gene knockout on metabolism

Although there has been a long history for the selection of *E. coli* mutants lacking activity of TCA cycle enzymes, most research has focused on analysis of their growth phenotype (Miles and Guest, 1989; Guest and Russell, 1992). Their research reveals that the mutants lacking any of the TCA cycle enzymes have a common phenotype: all fail to grow with acetate as a sole carbon source. Some TCA cycle mutants (*sucAB, mdh, sdhCDAB*, and *fumA*) grow normally on glucose minimal medium under anaerobiosis, which is attributed either to the lack of function of the enzyme in the branched mode or to the other enzymes that supply the missing biosynthetic intermediates. The enzymes CS (*gltA*), Acn (*acnA,B*), and ICDH (*icdA*) are responsible for glutamate synthesis and thus should be essential for both aerobic and anaerobic growth on minimal media. Considering several central roles of the TCA cycle, it is expected that the blockage in the TCA cycle pathway may cause flux re-routing, which absolutely exerts a different type of metabolic regulation and triggers the compensatory mechanism.

Both *icdA* mutant *E. coli* (JW 1122), and its parent strain *E. coli* BW 25113, were cultivated using LB medium with different carbon sources such as glucose and acetate, in order to elucidate the physiological responses to *icd* gene deletion (Kabir and Shimizu, 2004). Batch cultivation results of both strains grown on glucose under aerobic conditions are shown in Figure. 6.17. Batch cultivation under microaerobic conditions was also conducted with glucose as a sole carbon source, to observe the effects of the *icd* knockout gene on metabolism at a limited DO level (<1 ppm) (Figure 6.18). Figure 6.19 shows the batch cultivation results for the use of acetate as a carbon source under aerobic conditions. The growth parameters are summarized in Table 6.13, based on three different culture conditions. As can be seen in Figure 6.17, the wild-type *E. coli* utilizes glucose for cell growth with accumulation of acetate as the

Published by Woodhead Publishing Limited, 2013

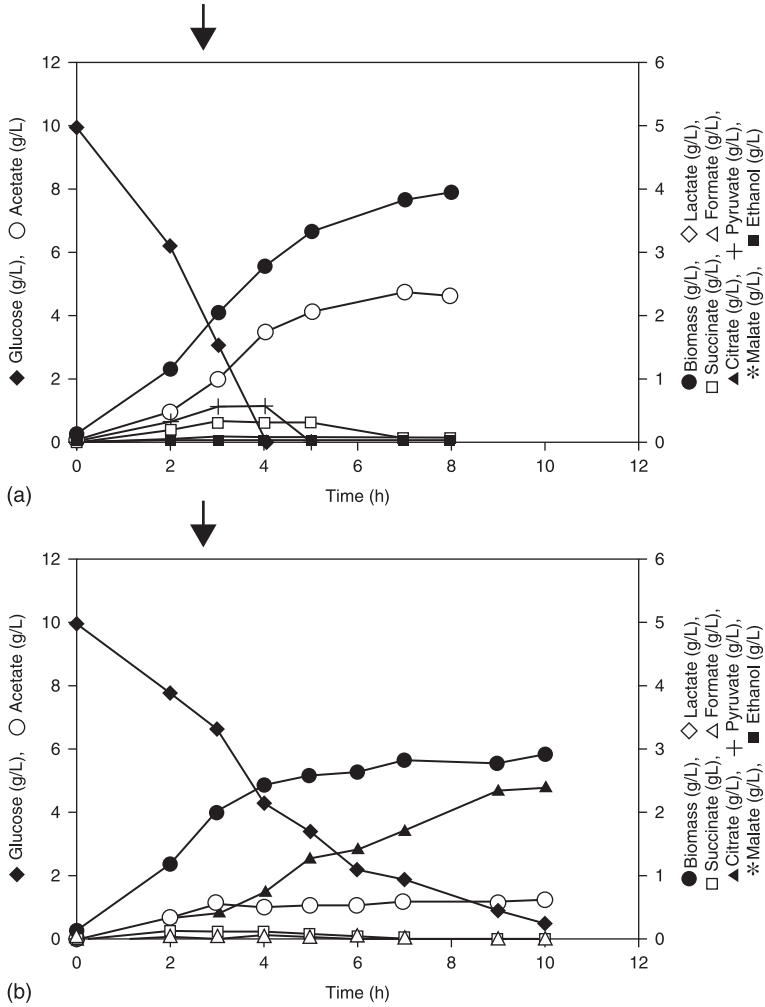

Figure 6.17 **Batch cultivation results of: parent *E. coli*; and (b) *icd mutant*, grown on glucose under aerobic conditions. The arrow indicates the sampling time for proteome analysis and for measurement of enzyme activity**

major by-product (Figure 6.17a), whereas the *icd* mutant consumes glucose for cell growth with slight accumulation of acetate (Figure 6.17b). Moreover, citrate accumulation (~2.40 g/l) is observed in the *icd* mutant. Other organic acids, such as lactate, succinate, formate, pyruvate, malate, and ethanol, are almost negligible in both the *icd* mutant and the parent

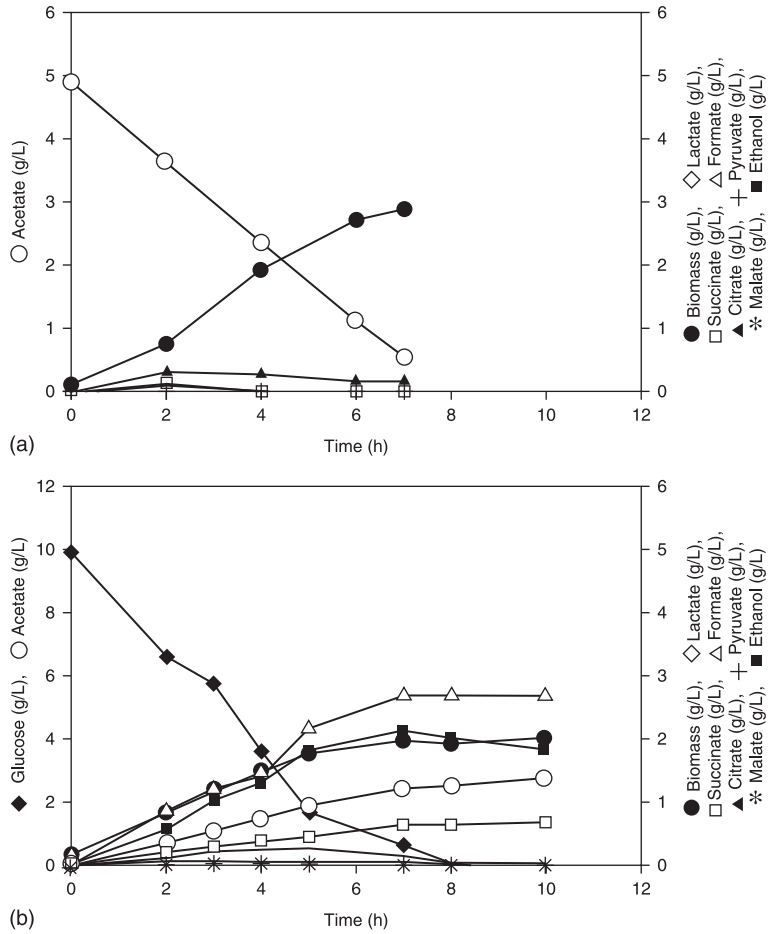

Figure 6.18 **Batch cultivation results of: (a) parent *E. coli*; and (b) *icd mutant*, grown on glucose under microaerobic conditions**

E. coli. Furthermore, the *icd* mutant shows higher specific CO_2 evolution rates (0.16 mM/gDCW/h), which is 60% higher compared to its parent *E. coli* (0.10 mM/gDCW/h) (Table 6.13). However, approximately 27% increase in the biomass yield on glucose is observed in the *icd* mutant compared to that of the parent *E. coli*. When cells are grown on glucose under microaerobic conditions, little difference in fermentation characteristics (Table 6.13) is observed where formate is the main by-product in both the *icd* mutant and the wild type *E. coli* followed by

Published by Woodhead Publishing Limited, 2013

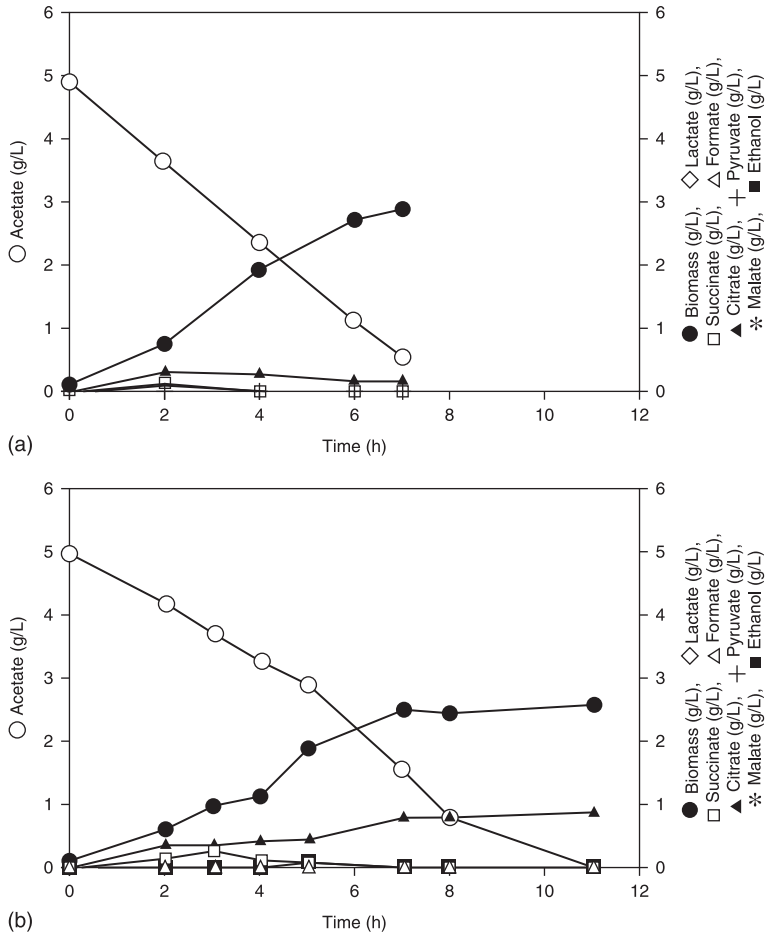

Figure 6.19 Batch cultivation results of: parent *E. coli* (a) and *icd mutant* (b) grown on acetate under aerobic conditions

ethanol, acetate, and succinate (Figures 6.18a,b). No citrate accumulation is observed in the *icd* mutant *E. coli* under microaerobic conditions. Similarly, when acetate is used as a sole carbon source, similar fermentation characteristics are observed between the two strains, except for a slight citrate accumulation in the *icd* mutant (Figures 6.19a,b).

Table 6.14 represents a summary of the mass spectrometry data, including predicted molecular masses, pI values, and protein identification. As shown in Table 6.15, the enzyme activity levels vary significantly in the *icd* mutant compared to the parent. To see how each enzyme activity

Table 6.13 Specific rate of parent and *icd* mutant grown on different carbon sources under different culture conditions. Standard deviations were calculated from four independent measurements (duplicate measurements from duplicate experiments). q_S – specific substrate uptake rate; μ – specific growth rate; $Y_{X/S}$ – biomass yield; q_{Ace} – specific acetate production rate; q_{O2} – specific oxygen uptake rate; qCO_2 – specific carbon dioxide evolution rate

Experiment		qS [g/gDCW/h]	μ [h-1]	$Y_{X/S}$ [gDCW/g substrate]	q_{Ace} [g/DCWg/h]	q_{O2} [mM/gDCW/h]	q_{CO2} [mM/gDCW/h]
Glucose (aerobic)	Parent	1.53(±0.05)	0.44(±0.03)	0.26(±0.04)	0.78(±0.05)	0.14(±0.03)	0.10(±0.03)
	Mutant	0.88(±0.03)	0.34(±0.01)	0.33(±0.02)	0.15(±0.02)	0.17(±0.04)	0.16(±0.01)
Glucose (microaerobic)	Parent	1.58(±0.11)	0.42(±0.06)	0.17(±0.01)	0.56(±0.11)	0.09(±0.02)	0.05(±0.02)
	Mutant	1.32(±0.04)	0.29(±0.05)	0.21(±0.05)	0.59(±0.13)	0.04(±0.01)	0.03(±0.01)
Acetate (aerobic)	Parent	0.33(±0.02)	0.32(±0.07)	0.79(±0.03)	—	0.37(±0.05)	0.29(±0.06)
	Mutant	0.36(±0.05)	0.32(±0.08)	0.79(±0.07)	—	0.29(±0.02)	0.22(±0.01)

is affected, the ratio of enzyme activity is calculated for the *icd* mutant over the corresponding value in the parent strain and the ratio values in the central metabolic map are annotated. Figure 6.20 shows such a metabolic map of *E. coli* grown on glucose under aerobic conditions, where the solid lines indicate up-regulation and the dotted lines represent down-regulation. The thickness of the lines is proportional to the magnitude of the ratio, that is, the thicker the line, the more regulated.

The Pgi and Fba are up-regulated significantly in the *icd* mutant compared to the parent, except Pfk. The two enzymes involved in the oxidative PP pathway, such as G6PDH and 6PGDH, are also affected significantly in the *icd* mutant grown on glucose under aerobic conditions. G6PDH and 6PGDH are increased by 1.77- and 1.42-fold in the *icd* mutant compared to that in the parent, respectively (Table 6.15

Table 6.14 **Summary of MALDI-TOF mass spectrometry data for protein spots showing altered expression levels on 2D gels for parent *E. coli* (WT) and *icd* mutant**

Spot number	Theoretical *pI/Mw* (kDa)	Experimental *pI/Mw* (kDa)	Gene name with protein identity	Abundance (*icd*-/WT) ratio
41	5.26/51.8	5.19/54.7	*glnA (Glutamine synthetase)*	0.161
35	6.05/56.7	6.23/55.9	*trpD (Anthranilate synthase component II)*	0.082
46	6.35/58.2	6.34/54.0	*cydA (Cytochrome BD-I oxidase subunit I)*	0.128
100	5.37/41.4	5.40/42.4	*sucC (Succinyl-CoA synthetase beta chain)*	0.152
103	6.01/41.2	6.03/41.9	*metB (Cystathionine gamma-synthase)*	0.089
115	6.58/35.4	6.72/38.7	*gapA (Glyceraldehyde 3-phosphate dehydrogenase A)*	0.059
123	6.90/36.2	6.89/37.9	*nuoH (NADH dehydrogenase I, chain H)*	0.032
170	5.99/32.2	6.77/32.2	*cyoA (Cytochrome O subunit 2)*	0.142

(*Continued*)

Table 6.14 Summary of MALDI-TOF mass spectrometry data for protein spots showing altered expression levels on 2D gels for parent *E. coli* (WT) and *icd* mutant (*Continued*)

Spot number	Theoretical *pI/Mw* (kDa)	Experimental *pI/Mw* (kDa)	Gene name with protein identity	Abundance (*icd*-/WT) ratio
381	6.31/29.6	6.16/29.8	*sucD (Succinyl-CoA synthetase alpha chain)*	0.071
202	—	6.70/27.1	*not detected*	0.034
210	6.31/26.8	6.80/26.2	*sdhB (Succinate dehydrogenase iron-sulfur protein)*	0.046
316	–	8.01/25.4	*not detected*	0.15
426	–	6.79/24.4	*not detected*	19.118
465	5.40/18.6	5.41/19.6	*nuoE (NADH dehydrogenase I, chain E)*	0.139
510	6.58/16.1	6.40/15.4	*rpiB (Ribose 5-phosphate isomerase B)*	0.159
644	6.56/12.0	6.93/11.8	*cyoD (Cytochrome O ubiquinol oxidase protein cyoD)*	6.305
761	–	6.83/10.6	*not detected*	0.156
616	5.46/14.9	5.42/14.8	*atpC (ATP synthase epsilon chain)*	6.997
498	4.72/19.2	4.59/16.1	*aroL (Shikimate kinase II)*	0.057
606	5.03/17.6	4.97/15.6	*bcp (Bacterioferritin comigratory protein)*	0.071
719	4.71/17.6	4.62/14.4	*greA (Transcription elongation factor greA)*	0.033

and Figure 6.20). The up-regulation of these two enzymes in the *icd* mutant is contrary to the slower growth rates, since both enzymes are known to be growth rate dependent (Wolf et al. 1979; Pease and Wolf, 1994).

Both enzymes G6PDH and 6PGDH in the PP pathway are known to be growth rate dependent. The reason for up-regulation of these

Published by Woodhead Publishing Limited, 2013

Table 6.15 Specific enzyme activities in cell extracts of parent and *icd* mutant grown on glucose under aerobic conditions. The unit of enzyme activity is nM/min/mg protein. Overall ED pathway enzyme was represented as mg pyruvate/min/mg protein. The ratio of enzyme activity was calculated for *icd* mutant over the corresponding value in the parent strain. Therefore, a value of 1.0 indicates no change. The mean value from four independent measurements (duplicate measurements from duplicate experiments) is presented with standard deviation

Enzyme with their corresponding gene name	Parent	*icdA* mutant	Ratio
Glucokinase (*glk*)	257.02 ± 25.13	175.25 ± 23.33	0.66
Phosphoglucose isomerase (*pgi*)	14.99 ± 2.84	31.83 ± 4.51	2.25
Phosphofructose kinase (*pfk*)	105.18 ± 13.09	112.11 ± 15.62	1.05
Fructose diphosphate aldolase (fba)	45.66 ± 17.05	52.14 ± 11.45	1.42
Glyceraldehyde-3-phosphate dehydrogenase (*gapA*)	64.26 ± 13.46	46.5 ± 10.73	0.70
3-phosphoglycerate kinase (*pgk*)	85.49 ± 12.32	82.18 ± 13.68	0.94
Pyruvate kinase (*pyk*)	161.36 ± 21.78	152.46 ± 23.17	0.93
Pyruvate dehydrogenase complex (*aceE, aceF* & *lpdA*)	14.69 ± 3.55	14.72 ± 3.82	0.98
Phosphoenol pyruvate carboxylase (*ppc*)	64.26 ± 5.24	50.07 ± 4.25	0.78
Phosphoenol pyruvate carboxykinase (*pckA*)	28.56 ± 11.37	42.92 ± 8.19	2.02
$NADP^+$-specific malic enzyme (*mae1*)	1.42 ± 1.31	11.8 ± 9.42	21.64
NAD^+-specific malic enzyme (*mae2*)	1.22 ± 1.15	1.25 ± 1.19	0.86
Glucose-6-phosphate dehydrogenase (*zwf*)	71.4 ± 7.81	125.18 ± 12.67	1.77
6-phosphogluconate dehydrogenase (*gnd*)	28.56 ± 9.94	33.98 ± 7.58	1.42
ED pathway enzyme (*edd* & *eda*)	3.64 ± 3.41	3.61 ± 3.43	0.78

(*Continued*)

Table 6.15 Specific enzyme activities in cell extracts of parent and *icd* mutant grown on glucose under aerobic conditions. The unit of enzyme activity is nM/min/mg protein. Overall ED pathway enzyme was represented as mg pyruvate/min/mg protein. The ratio of enzyme activity was calculated for *icd* mutant over the corresponding value in the parent strain. Therefore, a value of 1.0 indicates no change. The mean value from four independent measurements (duplicate measurements from duplicate experiments) is presented with standard deviation (Continued)

Enzyme with their corresponding gene name	Parent	*icdA* mutant	Ratio
Acetate kinase (*ack*)	113.16 ± 19.46	61.51 ± 6.37	0.59
Transhydrogenase (*udhA*, *pntA* & *pntB*)	26.59 ± 6.35	27.13 ± 5.18	1.08
Citrate synthase (*gltA*)	10.12 ± 3.27	38.28 ± 9.48	4.20
Isocitrate dehydrogenase (*icd*)	154.22 ± 26.55	1.43 ± 1.35	0.00
α-Ketog;utarate dehydrogenase complex (*sucA*, *sucB* & *lpdA*)	135.45 ± 24.11	33.19 ± 16.44	0.15
Fumarase (*fumA*)	105.73 ± 22.06	52.11 ± 17.51	0.41
Malate dehydrogenase (*mdh*)	35.56 ± 8.77	77.21 ± 14.74	2.33
Isocitrate lyase (*aceA*)	8.01 ± 2.93	149.65 ± 22.69	24.99
Malate synthase (*aceB*)	2.11 ± 1.73	48.90 ± 38.57	27.18

enzymes in the *icd* mutant may be due to the demand for NADPH, since intracellular NADPH concentrations are much lower in the mutant than in the parent strain (Table 6.16). Moreover, the extent of the regulation of these two enzymes may be accounted for by their

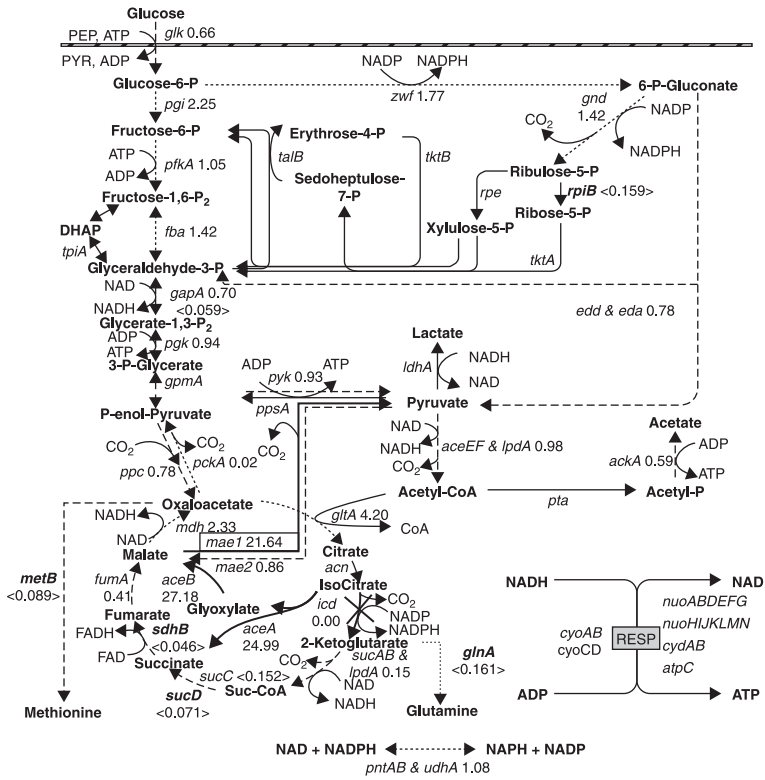

Figure 6.20 Relative protein and enzyme levels of *icd mutant* JW1122 from exponential growth phase in comparison to the parent *E. coli* BW25113 grown on glucose under aerobic conditions. The enzymes are annotated by their gene names. The numbers represent the up-regulation ratios in *icdA* mutant (JW1122) as compared to its parent. The genes with numbers in parentheses indicate the protein abundance ratios deduced from proteome analysis. The solid lines/genes indicate up-regulation, whereas the broken lines/genes for down-regulation.

individual allosteric control. Sugimoto and Shiio (1987) reported that G6PDH was allosterically inhibited by FDP and PRPP, and induced by glucose. However, 6PGDH is inhibited by FDP, PRPP, GAP, Ru5P, E4P, and NADPH, and induced by gluconate. Apparently, the shortage of FDP is facilitated and functions as a major activator to 6PGDH, due to significant up-regulation of Fba activity in the *icd* mutant (Table 6.13 and Figure 6.20). However, the protein encoded by *rpiB* is down-regulated in the *icd* mutant (Table 6.14). *E. coli* hosts two discernible Rpi activities (David and Wiesmeyer, 1970; Esseenberg and Cooper, 1975): a constitutive activity (*rpiA*) that accounts for at least 99% of the total Rpi and an inducible one (*rpiB*). The expression of *rpiB* is very low when cells are grown on complex media, even in the presence of D-ribose. The mode of its regulation is not known, but the involvement of a negative regulator (product of *rpiR*) is more likely (Skinner and Cooper 1971). The significant down-regulation of *rpiB* in the *icd* mutant may be due to inactivation of ICDH, which can efficiently induce *rpiR*, which in turn negatively regulates expression of the *rpiB* protein.

Among the TCA cycle enzymes, CS and MDH are up-regulated significantly in the *icd* mutant *E. coli* compared to its parent strain. It has been revealed that the enzymes at the branch point of the TCA cycle and glyoxylate shunt are regulated in the opposite way (LaPorte and

Table 6.16 **Measurement of intracellular metabolites for parent *E. coli* and *icd* mutant grown on glucose under aerobic conditions. Standard deviations were calculated from four independent measurements (duplicate measurements from duplicate cultures). DCW denotes dry cell weight**

	Concentration [*μM/gDCW*]			Ratio	
	Parent	*icdA⁻ mutant*		*Parent*	*icdA⁻ mutant*
ATP	97.01 ± 13.55	43.05 ± 18.35			
ADP	231.02 ± 11.29	169.07 ± 15.24	ATP/ADP	0.380	0.161
NADH	72.11 ± 9.27	64.03 ± 7.41			
NAD^+	181.15 ± 15.49	28.06 ± 6.76	$NADH/NAD^+$	0.379	2.658
NADPH	83.04 ± 8.32	49.05 ± 3.83			
$NADP^+$	232.06 ± 14.67	196.02 ± 16.52	$NADPH/NADP^+$	0.344	0.252

Published by Woodhead Publishing Limited, 2013

Koshland, 1983; Nimmo and Nimmo, 1984). It is shown that the knockout of the *icd* gene may induce glyoxylate shunt significantly, as is evidenced by the significant up-regulation of Icl and MS activity in the mutant compared to that in the parent strain (Table 6.15 and Figure 6.20).

Anaplerotic enzyme Ppc is down-regulated in the *icd* mutant compared to the parent strain (Table 6.15 and Figure. 6.20). However, Pck is up-regulated in the mutant. The reason may be due to the shortage of PEP in the *icd* mutant. Two other anaplerotic enzymes, such as the NAD^+ and $NADP^+$-specific malic enzymes, are regulated differently in the *icd* mutant. The activity of Mez ($NADP^+$-specific) is up-regulated significantly, whereas Sfc (NAD^+-specific) is down-regulated in the *icd* mutant compared to that in the parent (Table 6.15 and Figure 6.20). Acetate kinase (Ack) activity is down-regulated in the *icd* mutant, a result which is consistent with lower acetate production rates (Table 6.13).

Table 6.15 and Figure 6.20 imply that re-oxidation of the reducing power are more or less balanced in the mutant *E. coli*. The intracellular concentrations of ATP, ADP, NADH, NAD^+, NADPH, and $NADP^+$ are shown in Table 6.16. The intracellular concentrations of these metabolites are lower in the *icd* mutant than those in the parent. However, the NADH/NAD^+ ratio is higher in the *icd* mutant, whereas the ATP/ADP and NADPH/$NADP^+$ ratios are much lower in the mutant than in the parent strain.

Basically, ICDH is involved in the conversion of isocitrate to αKG, with concomitant generation of NAD(P)H and CO_2. Therefore, it is expected that the *icd* mutant can produce less CO_2. However, it is shown that specific CO_2 evolution rates are higher in the *icd* mutant than in the parent strain (Table 6.13). Enzyme activity measurements show that the *icd* gene knockout results in the activation of the glyoxylate shunt that ultimately increases the $NADP^+$-dependent malic enzyme, PckA, and Gnd (6PGDH) activity significantly in the mutant compared to the parent (Table 6.15 and Figure 6.20). This may be why higher CO_2 evolution rates are observed in the *icd* mutant than in the parent strain. The significant up-regulation of CS (GltA) in the *icd* mutant is consistent with other results (Park et al., 1994), where GltA activity levels are inversely proportional to growth rates. The NAD^+-specific malic enzyme is repressed by glucose and inhibition can be released by malate, whereas glucose and AcCoA repress the $NADP^+$-specific malic enzyme. Previous studies have shown that the NAD^+-specific malic enzyme takes part in catabolism of malate, controlling C_4-dicarboxylic acids as well as

amino acids in the cell, while the $NADP^+$-specific malic enzyme supplies AcCoA from MAL via PYR, which is utilized for biosynthesis and maintains the action of the TCA cycle (Murai et al., 1971). By this mechanism, the down-regulation of the NAD^+-specific malic enzyme may explain why the intracellular malate concentrations decrease due to a significant increase of MDH activity in the *icd* mutant (Table 6.15), which diverts more carbon flux from MAL to OAA as compared to the parent strain. The significant up-regulation of the $NADP^+$-specific malic enzyme may be due to the reduced intracellular AcCoA pool, which can relieve the inhibition to this enzyme. This speculation might be reflected by the down-regulation of GAPDH, Pgk, Pyk, PDHc, and Ack activity, which are directly and/or indirectly linked to AcCoA synthesis. The AcCoA pool is expected to decrease, since the entry to the TCA cycle seems to increase in the influx from glycolysis, which is inferred by increased CS (GltA) activity in the *icd* mutant compared to the parent strain (Table 6.15 and Figure 6.20). Moreover, down-regulation of GapA (GAPDH) activity in the *icd* mutant strain may be the effect of lower intracellular NAD^+ concentrations, which have been reported to restrict GAPDH activity in *E. coli* (Seta et al., 1997).

The protein encoded gene *atpC* (ATP synthase) is up-regulated significantly in the *icd* mutant compared to its parent strain (Table 6.14 and Figure 6.20). The reason for up-regulation may be due to lower ATP concentrations and lower ATP/ADP ratios in the *icd* mutant strain (Table 6.16), since the expression of *atpC* does not appear to be subject to substrate or growth rate control (Pedersen et al., 1978; Nielsen, 1984), or to respond to anaerobic or aerobic shifts (Smith and Neidhardt, 1983). A lower ATP/ADP ratio is responsible for a lower growth rate in the *icd* mutant than in the parent *E. coli*, since Brian et al. (2002) have shown that growth rates of the cells are modulated by the intracellular ATP/ADP ratio, i.e. the ATP/ADP ratio is proportional to cell growth rate. This result indicates that the *icd* mutant gains enough energy for growth that ultimately reduces specific growth rates in the *icd* mutant strain. Moreover, significant down-regulation of the proteins encoded by genes *nuoE*, *nuoH*, *cydA*, and *cyoA* is consistent with lower ATP, ADP, NADH, and NAD^+ concentrations, respectively (Table 6.16), in the *icd* mutant than in the parent strain, indicating that the *icd* gene knockout significantly affects the respiratory system and electron transport chain. Therefore, compensation of cellular respiratory components can be mediated by the protein encoded gene *cyoD*, which is up-regulated significantly in the *icd* mutant compared to the parent strain (Table 6.14 and Figure 6.20).

Published by Woodhead Publishing Limited, 2013

Down-regulation of the protein encoded genes *glnA*, *sucC*, *sucD*, *sdhB*, and *metB* in the *icd* mutant compared to the parent strain (Table 6.14 and Figure 6.20) may be due to the effects of *icd* gene deletion. Moreover, significant down-regulation of the protein encoded genes *trpD*, *aroL*, *bcp*, and *greA* in the *icd* mutant are also observed in Table 6.14. Down-regulation of the *trpD* gene encoding protein in the *icd* mutant might be the effect of the Trp repressor. The *E. coli* Trp repressor is one of the smallest proteins that shows sequence-specific DNA binding and is also allosterically controlled (Somerville, 1992), and this protein has been studied extensively by physical as well as genetic methods, yet its mode of DNA recognition remains controversial. It is of particular interest, as it binds to five diverse sequences in the *E. coli* genome. Four of these sequences are in promoters, in the *trpEDCBA* operon (Rose et al., 1973; Bennett et al., 1976), the *trpR* gene (Gunsalus and Yanofsky, 1980; Kelley and Yanofsky, 1982), the *aroH* gene (Zurawski et al., 1981; Grove and Gunsalus 1987), and the *mtr* gene (Heatwole and Somerville, 1991; Sarsero et al., 1991), respectively. The fifth site is within the leader region of the *aroL* gene (Heatwole and Somerville, 1992; Lawley and Pittard, 1994). These five operons control the biosynthesis and uptake of the amino acid tryptophan. The repressor binds to the operators only in the presence of tryptophan, repressing gene expression, hence controlling the intracellular level of its co-repressor. Consequently, significant down-regulation of the *aroL* gene encoding protein is reasonable in the *icd* mutant compared to the parent, since higher tryptophan synthesis is expected in the *icd* mutant strain as a compensatory function due to blockage of the *icd* pathway in the TCA cycle.

Furthermore, bacterioferritin co-migratory protein encoded gene *bcp* is down-regulated significantly in the *icd* mutant compared to the parent strain (Table 6.14). This result indicates that *E. coli* lacking the *icd* gene is less efficient to protect against toxicity of reactive oxygen species (ROS), since *E. coli* bacterioferritin co-migratory protein (BCP) has been categorized as a new member of the thiol-specific antioxidant protein (TSA)/alkyl hydroperoxide peroxidase C (*ahpC*) family, because BCP exhibits thioredoxin-dependent hydroperoxide peroxidase activity (Jeong et al., 2000). This might be another reason for lower growth rates of the *icd* mutant than in the parent strain grown on glucose (Table 6.13). However, the function of BCP has not yet been fully clarified, despite the wide distribution of BCP in most pathogenic bacteria, including *Haemophilus influenzae, Helicobactor pylori*, and *Mycobacterium tuberculosis*. Down-regulation of the protein encoded gene *greA* (transcription elongation factor) in the *icd* mutant indicates that

inactivation of ICDH greatly affects the regulation of transcription elongation and cleavage, since *greA* stimulates intrinsic nucleolytic activity of RNA polymerase (RNAP) and also has a role on RNA hydrolysis, which includes transcription proofreading, suppression of transcriptional pausing and arrest, and facilitation of RNAP transition from transcription initiation to transcription elongation (Fish and Kane, 2002).

6.8 Effect of *pfl* gene knockout on metabolism

In the case of anaerobic or microaerobic cultivation, NADH regeneration and ATP formation control metabolic fluxes at the branch points, such as PEP, PYR, and AcCoA (Zhu and Shimizu, 2004). As a result, the *pflA,B* gene knockout causes over-production of lactate (Zhu and Shimizu, 2004, 2005). Figure 6.21 shows the fermentation results of *E. coli* BW25113 and *E. coli pfl*B mutant grown on glucose. It indicates that the fermentation patterns of these two strains are similar under aerobic conditions, where the *E. coli pfl*B mutant produces less acetate. However, under microaerobic conditions (Figure 6.22), the results are different, and the *pfl*B mutant strain shows an almost homolactic acid fermentation as compared to that of *E. coli* BW25113. The concentrations of acetate and formate are about 3 g l^{-1} in the parent strain. However, no formate is detected in the culture of the *pfl*B mutant, and the acetate concentration is kept low at about 0.2–0.3 g l^{-1}. A similar fermentation pattern is found in the *pfl*A mutant (JW0885). Two other mutant strains, *pfl*C and *pfl*D, are also cultivated under microaerobic conditions, where the fermentation patterns of these two mutants are similar to that of the parent strain.

Specific glucose uptake rates and metabolite formation rates in these cultures are compared in Figure 6.23. It indicates that the glucose uptake rate is higher in the *pfl*B and *pfl*A mutants than in the parent strain, under either aerobic or microaerobic conditions. The lactate formation rate of the mutant strains of *pfl*A and *pfl*B is about 70-fold higher than in the parent strain. This results in the high yields of lactate production of more than about 70% from glucose (Figure 6.24B).

The *pfl*A mutant is also cultivated using several other carbon sources, i.e. gluconate, pyruvate, fructose, and glycerol, under microaerobic conditions. The results are shown in Tables 6.17 and 6.18. When using glucose as a carbon source, the *pfl*A mutant shows extensive homolactic

Published by Woodhead Publishing Limited, 2013

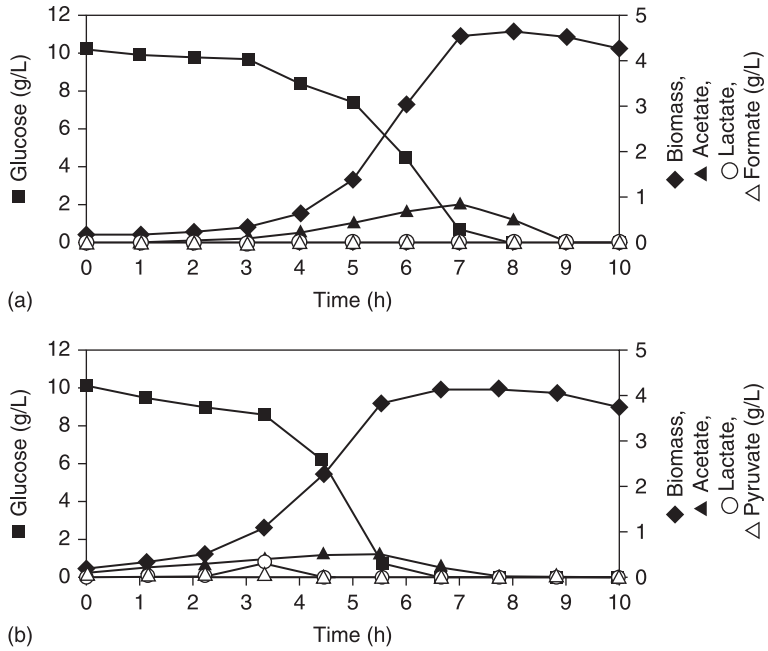

Figure 6.21 **The cultivation results of: (a) *E. coli* BW25113; and (b) the *pfl*B⁻ mutant (B) grown on glucose under the aerobic conditions. A *E. coli* BW25113, B *E. coli* *pfl*B⁻ mutant. ■ Glucose, ◆ biomass, ○ lactate, ▲ acetate, Δ formate, ◇ pyruvate**

acid fermentation in the microaerobic culture. However, a large amount of acetate is produced together with lactate, when gluconate or pyruvate is used as a carbon source. In particular, acetate instead of lactate is the major product when pyruvate is used as a carbon source. The fermentation patterns, when using fructose or glycerol as a carbon source, are similar to those when using glucose. However, fructose and glycerol uptake rates are significantly lower than glucose uptake rates (Table 6.17), and the lactate yields vary from 60% to more than 70% (Table 6.18). Succinate concentration is always very low. For the *pfl*A and *pfl*B mutants, the specific growth rate is lower under microaerobic conditions, especially when using glycerol as a carbon source.

Pfl activities in BW25113, *pfl*A, *pfl*B, *pfl*C, and *pfl*D mutants, using glucose as a carbon source under microaerobic conditions, are shown in Figure 6.25. It can be seen that Pfl is inactivated in *pfl*A and *pfl*B mutants.

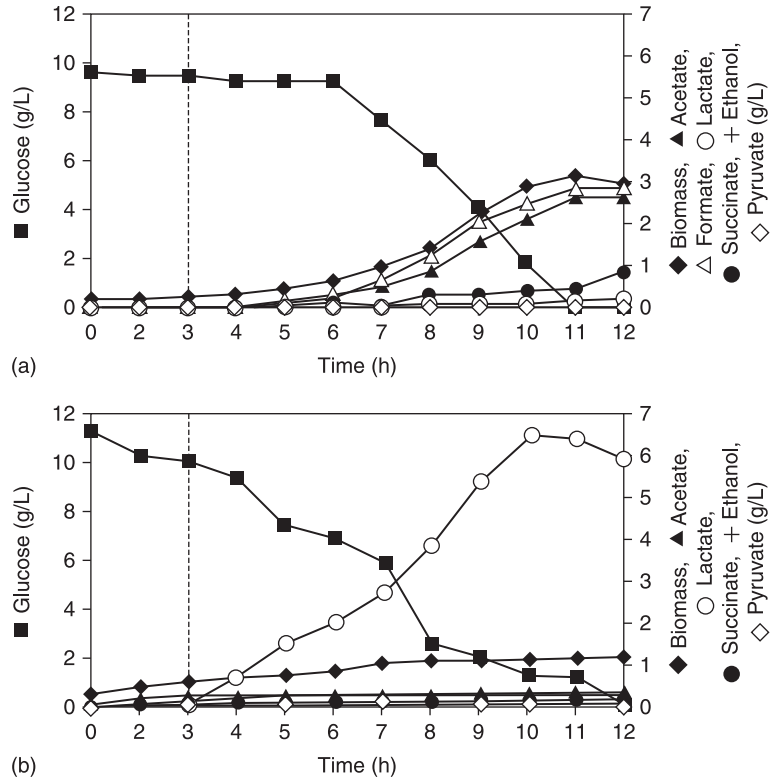

Figure 6.22 **The cultivation results of: (a) *E. coli* BW25113; and (b) the *pfl*B⁻ mutant, grown on glucose under the microaerobic conditions. The dotted line indicates the time when the culture was shifted from the aerobic conditions to the microaerobic conditions. A *E. coli* BW25113, B *pfl*B⁻ mutant. ■ Glucose, ◆ biomass, ● succinate, ○ lactate, ▲ acetate, △ formate, ◇ pyruvate, + ethanol**

However, Pfl activity in *pfl*C and *pfl*D mutants is comparable to those in the parent strain. The enzyme activities of the strains *E. coli* BW25113, and *pfl*A and *pfl*B mutants, grown on glucose under microaerobic conditions, are shown in Figure 6.26. The enzyme activity indicates that glycolytic enzymes, such as GAPDH and Pyk, are up-regulated in the *pfl*A and *pfl*B mutants as compared to the parent strain. By comparing the higher glucose uptake rates in the mutant strains, it can be seen that

Published by Woodhead Publishing Limited, 2013

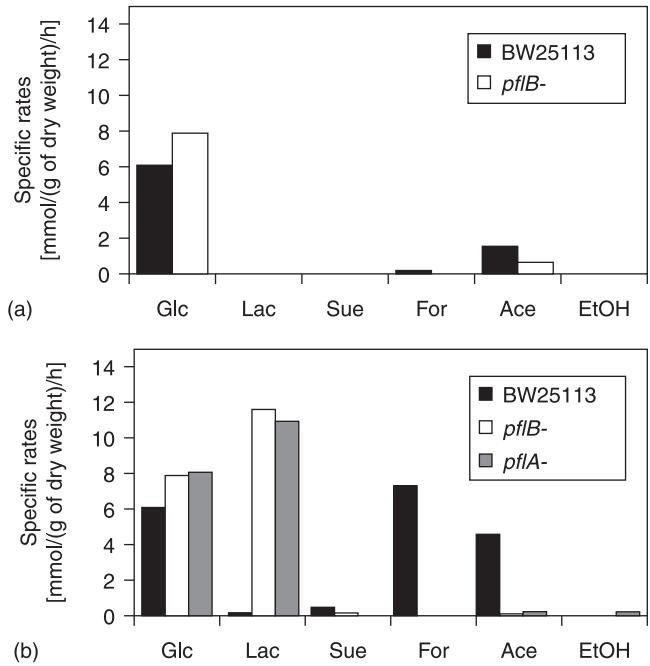

Figure 6.23 **The specific glucose uptake rates and the specific product formation rates for: (a) the aerobic conditions; and (b) the microaerobic conditions. *Glc* Glucose uptake rate; *Lac* lactate production rate; *Suc* succinate production rate; *For* formate production rate; *Ace* acetate production rate; *Etoh* ethanol production rate**

the glycolytic flux increases in the mutants. Higher glycolytic flux may be used to fulfill energy requirements. To maintain the glycolytic flux, PYR has to be assimilated, and the NADH produced by GAPDH must be reoxidized to NAD^+. LDH activity is 3-fold higher in the *pfl*A mutant, which is consistent with the higher lactate production. Another metabolic enzyme, ADH, is also slightly up-regulated for the mutants as compared to the parent strain. It is interesting to see that the activities of Ppc and Ack increase more than 100-fold in the mutants, suggesting that these two enzymes play important roles in the microaerobic growth of these two mutants. Ppc is the first enzyme for succinate production. Based on the activity of this enzyme, significant succinate production is expected in *pfl*A and *pfl*B mutants. However,

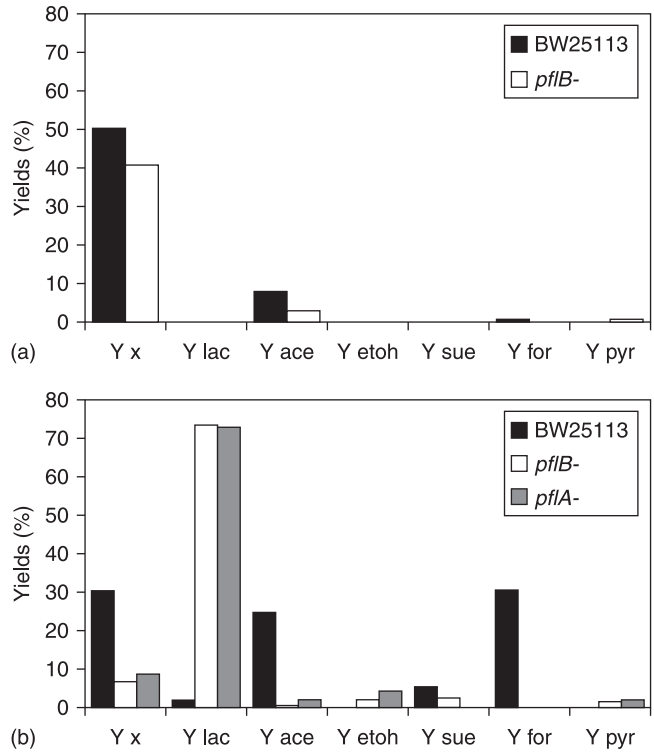

Figure 6.24 Biomass and metabolite yields on glucose for: (a) the aerobic conditions; and (b) the microaerobic conditions. Y_x Biomass yield on glucose; Y_{lac} lactate yield; Y_{ace} acetate yield; Y_{etoh} ethanol yield; Y_{suc} succinate yield; Y_{for} formate yield; Y_{pyr} pyruvate yield

Table 6.17 The specific carbon source uptake rates and product formation rates for the *E. coli pfl*A mutant using different carbon sources under microaerobic conditions. *q* is the specific rate calculated as the average rate during the exponential growth phase

Carbon source	*q* *(mmol (g dry weight)$^{-1}$ h^{-1}) for:					
	Substrate	Lactate	Succinate	Formate	Acetate	Ethanol
Glucose	8.15	11.01	0.0	0.0	0.27	0.2
Gluconate	6.57	8.22	0.21	0.0	5.63	0.32
Pyruvate	6.87	1.78	0.25	0.0	4.58	0.11
Fructose	3.21	4.42	0.0	0.0	0.23	0.0
Glycerol	1.33	0.83	0.0	0.0	0.05	0.0

Published by Woodhead Publishing Limited, 2013

Table 6.18 The yields (*Y*) of cell mass (*x*) and metabolites for different carbon sources for the *E. coli pfl*A mutant grown under microaerobic and the anaerobic conditions. *AN* – The *pfl*A mutant grown on glucose under anaerobic conditions filled with CO_2. *Y* values were calculated based on data in the exponential growth phase

Carbon source	Yields on carbon source (g g^{-1})%						
	$Y_{x/s}$	$Y_{lactate/s}$	$Y_{acetate/s}$	$Y_{ethanol/s}$	$Y_{succinate/s}$	$Y_{formate/s}$	$Y_{pyruvate/s}$
Glucose	8.1	72.5	1.1	3.8	0.0	0.0	1.1
Gluconate	8.1	57.4	26.2	1.1	1.9	0.0	1.0
Pyruvate	5.9	26.5	45.4	0.2	1.3	0	–
Fructose	9.7	69.0	3.7	0.0	0.0	0.0	1.2
Glycerol	0.0	61.1	2.6	0.0	0.0	0.0	0.0
Glucose (AN)	6.7	48.2	0.6	–	3.6	0.0	–

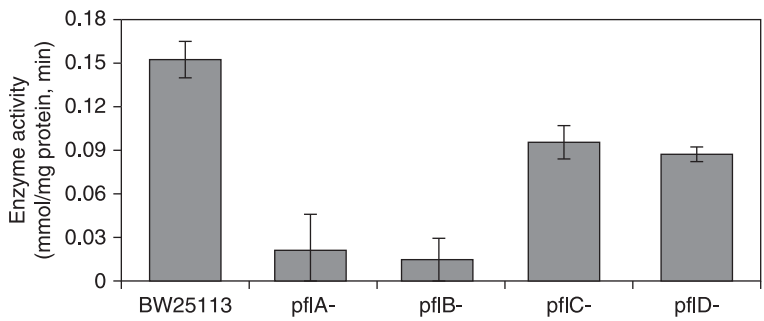

Figure 6.25 The pyruvate formate lyase activities of *E. coli pfl* mutants and the parent strain *E. coli* BW25113

succinate production is even lower in the mutant strains. One possible reason may be due to a CO_2 shortage in the microaerobic cultivation of the mutants, since CO_2 is required for the Ppc reaction to form OAA. By supplying CO_2, succinate production is slightly increased in the *pfl*A mutant (Table 6.18). However, it is still lower than that in the parent strain. Therefore, the shortage of PEP may be the most plausible reason for the lower succinate production.

Enzyme activities are also assayed for the *pfl*A mutant grown on different carbon sources (Table 6.19). Enzyme activities of GAPDH and LDH show almost the same behavior, which means that higher LDH

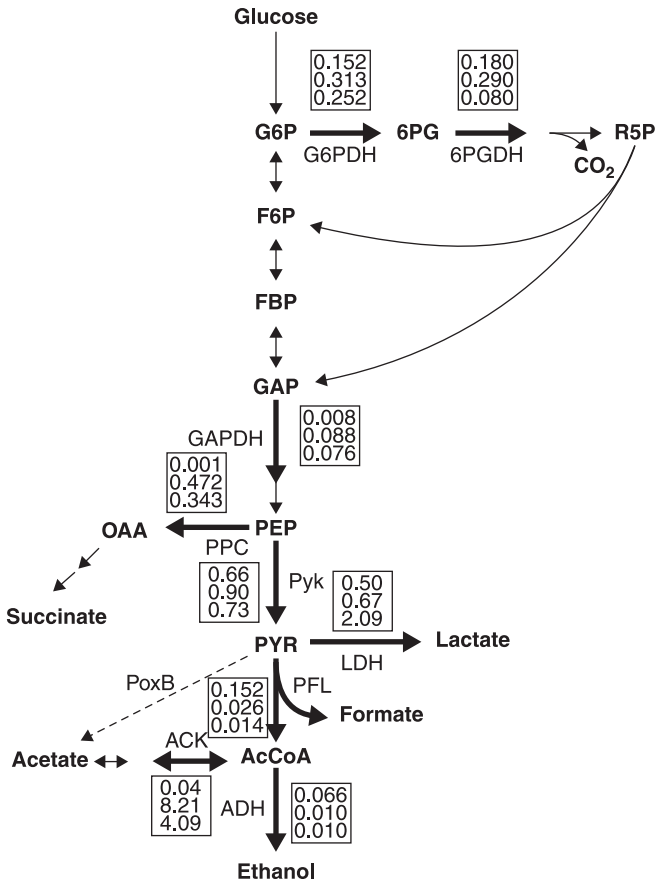

Figure 6.26 **Enzyme activities for strains grown on glucose in the microaerobic conditions. The values in the *boxes* show enzyme activities. First row *E. coli* BW25113; second row *pfl*Bmutant; *third row pfl*A mutant. The *red lines* indicate the up-regulation of the enzymes of *pfl*A and *pfl*B mutants, compared to that of the parent strain**

activity causes higher GAPDH activity when using different carbon sources, implying a coupling between these two enzymes. Another interesting phenomenon is that Ack activity varies dramatically, depending on the carbon source. Compared to using glucose as a carbon source, Ack activity is about 10-fold higher in cells using gluconate or PYR as a carbon source, while this enzyme activity is reduced 50- to 100-fold when using glycerol or fructose as a carbon source. Ppc activity is highest when using

Published by Woodhead Publishing Limited, 2013

Table 6.19 Enzyme activities for the *E. coli pfl*A mutant grown on different carbon sources in the microaerobic conditions

Carbon source	Enzyme activity (mmol (mg protein)$^{-1}$ min^{-1})							
	G6PDH	6PGDH	GAPDH	PYK	LDH	PPC	ACK	ADH
Glucose	0.252±0.019	0.080±0.003	0.076±0.003	0.73±0.04	2.09±0.12	0.343±0.032	4.09±0.77	0.010±0.001
Gluconate	0.449±0.02	0.244±0.009	0.126±0.005	0.90±0.04	4.38±0.42	0.084±0.010	38.15±2.5	ND
Pyruvate	0.264±0.019	ND	ND	ND	0.42±0.04	ND	39.82±2.8	ND
Fructose	0.170±0.019	0.066±0.004	0.030±0.006	0.88±0.09	0.6±0.07	0.013±0.001	0.036±0.006	0.015±0.002
Glycerol	0.141±0.013	0.098±0.005	0.026±0.002	0.44±0.03	0.52±0.10	0.025±0.002	0.072±0.009	0.006±0.001

glucose as a carbon source, but it is significantly lower when using fructose or glycerol as a carbon source. ADH activity is low when using fructose, glycerol, gluconate, glucose, or PYR as the carbon source.

Table 6.20 shows the intracellular metabolite concentrations for the three strains grown on glucose in aerobic and microaerobic conditions. In aerobic conditions, intracellular FDP(FBP) and PYR are significantly accumulated in the *pfl*B mutant, where the intracellular FBP concentrations increase to 35.89 μ mol (g dry weight)$^{-1}$, while PYR increase to 34.60 μ mol (g dry weight)$^{-1}$. Under microaerobic conditions, ATP/AMP ratios in the *pflA* and *pflB* mutants are significantly lower than in the parent strain. This suggests that the mutant strains require more ATP than the parent strain. Intracellular FBP and PYR concentrations are significantly increased and the NADH/NAD$^+$ ratios are 4- to 7-fold higher compared to those in the parent strain (Zhu and Shimizu, 2004).

Table 6.21 shows intracellular metabolite concentrations in the *pfl*A mutant grown on different carbon sources under microaerobic conditions. It indicates that the intracellular PYR concentrations are related to FBP concentrations. When using PYR as a carbon source, the high intracellular PYR concentrations are found together with high FBP concentrations, which are 10-fold higher than when using glucose as a carbon source. The NADH/NAD$^+$ ratio is highest when using glycerol as a carbon source and this ratio is relatively low when using gluconate or PYR as a carbon source.

Production of pure D-lactate using the *E. coli pfl* mutant strain has been reported (Pascal et al., 1981; Zhou et al., 2003), and the main characteristics are shown in Figure 6.27. The *pfl* gene knockout blocks the main PYR assimilation pathway under microaerobic or anaerobic conditions. This mutant may cause the shortage of AcCoA. In *E. coli*, the Ack–Pta pathway is related to the AcCoA pool. This pathway has two directions. One direction is to excrete acetate and produce 1 mol ATP. The other direction is to utilize acetate by consuming 1 mol ATP to produce intracellular AcCoA (Brown et al., 1977; Kumari et al., 2000). Since AcCoA formation through Pfl is deficient in the two *pfl* mutants, Ack–Pta reactions may occur in the direction of forming AcCoA using acetate and ATP for biomass formation. This may be the reason why Ack activity is up-regulated in the *pfl*A and *pfl*B mutants under microaerobic conditions (Figure 6.26).

Since ATP can only be generated through glycolysis in oxygen-limited conditions, and it is known that the glycolytic flux is controlled by the demand for ATP (Koebmann et al., 2002), glycolysis has to show a stepping-up to fulfill the energy requirement in microaerobic or anaerobic conditions. In the *pfl* gene-knockout cells, energy generation is further reduced since the cell cannot use Ack to produce ATP through acetate

Published by Woodhead Publishing Limited, 2013

Table 6.20 Intracellular metabolite concentrations in cells grown on glucose

Metabolite	Intracellular concentration [μ mol (g dry weight)$^{-1}$ cell^{-1}]				
	Aerobic conditions		Microaerobic conditions		
	Wild	*pfl*B	Wild	*pfl*B	*pfl*A
G6P	0.591±0.001	0.753±0.050	0.049±0.009	0.133±0.020	1.093±0.006
FBP	1.347±0.010	35.89±0.12	4.593±0.021	41.32±0.11	16.41±0.11
PEP	1.35±0.30	0.67±0.11	0.32±0.12	0.84±0.14	0.12±0.04
PYR	0.53±0.01	34.60±0.20	8.21±0.01	67.97±0.20	25.49±0.01
AcCoA	0.144±0.006	0.012±0.001	0.066±0.002	0.070±0.001	0.050±0.001
ATP	0.375±0.015	0.442±0.045	0.087±0.013	0.044±0.014	0.052±0.012
ADP	1.253±0.014	0.922±0.011	0.380±0.006	0.342±0.006	0.195±0.010
AMP	0.392±0.010	0.515±0.012	0.214±0.006	0.193±0.006	0.197±0.004
NADH	0.026±0.001	0.028±0.005	0.018±0.002	0.029±0.003	0.056±0.001
NAD^+	0.018±0.002	0.312±0.002	0.143±0.001	0.050±0.001	0.060±0.002
ATP/AMP	0.957	0.858	0.407	0.228	0.264
$NADH/NAD^+$	1.44	0.09	0.13	0.58	0.93

Table 6.21 Intracellular metabolite concentrations in the *E. coli pfl*A mutant grown on different carbon sources in microaerobic conditions

Metabolite	Intracellular concentration [μ mol (g dry weight)$^{-1}$ cell^{-1}]				
	Glucose	Gluconate	Pyruvate	Fructose	Glycerol
G6P	1.093±0.006	0.123±0.001	0.120±0.001	0.240±0.001	0.045±0.003
FBP	16.41±0.11	27.08±0.10	164.9±2.7	28.92±0.04	33.02±0.04
PEP	0.12±0.04	0.22±0.11	0.50±0.13	0.45±0.13	0.10±0.05
PYR	25.49±0.01	41.81±0.70	250.6±0.85	47.22±0.50	52.98±0.30
AcCoA	0.050±0.001	0.003±0.001	0.039±0.004	0.132±0.035	0.037±0.001
ATP	0.052±0.012	0.008±0.004	0.034±0.011	0.027±0.006	0.056±0.026
ADP	0.195±0.010	0.143±0.003	0.835±0.011	0.458±0.092	0.531±0.091
AMP	0.197±0.004	0.226±0.007	0.932±0.049	0.127±0.013	0.499±0.006
NADH	0.056±0.001	0.032±0.002	0.016±0.002	0.092±0.012	0.085±0.020
NAD^+	0.060±0.002	0.046±0.001	0.032±0.001	0.244±0.003	0.037±0.001
ATP/AMP	0.264	0.035	0.036	0.213	0.112
$NADH/NAD^+$	0.93	0.7	0.5	0.38	2.3

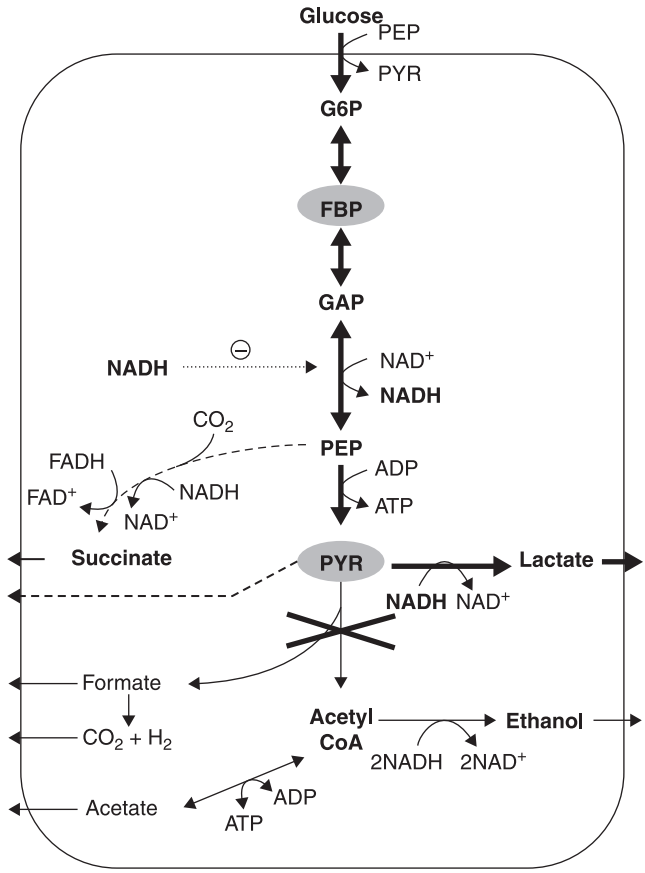

Figure 6.27 **Metabolic regulation mechanisms of lactate production in *E. coli pfl*A and *pfl*B mutants**

formation under microaerobic conditions. However, the up-regulated Pta–Ack pathway consumes more ATP to form AcCoA. This results in a considerably lower ATP/AMP ratio in the cell than in the parent strain (Table 6.20). The energy requirement will further promote glycolytic flux, which is reflected by the higher glucose uptake rate in the *pfl* mutant under microaerobic conditions (Figure 6.23b).

During glycolysis, the reaction through GAPDH produces NADH. This NADH must be regenerated to maintain the glycolytic flux, which is essential for ATP generation. In aerobic conditions, this regeneration can be achieved by the respiratory chain. However, the NAD^+ can only be regenerated through fermentative pathways in the anaerobic conditions in *E. coli*. However, PYR produced from glycolysis has to be assimilated.

Several pathways can be used to maintain the stoichiometric balance and the intracellular redox balance; one of these is to produce ethanol through ADH. However, this pathway needs AcCoA, which is not present in sufficient amounts in the *pfl* mutant strains.

Another pathway is to produce succinate through Ppc and the reducing arm of the TCA cycle. Succinate production is attained by using 1 mol of NADH and 1 mol of $FADH_2$, which is favorable from a redox balance point of view. Note that the reaction through Ppc requires PEP as well as CO_2, which may limit the flux through this pathway for *pfl* mutants. With supplementation of CO_2 in the medium, succinate production is slightly enhanced but not as much as expected (Table 6.18), which indicates that the Ppc reaction is not mainly limited by CO_2. The reactions through Ppc, Pyk, and PTS, as well as cell synthesis, compete for PEP as the substrate. Note that the reaction through Pyk produces 1 mol ATP, and PTS is essential for energy generation. It can be seen that the enzyme activity of both Ppc and Pyk increases in the mutants as compared to the wild type (Figure 6.26). The low succinate production through Ppc indicates that ATP demand is favored over intracellular redox balance. This is consistent with the previous reports, indicating that instead of the amplification of Ppc, introduction of an exogenous PYR carboxylase or malic enzyme into *E. coli* can significantly improve succinate production under anaerobic conditions, since Pyc is not competitive with Pyk and PTS in such a case (Gokarn et al., 1998, 2000; Hong and Lee, 2001; Vemuri et al., 2002).

Another possibility is that PYR can be directly excreted, but this is unfavorable from the intracellular redox balance point of view. The accumulated PYR will allosterically activate LDH. Finally, the *E. coli pfl* mutant uses LDH exclusively to regenerate NAD^+. In conclusion, glycolysis is promoted by *pfl* mutation under microaerobic conditions due to the energy requirement for cell growth, and lactate production is enhanced from the points of stoichiometric balance and intracellular redox balance to maintain glycolysis.

It is shown that PYR and FBP are significantly accumulated in *pfl*A mutants, when using different carbon sources. PYR accumulation may be considered as the result of *pfl* knockout, since Pfl is the main PYR assimilation pathway under microaerobic conditions. As previously discussed, the *pfl* gene-knockout results in a significantly higher intracellular $NADH/NAD^+$ ratio. Since GAPDH is competitively inhibited by NADH (Garrigues et al., 1997), FBP cannot be adequately assimilated through glycolysis, thus the intracellular FBP concentrations are high.

Published by Woodhead Publishing Limited, 2013

The NADH/NAD^+ ratio also affects the metabolite production pattern (Riondet et al., 2000). Since most of the NADH is produced by the reaction through GAPDH, NADH production is variable when using different carbon sources. It is clear that the cell will produce less NADH when using gluconate or PYR as a carbon source. This is confirmed by the lower NADH/NAD^+ ratio when using gluconate or PYR as a carbon source than when using glucose (Table 6.21). The activity of GAPDH is significantly higher when using gluconate as a carbon source (Table 6.19), which indicates the partial release of NADH inhibition on this enzyme. Correspondingly, the lactate yields, when using gluconate or PYR, are lower, which again confirms that lactate production in *pfl* mutants is promoted by the intracellular redox balance.

The results using gluconate or pyruvate as a carbon source may also be distinguished from those using other carbon sources, because of the significantly lower ATP/AMP ratio in the *pfl*A mutant (Table 6.21), which is less than one-seventh of that when using glucose as a carbon source. One reason may be due to the difference in the metabolic networks used; when using gluconate as a carbon source, some of the carbon atoms will go directly to PYR through the Entner-Doudoroff pathway, which reduces the flux through glycolysis where ATP is generated. The other reason may be due to the activation of Ack. It should be noted that the activity of Ack is up-regulated about 10-fold when using gluconate or pyruvate as a carbon source. As previously discussed, the Ack–Pta pathway will occur in the direction of AcCoA synthesis. It may utilize ATP for this pathway to form AcCoA, and finally result in a lower ATP/AMP ratio. There is significant acetate production when using gluconate or PYR as a carbon source. One possibility is that some other back-up systems of Pfl are used to produce AcCoA using PYR. However, since there was no formate detected in the medium, and at the same time the CO_2 concentration in the effluent gas is not higher than the parent strain, the acetate may not be produced from the Ack–Pta pathway. The other possibility may be the activation of PoxB, which is shown to have some relationship with Ack (Abdel-Hamid et al., 2001). When PoxB is inactivated, Ack activity is also relatively low. However, the activity of Ack increases several-fold when PoxB is activated and the increase is 13- to 20-fold in the PDH-E1P-null strains. Consistent with this research, the significant induction of Ack in the *pfl*A mutant may be related to the activation of PoxB, which produces acetate and the cell utilizes the Ack–Pta pathway to supplement the AcCoA pool. In comparison, Ack activity is much lower when using glycerol as a carbon source. Considering the significantly

higher NADH/NAD^+ ratio when using glycerol, the result suggests that the redox balance is less important for metabolism.

6.9 Effect of *ldhA* gene knockout on metabolism

When *E. coli* converts sugars to pyruvate under anaerobic conditions, two major alternative pathways exist for the formation of terminal fermentation products from PYR. The first pathway involves the conversion of PYR to AcCoA and formate by the enzyme Pfl (Gottschalk, 1985). Subsequently, AcCoA is transformed to an approximately equal mixture of ethanol and acetate (Stokes, 1949). The other alternative pathway involves the direct conversion of PYR to lactate in a single step by means of LDH (Tarmy and Kaplan, 1968a,b). The conversion of L- or D-lactate to PYR is catalyzed by two separate isomer-specific flavoproteins, which are often called LDHs but better regarded as lactate oxidases. Basically, *E. coli* has two such enzymes to use when lactate is the sole carbon source and when oxygen or nitrate is available as terminal electron acceptors (Haugaard, 1959; Kline and Mahler, 1965). These flavoproteins are in fact membrane-bound components in the electron transport chain. The conversion of pyruvate to lactate under anaerobic conditions is catalyzed by the third enzyme, LDH, which is a soluble and NADH-linked enzyme, and produces D-lactate (Tarmy and Kaplan, 1968a,b). The fermentative LDH has been purified, is allosterically activated by its substrate PYR, and is induced approximately 10-fold in anaerobically grown cultures at acidic pH (Tarmy and Kaplan, 1968a,b).

Mutants deficient in the fermentative NAD-linked LDH have been studied (Mat-Jan et al., 1989). It is shown that *ldhA* mutants have little effect on cell growth, and convert sugars to a variety of other metabolites. The mutants are tested for aerobic and anaerobic growth on a variety of sugars, such as glucose, fructose, maltose, rhamnose, xylose, sorbitol, and gluconate in minimal medium and the results are almost identical. However, introduction of plasmids carrying *ldhA* genes into the *ldhA* mutant and parent *E. coli* have also been studied (Yang et al., 1999). Over-expression of LDH in the parent strain increases the lactate synthesis rate from 0.19 to 0.40 mM/g/h, when LDH activities increase from 1.3 to 15.3 units. Even an increase of more than 10 times in the LDH activity fails to divert a large fraction of the carbon flux to lactate; the majority of the flux is channeled

Published by Woodhead Publishing Limited, 2013

through the AcCoA branch. Here, the effect of the *ldhA* gene knockout on metabolism of *E. coli* under anaerobic conditions is explained (Figure 6.28).

Both *E. coli* BW25113 and its *ldhA* mutant (JW1375) are cultivated anaerobically on glucose as a sole carbon source (Kabir et al., 2005). Batch cultivation results for both strains grown on glucose under

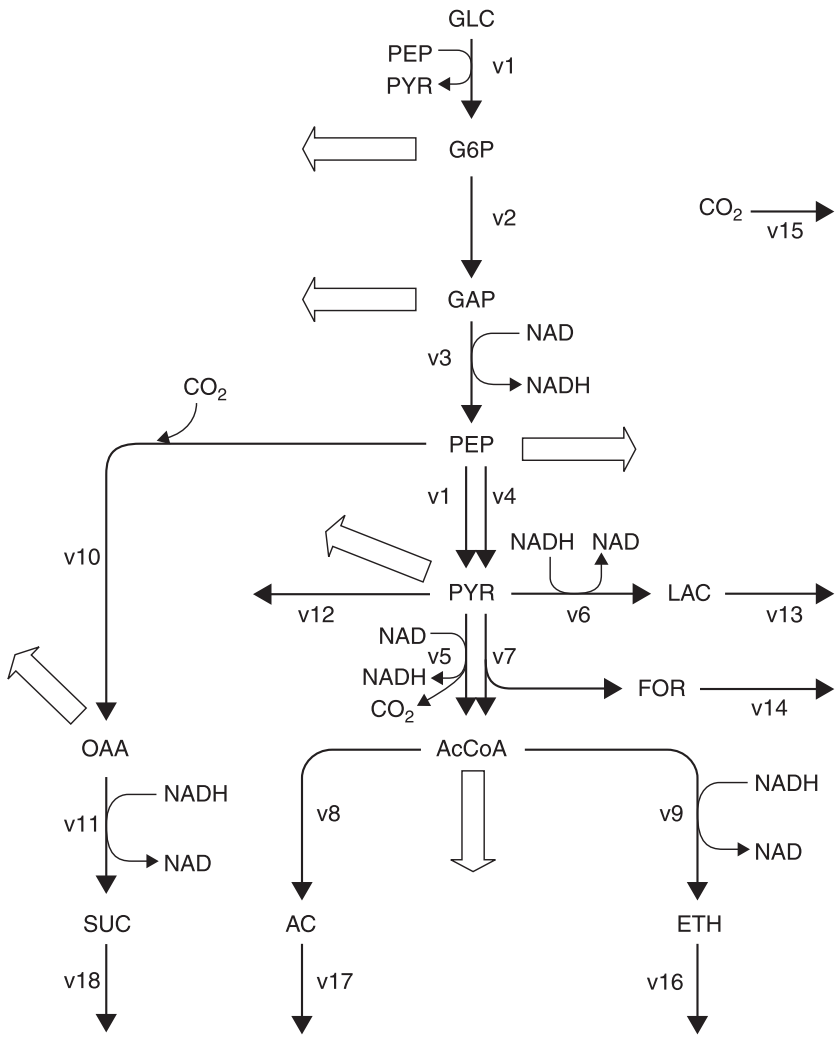

Figure 6.28 **Fermentative pathways of *E. coli* grown on glucose. ⇨ indicates biomass formation flux. The fluxes through each pathway are designated v_1 through v_{18}**

anaerobic conditions are shown in Figure 6.29. Growth parameters at the exponential growth phase are shown in Table 6.22. The growth rate of the *ldhA* mutant is slightly lower (13.33% decrease) at a lower glucose consumption rate compared to the parent strain. However, the biomass yield on glucose changed little in the *ldhA* mutant as compared to the parent strain. Table 6.22 shows that the extracellular formate, acetate, ethanol, pyruvate, and glutamate production rates increase by about 13.2, 17.7, 13.2, 55.6, and 156.0%, respectively, in the *ldhA* mutant as compared to the parent strain. However, extracellular production rates of citrate, malate, and succinate are reduced in the *ldhA* mutant as compared to the parent strain.

As shown in Table 6.23, enzyme activity levels vary significantly in the *ldhA* mutant, as compared to those in the parent strain. Although the glycolytic enzymes, such as Glk and Pgi, are down-regulated, Pfk, GAPDH, Pgk, Pyk, and PDHc are up-regulated significantly in the *ldhA* mutant as compared to the parent strain, although Fba is not. Although the conversion of PYR to AcCoA through Pfl is the major pathway under anaerobic conditions, the PDH enzyme is up-regulated (Spencer and Guest, 1985; Kaiser and Sawer, 1994).

The activity of G6PDH increases by 38.70%, whereas 6PGDH activity decreases by 28.75% in the *ldhA* mutant compared to the parent stain. The down-regulation of 6PGDH agrees with the slower growth rate of the *ldhA* mutant, since this enzyme is known to be growth rate dependent (Pease and Wolf, 1994).

Citrate synthase (CS) is up-regulated by 1.45-fold in the *ldhA* mutant compared to the parent strain (Table 6.23). This up-regulation causes an increase in the carbon flux from citrate to glutamate via α-KG, as is evidenced by the up-regulation of ICDH, higher glutamate production rate (Table 6.22), and high concentration of intracellular α-KG (Figure 6.30) in response to *ldhA* gene deletion. Moreover, the activities of MDH and Fum are also up-regulated in the *ldhA* mutant compared to those in the parent strain.

The anaplerotic enzyme Ppc, which is also known to contribute to catabolic succinate formation under anaerobic conditions, is down-regulated in the *ldhA* mutant compared to the parent strain (Table 6.24). However, Pck is up-regulated significantly in the mutant. This is mainly due to the shortage of PEP in the *ldhA* mutant, as evidenced by the measurement of intracellular PEP concentration (Figure 6.30). The activity of $NADP^+$-specific malic enzyme ($NADP^+$-Mez) remains unchanged, whereas the NAD^+-specific malic enzyme (NAD^+-Mez) is up-regulated significantly in the *ldhA* mutant compared to that in the

Published by Woodhead Publishing Limited, 2013

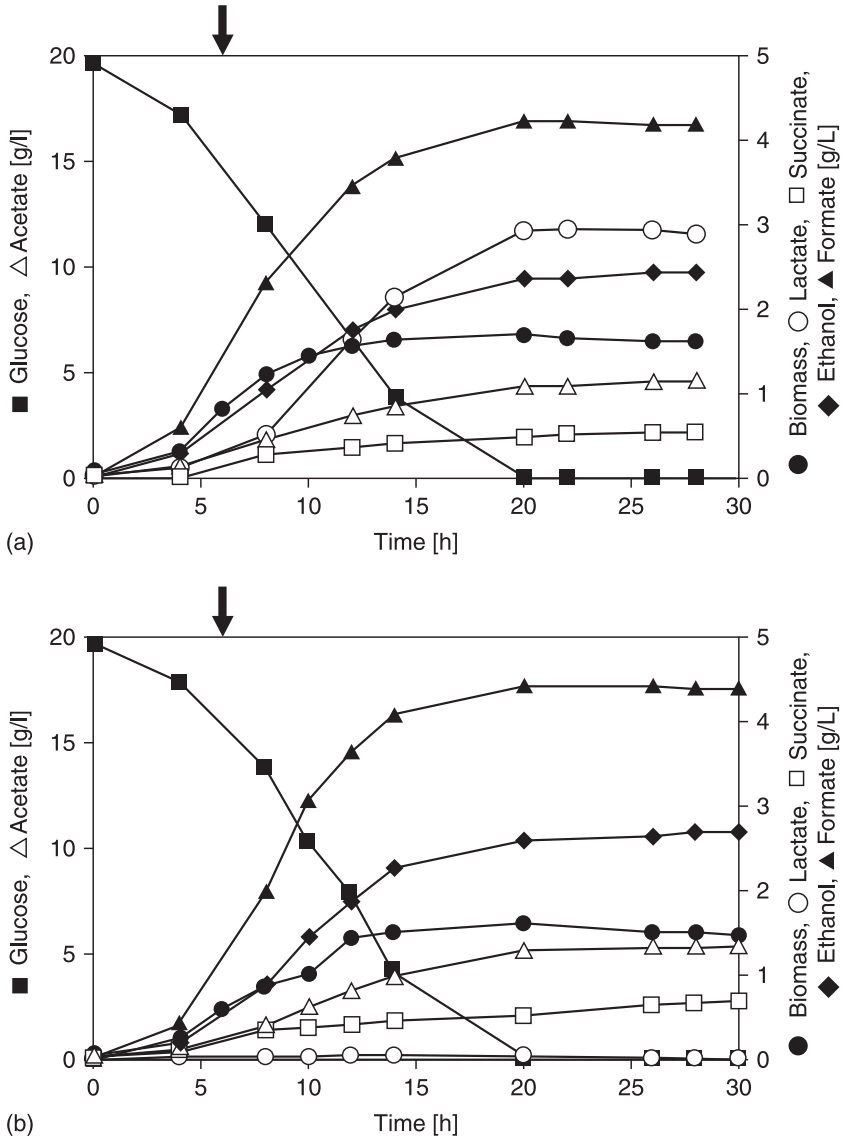

Figure 6.29 Batch cultivation results of: (a) parent *E. coli*; and (b) *ldhA* mutant *E. coli*; grown on glucose under anaerobic conditions. The arrow indicates the sampling time for RT-PCR analysis, measurement of enzyme activities, and intracellular metabolites

Table 6.22 Specific rates of parent and *ldhA* mutant *E. coli* grown on glucose under anaerobic conditions. Standard deviations were calculated from four independent measurements (duplicate measurements from duplicate experiments). μ – specific growth rate; q – specific uptake/production rate; $Y_{X/S}$ – biomass yield

Parameter	BW 25113 (Parent)	JW 1375 (*ldhA*$^-$)	Ratio (*ldhA*$^-$/Parent)
μ [h^{-1}]	0.16 ± 0.01	0.14 ± 0.01	0.87
$Y_{X/S}$ [$g.g^{-1}$]	0.12 ± 0.01	0.12 ± 0.01	1.00
q_{GLC} [$mmol.gDCW^{-1}.h^{-1}$]	7.49 ± 0.75	6.85 ± 0.68	0.92
q_{ACE} [$mmol.gDCW^{-1}.h^{-1}$]	4.70 ± 0.47	5.53 ± 0.55	1.18
q_{LAC} [$mmol.gDCW^{-1}.h^{-1}$]	1.84 ± 0.18	UD*	—
q_{FOR} [$mmol.gDCW^{-1}.h^{-1}$]	7.46 ± 0.74	8.45 ± 0.84	1.13
q_{ETH} [$mmol.gDCW^{-1}.h^{-1}$]	3.79 ± 0.38	4.29 ± 0.43	1.13
q_{PYR} [$mmol.gDCW^{-1}.h^{-1}$]	0.10 ± 0.01	0.16 ± 0.02	1.56
q_{SUC} [$mmol.gDCW^{-1}.h^{-1}$]	0.38 ± 0.04	0.31 ± 0.03	0.82
q_{CIT} [$\mu mol.gDCW^{-1}.h^{-1}$]	1.74 ± 0.20	1.48 ± 0.20	0.83
q_{GLU} [$\mu mol.gDCW^{-1}.h^{-1}$]	1.60 ± 0.20	4.08 ± 0.50	2.56
q_{MAL} [$\mu mol.gDCW^{-1}.h^{-1}$]	19.1 ± 2.01	16.1 ± 2.03	0.82
Carbon recovery [%]	88.37 ± 8.1	90.87 ± 14.3	

*UD: undetected

parent strain (Table 6.23), implying that the inactivation of the *ldhA* gene leads to the production of malate from pyruvate, while the parent strain produces MAL from PEP in two-step reactions catalyzed by Ppc and MDH. This result is consistent with the study of Stols and Donnelly (1997), where inactivation of the *ldhA* gene produces malic acid from pyruvate. Acetate kinase (Ack) activity is up-regulated in the *ldhA* mutant, compared to the parent strain. This result is consistent with the higher acetate production rates (Table 6.22). The activity of soluble transhydrogenase (THD) encoded by *udhA*, which catalyzes the conversion of NAD^+ and NADPH to NADH and $NADP^+$, is almost unchanged in the *ldhA* mutant compared to the parent strain (Table 6.23), implying that re-oxidation of reducing power is balanced in the mutant.

The relative expressions of *ptsG*, *pgi*, *fbaA*, *gapA*, *pgk*, *aceE*, and *aceF* involved in the glycolysis are significantly up-regulated in the

Published by Woodhead Publishing Limited, 2013

Table 6.23 **Specific enzyme activities in cell extracts of parent and *ldhA* mutant *E. coli* grown on glucose under anaerobic conditions. The unit of enzyme activity is nmol/min/mg protein. Overall ED pathway enzyme was represented as mg pyruvate/min/mg protein. The ratio of enzyme activity was calculated for *ldhA* mutant over the corresponding value in the parent strain. Therefore, a value of 1.0 indicates no change. ND indicates not detected**

Enzyme (abbreviated name)	Parent	Δ*ldhA*	Ratio
Glucokinase (Glk)	187 ± 13	138 ± 12	0.7
Phosphoglucose isomerase (Pgi)	684 ± 48	537 ± 35	0.8
Glucose-6-phosphate dehydrogenase (G6PDH)	61 ± 9	84 ± 12	1.4
6-phosphogluconate dehydrogenase (6PGDH)	105 ± 7	75 ± 5	0.7
ED pathway enzyme (6PGD & 2KDPGA)	1 ± 0.1	1 ± 0.1	1.0
Phosphofructose kinase (Pfk)	158 ± 11	191 ± 13	1.2
Fructose diphosphate aldolase (Fba)	175 ± 12	178 ± 12	1.0
GAP dehydrogenase (GAPDH)	301 ± 21	358 ± 25	1.2
3-phosphoglycerate kinase (Pgk)	74 ± 5	84 ± 6	1.1
Phosphoenol pyruvate carboxylase (Ppc)	97 ± 7	40 ± 3	0.4
Phosphoenol pyruvate carboxykinase (Pck)	34 ± 2	62 ± 5	1.8
Pyruvate kinase (Pyk)	265 ± 19	330 ± 12	1.3
Pyruvate dehydrogenase complex (PDH)	13 ± 1	23 ± 2	1.8
Acetate kinase (Ack)	522 ± 36	636 ± 44	1.2
Lactate dehydrogenase (LDH)	151 ± 11	ND	—
Citrate synthase (CS)	49 ± 10	71 ± 15	1.4
Isocitrate dehydrogenase (ICDH)	43 ± 9	72 ± 15	1.7
Isocitrate lyase (Icl)	1 ± 0.1	1 ± 0.1	1.0
Malate synthase (MS)	1 ± 0.1	1 ± 0.1	1.0
α-Ketoglutarate dehydrogenase (α-KGDH)	ND	ND	—
Malate dehydrogenase (MDH)	37 ± 5	59 ± 8	1.6
NADP+-specific malic enzyme ($NADP^+$-Mez)	1 ± 0.1	1 ± 0.1	1.0
NAD+-specific malic enzyme (NAD^+-Mez)	2 ± 0.1	16 ± 1	7.9
Fumarase (Fum)	15 ± 2	20 ± 2	1.4
Transhydrogenase (THD)	23 ± 2	23 ± 2	1.0

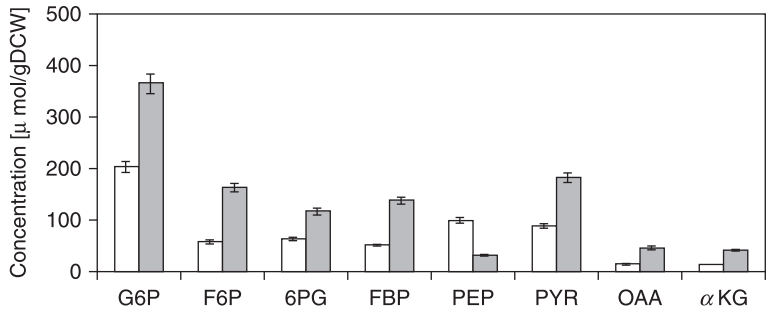

Figure 6.30 **Intracellular metabolite concentrations in the central metabolic pathways at the exponential growth phase for both *ldhA* mutant and parent *E. coli* (see Materials and Methods for details). □, parent; ■, mutant**

mutant compared to those in the parent strain (Figure 6.31a). The down-regulation of *pykA*, but not *pykF*, in the *ldhA* mutant, indicates that these two isozymes are differentially regulated. The *ppc* gene is down-regulated by almost 25%, whereas *pckA* is up-regulated by about 52% in the *ldhA* mutant compared to the parent strain, a result that is consistent with the measurement of enzyme activity (Table 6.23). Among the PP pathway genes, the relative expression level of *zwf* is slightly up-regulated, whereas all other genes, except *gnd*, are almost unchanged in the *ldhA* mutant compared to the parent strain (Figure 6.31b). Along the fermentative pathway, the expression levels of *ack*, *adhE*, and *pflA* are also up-regulated significantly in the *ldhA* mutant.

Of the TCA cycle, *gltA*, *acnB*, *icdA*, and *mdh* transcripts are up-regulated significantly in the *ldhA* mutant compared to those in the parent strain (Figure 6.31c). This up-regulation is consistent with the fact that most of the TCA cycle genes, such as *gltA* (Park et al., 1994), *mdh* (Park et al., 1995b), and *icdA* (Saier and Ramseier, 1996), are known to be regulated by several global regulators, such as Fnr, ArcA, and Cra (or FruR), whose encoded genes are also up-regulated in the *ldhA* mutant (Figure 6.31d). The expression levels of the genes involved in protein secretion and disulfide bond formation, such as *secA*, *lepB*, and *dsbA*, are up-regulated slightly in the *ldhA* gene knockout *E. coli* (Figure 6.31c). This result suggests that *ldhA* gene deletion may modulate the activity of protein secretion and disulfide bond formation. The transcript levels of *rpoE* and *rpoH* (encoding σ^E and σ^{32}, respectively) are increased by 1.2-fold,

Published by Woodhead Publishing Limited, 2013

whereas *rpoD* (encoding σ^{70}) is almost unregulated in the mutant (Figure 6.31d). The significant up-regulation of heat shock genes, such as *dnaJ, grpE, groS*, and *fkpA*, in the mutant correspond to the fact that the heat shock gene expression is largely proportional to the amount of σ^{32}, though the level of σ^{32} activity is known to be regulated at multiple stages, including translational efficiency and protein stability (Straus et al., 1987).

Intracellular metabolite concentrations of G6P, F6P, 6PG, FBP, PYR, OAA, and α-KG are increased in the *ldhA* mutant, as compared to those of the parent strain. In contrast, the intracellular concentration of PEP decreases in the *ldhA* mutant, implying that the intracellular PEP is limiting in the mutant. The reason is mainly due to the significant up-regulation of Pyk and PDH activities (Table 6.23) that channel more carbon flux toward the formate, acetate, and ethanol pathways, from the PYR and AcCoA pool, as evidenced by their increased specific rate (Table 6.22), as well as increased NAD^+-Mez activity to replenish C_4 intermediates in the TCA cycle, such as OAA.

Deletion of the LDH pathway blocks carbon flow from pyruvate and results in a higher rate of pyruvate excretion. Metabolic flux analysis shows that most of the carbon flux in *ldhA* mutant *E. coli* is forced through formate, acetate, and ethanol production pathways, resulting in a concomitant increase in these fluxes, though little increase in fluxes through the glycolytic pathway is observed (Figure 6.32). This result is consistent with the study of Yang et al. (1999), where they observed that an *E. coli* mutant strain deficient in *ackA, pta*, and *ldhA* major carbon flux was forced through ethanol and formate production pathways.

When PEP is converted to MAL via OAA by Ppc and MDH, the free energy is wasted. In contrast, one ATP is produced when PEP is directly converted to pyruvate by Pyk (Figure 6.32). Therefore, a large fraction of PEP is channeled through the Pyk pathway and this might be why the *ldhA* mutant induces the sfcA pathway to supply the C_4 intermediates in the TCA cycle for conserving the free energy of PEP, as evidenced by the significant up-regulation of the NAD^+-Mez enzyme (Table 6.23). However, the up-regulation of this pathway cannot increase the specific production rate of malic acid and succinic acid (Table 6.22). The reason is mainly due to lower PEP concentrations in the *ldhA* mutant strain (Figure 6.30). Since PEP is an essential intermediate to supply the precursor metabolites for biomass production as well as amino acid biosynthesis, the demand for intracellular PEP in the *ldhA* mutant is maintained through redirecting the flux from OAA.

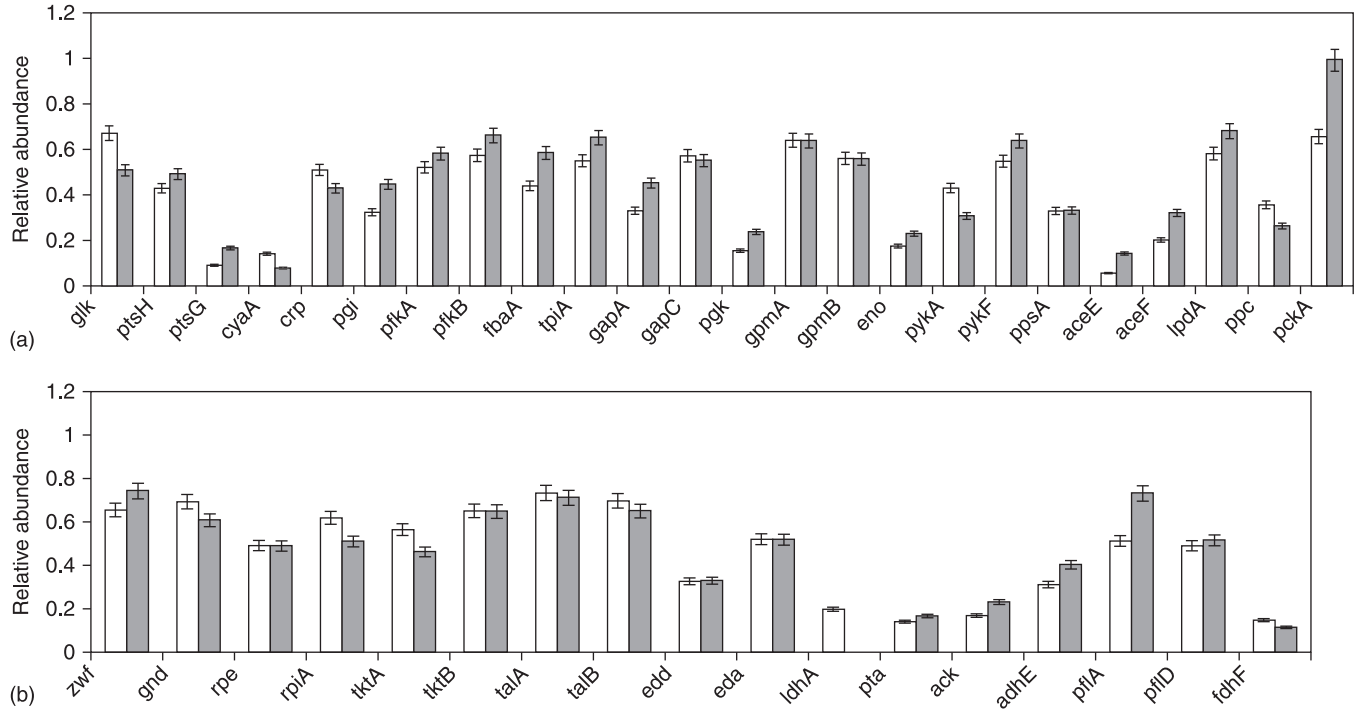

Figure 6.31 Comparison of gene expressions for parent (□) and *ldhA* mutant *E. coli* (■):(a) Transport and glycolytic pathway genes; (b) PP pathway and fermentative genes;

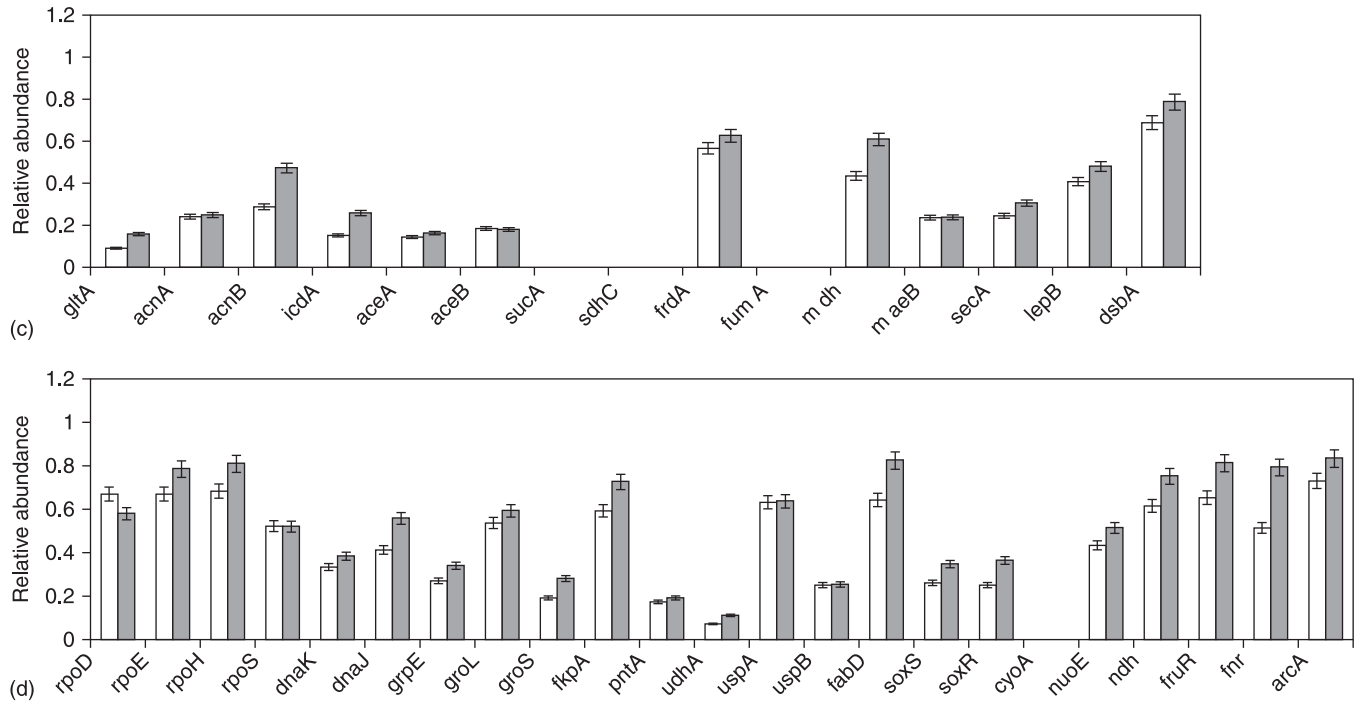

Figure 6.31 (C*ontinued*) (c) Genes involved in TCA cycle and protein synthesis; and (d) Genes involved in sigma factor, heat shock, NADPH re-oxidation, respiration, global, and other regulations (d). No RT-PCR amplifications were obtained for *sucA, sdhC, fumA*, and *cyoA*

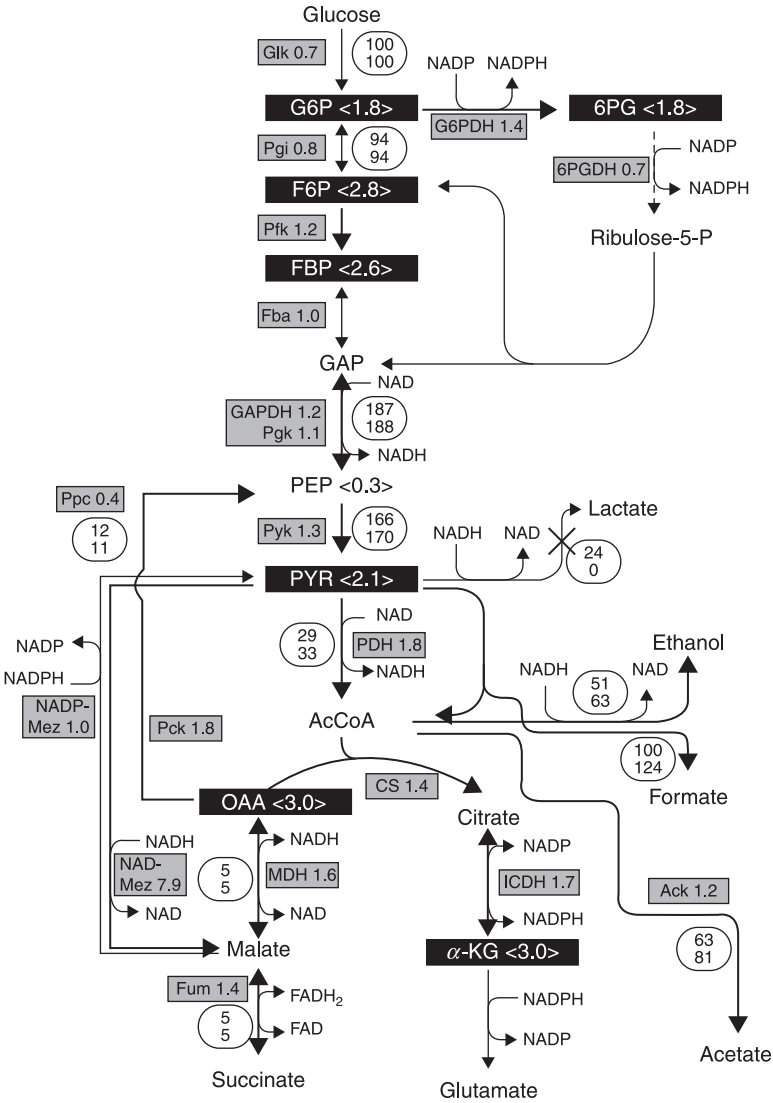

Figure 6.32 Anaerobic metabolism of glucose in *E. coli*. The value beside the intracellular metabolite and the enzyme in gray box is the relative value for *ldhA* mutant compared to the parent strain. The oval box represents the flux data; upper value, parent strain and lower value, *ldhA* mutant. The cross represents knockout of *ldhA* gene. Thick line, up-regulation; dotted line, down-regulation

Published by Woodhead Publishing Limited, 2013

The product of the global regulatory gene *cra* (*fruR*) is known to control the transcriptional expressions of numerous genes concerned with carbon and energy metabolism. The genes *ptsHI*, *pfkA*, *adhE*, and *pykF* are regulated negatively, whereas the genes *ppsA*, *pckA*, *icdA*, and *cydAB* are regulated positively by the product of *cra* (*fruR*) gene, as explained in Chapter 3. Gene expression analysis shows a slight up-regulation of *ptsH*, *pfkAB*, *pykF* (Figure 6.31a), and *adhE* (Figure 6.31b) genes in the *ldhA* mutant, compared to those in the parent strain. The reason is due to the higher concentration of FDP in the *ldhA* mutant (Figure 6.30), since the effect of the Cra protein on the transcription is counteracted by a high concentration of FDP, which promotes catabolite repression of Cra-activated operons and catabolite activation of Cra-repressed operons (Saier and Ramseier, 1996). However, although the higher concentrations of FDP are observed in the mutant, the genes *icdA* (Figure 6.31c) and *pckA* (Figure 6.31a) are found to be up-regulated, implying that *cra* (*fruR*) does not act alone to exert its multifarious effects but interacts with other pleiotropic regulators to create a network of transcriptional effects that serve to co-ordinate the effects of various bacterial sensing devices.

Although the activity of Pgi is down-regulated, the gene *pgi* is up-regulated by 1.4-fold in the *ldhA* mutant compared to the parent strain. This is mainly due to the higher concentrations of 6PG in the *ldhA* mutant, since 6PG is known to inhibit Pgi activity (Schreyer and Bock, 1980); an artifact that the activity of enzymes are regulated by reversible binding of effectors, covalent modification, and alteration of enzyme concentration, whereas transcript levels are influenced by both transcriptional activity and mRNA stability (Martin, 1987). Although a slight up-regulation of the *zwf* gene is observed, the enzyme activity of G6PDH increases significantly in the *ldhA* mutant. The reason is due to the demand for NADPH for glutamate synthesis, of which specific production rates are increased by 2.5-fold (150%) in the *ldhA* mutant compared to the parent strain (Table 6.22). A slight up-regulation of the *zwf* gene may be due to the effect of *soxS* and *soxR*, which was found to be up-regulated in the *ldhA* mutant (Figure 6.31d), since the *soxS* gene product has been found to act as a transcriptional activator of at least 10 genes, including *zwf* (Li and Demple, 1994). Based on the study of gene expressions, enzyme activities, and intracellular metabolite concentrations, together with metabolic flux analysis, the overall regulation mechanisms for *E. coli* grown on glucose minimal medium under anaerobic conditions in response to *ldhA* gene deletion are shown in Figure 6.32.

The soluble NADH-linked LDH is responsible for the formation of lactate from pyruvate (Tarmy and Kaplan, 1968a,b). This reaction consumes one NADH per three carbons, thus balancing out the NADH produced through GAPDH in glycolysis. Therefore, deletion of the *ldhA* gene may result in a reducing power imbalance in *E. coli*. However, the overall NADH balance calculated, based on the metabolic flux distribution, indicates that NADH production and consumption are almost the same in both the *ldhA* mutant and the parent strain (Figure 6.33). The reason is mainly due to the increased carbon flux through the ethanol pathway in the *ldhA* mutant from pyruvate node via AcCoA, since 4 moles of NADH are needed to metabolize 2 moles of AcCoA for the production of 2 moles of ethanol.

Table 6.24 indicates that enzyme activity is correlated approximately with gene expressions, whilst flux values do not necessarily correlate with enzyme activities. Basically, the flux is determined not only by the enzyme activity but also by the concentration of substrates, effectors, and inhibitors. The lower flux ratio through Pyk, as compared to the enzyme activity and mRNA transcript ratio, is mainly due to the decreased concentration of PEP, which is the substrate of pyruvate kinase reaction.

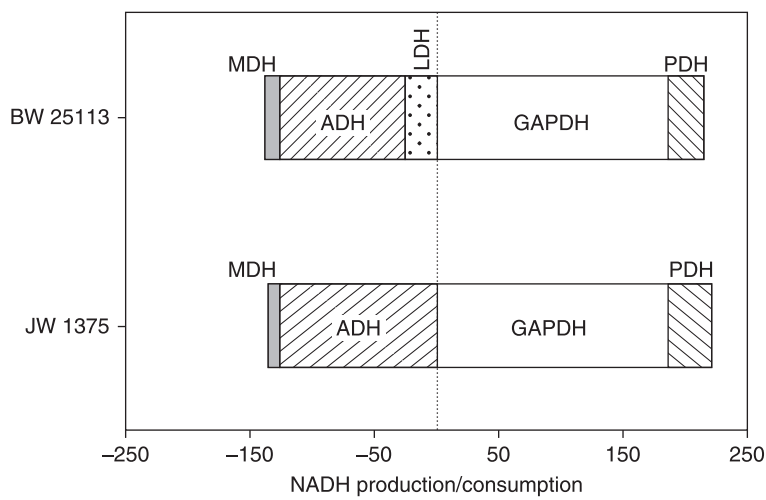

Figure 6.33 **NADH balances in both *ldhA* mutant and parent *E. coli* calculated based on the metabolic fluxes. +: NADH production; −: NADH consumption**

Published by Woodhead Publishing Limited, 2013

Table 6.24 **Comparison between the ratios of gene expressions, enzyme activities, and metabolic fluxes in *E. coli* grown on glucose under anaerobic conditions**

Gene	*IdhA mutant versus parent* E. coli		
	Flux Ratio	Enzyme Ratio	Transcript Ratio
glk	1.00	0.72	0.76
pgi	1.01	0.79	1.41
gapA	1.01	1.19	1.36
pykF	1.05	1.29 (pykAF)	1.16
aceEF & lpdA	1.16	1.84 (PDH)	1.86[(a)]
pfl	1.24	–	1.25[(b)]
ack	1.28	1.22	1.35
adhE	1.23	–	1.29
ppc	0.89	0.41	0.74
mdh	0.89	1.60	1.39

[(a)] average value of *aceE, aceF* and *lpdA* gene expressions which encode pyruvate dehydrogenase complex (PDH)
[(b)] average value of *pflA* and *pflD* gene expressions

6.10 References

Abdel-Hamid, A.M., Attwood, M.M., and Guest, J.R. (2001) 'Pyruvate oxidase contributes to the aerobic growth efficiency of *Escherichia coli*', *Microbiology*, 147: 1483–98.

Aristidou, A.A., San, K.Y., and Bennett, G..N. (1995) 'Metabolic engineering of *Escherichia coli* to enhance recombinant protein production through acetate reduction,' *Biotechnology Progress*, 11: 475–8.

Baba, T., Ara, T., Hasegawa, M., Takai, Y., Okumura, Y. et al. (2006) 'Construction of *Escherichia coli* K-12 in frame, single-gene knockout mutants: the Keio collection,' *Molecular Systtems Biology*, msb 4100050-E1.

Bennett, G.N., Schweingruber, M.E., Brown, K.D., Squires, C., and Yanofsky, C. (1976) 'Nucleotide sequence of region preceding *trp* mRNA initiation site and its role in promoter and operator function', *Proceedings of the National Academy of Sciences of USA*, 73: 2351–5.

Brian, J.K., Westerhoff, H.V., Snoep, J.L., Nilsson, D., and Jensen, P.R. (2002) 'The glycolytic flux in *Escherichia coli* is controlled by the demand for ATP', *Journal of Bacteriology*, 184: 3909–16.

Brice, C.B. and Kornberg, H.L. (1968) 'Genetic control of isocitrate lyase activity in *Escherichia coli*', *Journal of Bacteriology*, 96: 2185–6.

Brown, T.D.K., Jones-Mortimer, M.C., and Kornberg, H.L. (1977) 'The enzymic interconversion of acetate and acetyle-coenzyme A in *Escherichia coli*', *Journal of General Microbiology*, 102: 327–36.

Chambost, J.P. and Fraenkel, D.G. (1980) 'The use of 6-labeled glucose to assess futile cycling in *Escherichia coli*', *Journal of Biological Chemistry*, 255: 2867–9.

Chang, Y.Y., Wang, A.Y., and Cronan, J.E. Jr. (1994) 'Expression of *Escherichia coli* pyruvate oxidase (PoxB) depends on the sigma factor encoded by the *rpoS* (*katF*) gene', *Molecular Microbiology*, 11: 1019–28.

Chang, D., Jung, H., Rhee, J., and Pan, J. (1999) 'Homofermentative production of D-lactate or L-lactate in metabolically engineered *Escherichia coli* RR1', *Applied Environmental Microbiology*, 65: 1384–9.

Chao, Y.P. and Laio, J.C. (1994) 'Metabolic responses to substrate futile cycling in *Escherichia coli*', *Journal of Biological Chemistry*, 269: 5122–6.

Chassagnole, C., Noisommit-Rizzi, N., Schmid, J.W., Mauch, K., and Reuss, M. (2000) 'Dynamic modeling of the central carbon metabolism of *Escherichia coli*', *Biotechnology and Bioengineering*, 79: 53–73.

Choi, I.Y., Sup, K.I., Kim, H.J., and Park, J.W. (2003) 'Thermosensitive phenotype of *Escherichia coli* mutant lacking NADP(+)-dependent isocitrate dehydrogenase', *Redox Report*, 8: 51–6.

Clark, D.P. and Cronan, J.E. (1996) 'Two-carbon compounds and fatty acids as carbon sources', in: Escherichia coli *and* Salmonella typhimurium: *Cellular and Molecular Biology*, 2nd edition, edited by F.C. Neidhardt et al. Washington, DC: American Society of Microbiology Press. pp. 343–57.

Cronan, J.E. Jr. and LaPorte, D. (1999) 'Tricarboxylic acid cycle and glyoxalate bypass', in: Escherichia coli *and* Salmonella typhimurium: *Molecular Biology*, 2nd edition, edited by F.C. Neidhardt et al. Washington, DC: American Society of Microbiology Press. pp. 343–57.

Dalal, F. and Fraenkel, D.G. (1983) 'Assessment of a futile cycle involving reconversion of fructose-6-phosphate to fructose-1,6-biphosphate during gluconeogenic growth of *Escherichia coli*', *Journal of Bacteriology*, 153: 390–4.

David, J. and Wiesmeyer, H. (1970) 'Regulation of ribose metabolism in *E. coli* II: Evidence for two ribose-5-phosphate isomerase activities', *Biochimica et Biophysica Acta*, 208: 56–67.

Dessein, A., Schwartz, M., and Ullmann, A. (1978) 'Catabolite repression in *Escherichia coli* mutants lacking cyclic AMP', *Molecular and General Genetics*, 162: 83–7.

Dietrich, J. and Henning, U. (1970) 'Regulation of pyruvate dehydrogenase complex synthesis in *Escherichia coli* K12', *European Journal of Biochemistry*, 14: 258–69.

El-Mansi, E.M. and Holms, W.H. (1989) 'Control of carbon flux to acetate excretion during overflow in *Escherichia coli*', *Biotechnology and Bioengineering*, 35: 732–8.

Esseenberg, M.K. and Cooper, R.A. (1975) 'Two ribose-5-phosphate isomerase from *Escherichia coli* K-12: Partial characterization of the enzymes and consideration of their possible physiological roles,' *European Journal of Biochemistry*, 55: 323–32.

Published by Woodhead Publishing Limited, 2013

Farmer, W.R. and Liao, J.C. (1997) 'Reduction of aerobic production by *Escherichia coli*', *Applied Environmental Microbiology*, 63: 3205–10.
Fischer, E. and Sauer, U. (2003) 'A novel metabolic cycle catalyzes glucose oxidation and anaplerosis in hungry *Escherichia coli*,' *Journal of Biological Chemistry*, 278: 46446– 51.
Fish, R.N. and Kane, C.M. (2002) 'Promoting elongation with transcript cleavage stimulatory factors', *Biochimica et Biophysica Acta*, 1577: 287–307.
Fraenkel, D.G. (1968) 'Selection of mutants lacking glucose-6-phosphate dehydrogenase or gluconate-6-phosphate dehydrogenase', *Journal of Bacteriology*, 95: 1267–71
Fraenkel, D.G. (1999) 'Glycolysis', in: Escherichia coli *and* Salmonella: *Cellular and Molecular Biology*, edited by F.C. Neidhardt et al. Washington, DC: American Society of Microbiology Press, Mira Digital Publishing.
Garrigues, C., Loubiere, P., Nic, D., Lindley, N.D., and Cocaign-Bousquet, M. (1997) 'Control of the shift from homolactic acid to mixed-acid fermentation in *Lactococcus lactis*: Predominant role of the NADH/NAD^+ ratio', *Journal of Bacteriology*, 179: 5282–7.
Gokarn, R.R., Altman, E., and Eiteman, M.A. (1998) 'Metabolic analysis of *Escherichia coli* in the presence of and absence of pyruvate carboxylase', *Biotechnology Letters*, 20: 795–8.
Gokarn, R.R., Eiteman, M.A., and Altman, E. (2000) 'Metabolic analysis of *Escherichia coli* in the presence and absence of carboxylating enzymes phosphoenolpyruvate carboxylase and pyruvate carboxylase', *Applied Environmental Microbiology*, 66: 1844–50.
Gottschalk, G. (1985) *Bacterial Metabolism*, 2nd edition. New York: Springer Verlag.
Grabau, C. and Cronan, J.E. Jr. (1984) 'Molecular cloning of the gene (poxB) encoding the pyruvate oxidase of *Escherichia coli*, a lipid-activated enzyme', *Journal of Bacteriology*, 160: 1088–92.
Grove, C.L. and Gunsalus, R.P. (1987) 'Regulation of the *aroH* operon of *Escherichia coli* by the Tryptophan repressor', *Journal of Bacteriology*, 169: 2158–64.
Guest, J.R. and Russell, G.C. (1992) 'Complexes and complexities of the citric acid cycle in *Escherichia coli*', *Current Topics in Cellular Regulation*, 33: 231–47.
Gunsalus, R.P. and Yanofsky, C. (1980) 'Nucleotide sequence and expression of *Escherichia coli trpR*, the structural gene for the *trp* aporepressor', *Proceedings of the NationalAcademy of.Sciences of the USA*, 77: 7117–21.
Han, K., Lim, H.C., and Hong, J. (1992) 'Acetic acid formation in *Escherichia coli* fermentation', *Biotechnology and Bioengineering*, 39: 663–71.
Haugaard, N. (1959) 'D- and L-lactic acid oxidases of *Escherichia coli*', *Biochimica et Biophysica Acta*, 31: 66–77.
Heatwole, V.M. and Somerville, R.L. (1991) 'The tryptophan-specific permease gene, *mtr*, is differentially regulated by the tryptophan and tyrosine repressors in *E. coli* K12', *Journal of Bacteriology*, 174: 3601–4.
Heatwole, V.M. and Somerville, R.L. (1992) 'Synergism between the *trp* repressor and *tyr* repressor in repression of the *aroL* promoter of *Escherichia coli* K12', *Journal of Bacteriology*, 174: 331–5.

Holger, J., Bernhard, K., Peter, K., and Karl-Dieter, E. (1996) 'Mutants that show increased sensitivity to hydrogen peroxide reveal an important role for the pentose phosphate pathway in protection of yeast against oxidative stress', *Molecular and General Genetics*, 252: 456–64.

Hong, S.H. and Lee, S.Y. (2001) 'Metabolic flux analysis for succinic acid production by recombinant *Escherichia coli* with amplified malic enzyme activity', *Biotechnology and Bioengineering*, 74: 89–95.

Hoyt, J.C. and Reeves, H.C. (1988) '*In vivo* phosphorylation of isocitrate lyase from *Escherichia coli* D5H3G7', *Biochemical and Biophysical Research Communications*, 153: 875–80.

Hua, Q. Yang, C., Baba, T., Mori, H., and Shimizu, K. (2003) 'Responses of the central carbon metabolism in *Escherichia coli* to phosphoglucose isomerase and glucose-6-phosphate dehydrogenase knockouts', *Journal of Bacteriology*, 185: 7053–67.

Ishii, N., Nakahigashi, K., Baba, T., Robert, M., Soga, T. et al. (2007) 'Multiple high throughput analyses monitor the response of *E. coli* to perturbations', *Science*, 316: 593–7.

Iuchi, S. and Lin, E.C.C. (1992) 'Purification and phosphorylation of the Arc regulatory components of *Escherichia coli*', *Journal of Bacteriology*, 174: 5617–23.

Jeong, W. Cha, M.K., and Kim, I.H. (2000) 'Thioredoxin-dependent hydroperoxide peroxidase activity of bacterioferritin co-migratory protein (BCP) as a new member of the thiol-specific antioxidant protein (TSA)/alkyl hydroperoxide peroxidase C (*ahpC*) family', *Journal of Biological Chemistry*, 275: 2924–30.

Jiang, G.R., Nikolova, S., and Clark, D.P. (2001) 'Regulation of *ldhA* gene, encoding the fermentative lactate dehydrogenase of *Escherichia coli*', *Microbiology*, 147: 2437–46.

Kabir, M. and Shimizu, K. (2004) 'Metabolic regulation analysis of *icd*-gene knockout *Escherichia coli* based on 2D electrophoresis with MALDI-TOF mass spectrometry and enzyme activity measurements', *Appl. Microbiol. Biotechnol.*, 65: 89–96.

Kabir, M., Ho, P.Y., and Shimizu, K. (2005) 'Effect of *ldh*A gene deletion on the metabolism of *E. coli* based on gene expression, enzyme activities, intracellular metabolite concentrations, and metabolic flux distribution', *Biochemistry Engineering Journal*, 26: 1–11.

Kaiser, M. and Sawer, G. (1994) 'Pyruvate formate-lyase is not essential for nitrate respiration by *Escherichia coli*', *FEMS Microbiology Letters*, 117: 163–8.

Kedar, P., Colah, R., and Shimizu, K. (2007) 'Proteomic investigation on the *pyk-F* gene knockout *Escherichia coli* for aromatic amino acid production', *Enzyme and Microbial Technology*, 41: 455–65.

Kelley, R.L. and Yanofsky, C. (1982) 'Trp aporepressor production is controlled by autogenous regulation and inefficient translations', *Proceedings of the National Academy of Sciences of USA*, 79: 3120–4.

Kleman, G.L. and Strohl, W.R. (1994) 'Acetate metabolism by *Escherichia coli* in high-cell-density fermentation', *Applied Environmental Microbiology*, 60: 3952–8.

Published by Woodhead Publishing Limited, 2013

Kline, E.S. and Mahler, E.R. (1965) 'The lactic acid dehydrogenases of *Escherichia coli*', *Annual New York Academic Science*, 119: 905–17.

Koebmann, B.J., Westerhoff, H.V., Snoep, J.L., Nilsson, D., and Jensen, P.R. (2002) 'The glycolytic flux in *Escherichia coli* is controlled by the demand for ATP', *Journal of Bacteriology*, 184: 3909–16.

Krebs, A. and Bridger, W.A. (1980) 'The kinetic properties of phosphoenolpyruvate carboxykinase of *Escherichia coli*', *Canadian Journal of Biochemistry*, 58: 309–18.

Kumari, S., Tishel, R., Eisenbach, M., and Wolfe, A.J. (1995) 'Cloning, characterization, and functional expression of *acs*, the gene which encodes acetyl coenzyme A synthetase in *Escherichia coli*', *Journal of Bacteriology*, 177: 2878–86.

Kumari, S., Beatty, C.M., Browning, D.F., Busby, S.J.W., Simel, E.J. et al. (2000) 'Regulation of acetyl coenzyme A synthetase in *Escherichia coli*', *Journal of Bacteriology*, 182: 4173–9.

LaPorte, D.C. and Koshland, D.E. Jr. (1983) 'Phosphorylation of isocitrate dehydrogenase as a demonstration of enhanced sensitivity in covalent regulation', *Nature*, 305: 286–90

LaPorte, D.C., Thorsness, P.E., and Koshland, D.E. Jr. (1985) 'Compensatory phosphorylation of isocitrate dehydrogenase. A mechanism for adaptation to the intracellular environment', *Journal of Biological Chemistry*, 260: 10563–8.

Lawley, B. and Pittard, A.J. (1994) 'Regulation of *aroL* expression by TyrR protein and Trp repressor in *E. coli* K12', *Journal of Bacteriology*, 176: 6921–30.

Lemaster, D.M. and Cronan, J.E. Jr. (1982) 'Biosynthetic production of ^{13}C-labeled amino acids with site-specific enrichment', *Journal of Biological Chemistry*, 257: 1224–30.

Li, M., Yao, S., and Shimizu, K. (2006a) 'Effect of *lpdA* gene knockout on the metabolism in *Escherichia coli* based on enzyme activities, intracellular metabolite concentrations and metabolic flux analysis by ^{13}C-labeling experiments', *Journal of Biotechnology*, 122: 254–66.

Li, M., Ho, P.Y., Yao, S., and Shimizu, K. (2006b) 'Effect of *sucA* or *sucC* gene knockout on the metabolism in *Escherichia coli* based on gene expressions, enzyme activities, intracellular metabolite concentrations and metabolic fluxes by ^{13}C-labeling experiments', *Biochemical Engineering Journal*, 30: 286–96.

Li, Z. and Demple, B. (1994) '*SoxS* an activator of superoxide stress genes in *Escherichia coli*: purification and interaction with DNA', *Journal of Biological Chemistry*, 269: 18371–7.

Maaheimo, H., Fiaux, J., Cakar, Z.P., Bailey, J.E., Sauer, U., and Szyperski, T. (2001) 'Central carbon metabolism of *Saccharomyces cerevisiae* explored by biosynthetic fractional of common amino acids', *European Journal of Biochemistry*, 268: 2464–79.

Maloy, S.R. and Nunn, W.D. (1981) 'Role of gene fadR in *Escherichia coli* acetate metabolism', *Journal of Bacteriology*, 148: 83–90.

Martin, B.R. (1987) 'The regulation of enzyme activity', in: *Metabolic Regulation: A Molecular Approach*, edited by B.R. Martin. Oxford: John Wiley & Co. pp 12–27.

Mat-Jan, F., Alam, K.Y., and Clark, D.P. (1989) 'Mutants of *Escherichia coli* deficient in the fermentative lactate dehydrogenase', *Journal of Bacteriology*, 171: 342–8.

Mat-Jan, F., Williams, C.R., and Clark, D.P. (1989) 'Anaerobic growth defects resulting from gene fusions affecting succinyl-CoA synthetase in *Escherichia coli* K12', *Molecular and General Genetics*, 215: 276–80.

Matsushita, K., Arents, J.C., Bader, R., Yamada, M., Adachi, O., and Postma, P.W. (1997) '*Escherichia coli* is unable to produce pyrroloquinoline quinine (PQQ)', *Microbiology*, 143: 3149–56.

McCammon, M.T., Epstein, C.B., Przybyla-Zawislak, B., McAlister-Henn, L., and Butow, R.A., (2003) 'Global transcription analysis of Krebs tricarboxylic acid cycle mutants reveals an alternating pattern of gene expression and effects on hypoxic and oxidative genes', *Molecular Biology of the Cell*, 14: 958–72.

Miles, J.S. and Guest, J.R. (1989) 'Molecular genetic aspects if the citric acid cycle of *Escherichia coli*', *Biochemical Society Symposium*, 54: 45–65.

Morita, T., Waleed, E., Yuya, T., Toshifumi, I., and Hiroji, A. (2003) 'Accumulation of glucose 6-phosphate or fructose 6-phosphate is responsible for destabilization of glucose transporter mRNA in *Escherichia coli*', *Journal of Biological Chemistry*, 278: 15246–608.

Murai, T.M., Tokushige, M., Nagai, J., and Katsuki, H. (1971) 'Physiological functions of NAD+- and NADP+-linked malic enzymes in *E. coli*', *Biochemical and Biophysical Research Communications*, 43: 875–81.

Nakano, M.M., Zuber, P., and Sonenshein, A. (1998) 'Anaerobic regulation of *Bacillus subtilis* krebs cycle genes', *Journal of Bacteriology*, 180: 3304–11.

Neidhardt, F.C. (1996) Escherichia coli *and* Salmonella: *Cellular and Molecular Biology*, 2nd edition. Washington, DC: American Society of Microbiology Press. pp. 189–98.

Nielsen, J. (1984) 'Structure and expression of the ATP synthase operon of *Escherichia coli*', Ph.D. thesis, Technical University of Denmark, Lyngby, Denmark.

Nimmo, G.A. and Nimmo, H.G. (1984) 'The regulatory properties of isocitrate dehydrogenase kinase and isocitrate dehydrogenase phosphatase from *Escherichia coli* ML308 and the roles of these activites in the control of isocitrate dehydrogenase', *European Journal of Biochemistry*, 141: 409–14.

Nimmo, H.G., Borthwick, A.C., el-Mansi, E.M., Holms, W.H., MacKintosh, C., and Nimmo, G.A. (1987) 'Regulation of the enzymes at the branchpoint between the citric acid cycle and the glyoxylate bypass in *Escherichia coli*', *Biochemical Society Symposium*, 54: 93–101.

Notley, L. and Ferenci, T. (1996) 'Induction of RpoS-dependent functions in glucose-limited continuous culture: What level of nutrient limitation induces the stationary phase of *Escherichia coli*', *Journal of Bacteriology*, 178: 1465–8.

Oh, M.K., Rohlon, L., Kao, K., and Liao, J.C. (2002) 'Global expression profiling of acetate-grown *E. coli*', *Journal of Biological Chemistry*, 277: 13175–83.

Park, S.J., McCabe, J., Turna, J., and Gunsalus, R.P. (1994) 'Regulation of citrate synthase (*gltA*) gene of *Escherichia coli* in response to anaerobiosis and carbon supply: Role of the *arcA* gene product', *Journal of Bacteriology*, 176: 5086–92.

Published by Woodhead Publishing Limited, 2013

Park, S.J. and Gunsalus, R.P. (1995) 'Oxygen, iron, carbon, and superoxide control of the fumarase fumA and fumC genes of *Escherichia coli*: Role of the arcA, fnr, and soxR gene products', *Journal of Bacteriology*, 177: 6255–62.

Park, S.J., Cotter, P.A., and Gunsalus, R.P. (1995b) 'Regulation of malate dehydrogenase (mdh) gene expression in *Escherichia coli* in response to oxygen, carbon, and heme availability', *Journal of Bacteriology*, 177: 6652–6.

Park, S.J., Chao, G., and Gunsalus, R.P. (1997) 'Aerobic regulation of the sucABCD genes of *Escherichia coli*, which encode α-ketoglutarate dehydrogenase and succinyl coenzyme A synthetase: Roles of arcA, fnr, and the upstream sdhCDAB promoter', *Journal of Bacteriology*, 179: 4138–42.

Pascal, M.C., Chippaux, M., Abou-Jaoudé, A., Blaschkowski, H.P., and Knappe, J. (1981) 'Mutants of *Escherichia coli* K12 with defects in anaerobic pyruvate metabolism', *Journal of General Microbiology*, 124: 35–42.

Pease, A.J. and Wolf, J.R.E. (1994) 'Determination of the growth rate-regulated steps in expression of the *Escherichia coli* K-12 *gnd* gene', *Journal of Bacteriology*, 176: 115–22.

Pedersen, S., Block, P.L., Reeh, S., and Neihardt, F.C. (1978) 'Patterns of protein synthesis in *E. coli*: A catalog of the amount of 140 individual proteins in different growth rates', *Cell*, 14: 179–86.

Peng, L., Arauzo, M., and Shimizu, K. (2004) 'Metabolic flux analysis for a *ppc* mutant *Escherichia coli* based on 13C-labeling experiments together with enzyme activity assays and intracellular metabolite measurements', *FEMS Microbiology Letters*, 235: 17–23.

Perrenoud, A. and Sauer, U. (2005) 'Impact of global transcriptional regulation by arcA, arcB, Cra, Crp, Cya, Fnr, and Mlc on glucose catabolism in *Escherichia coli*', *Journal of Bacteriology*, 187: 3171–9.

Ponce, E., Martinez, A., Bolivar, F., and Valle, F. (1998) 'Stimulation of glucose catabolism through the pentose pathway by the absence of the two pyruvate kinase isoenzymes in *Escherichia coli*', *Biotechnology and Bioengineering*, 58: 292–5.

Ramseier, T.M., Chie, S.Y., and Saier, M.H. Jr. (1996) 'Co-operative interaction between Cra and Fnr in the regulation of the *cydAB* operon of *Escherichia coli*', *Current Microbiology*, 33: 270–4.

Riondet, C., Cachon, R., Waché, Y., Alcaraz, G., and Diviès, C. (2000) 'Extracellular oxido-reduction potential modifies carbon and electron flow in *Escherichia coli*', *Journal of Bacteriology*, 182: 620–6.

Rose, J.K., Squires, C.L., Yanofsky, C., Yang, H., and Zubay, G. (1973) 'Regulation of *in vitro* transcription of the tryptophan operon by purified RNA polymerase in the presence of partially purified repressor and tryptophan', *Nature New Biology Archive*, 245: 133–7.

Saier, M.H. Jr., and Ramseier, T.M. (1996) 'The catabolite repressor/activator (Cra) protein of enteric bacteria', *Journal of Bacteriology*, 178: 3411–7.

Sarsero, J.P., Wookey, P.J., and Pittard, A.J. (1991) 'Regulation of the expression of *Escherichia coli* K12 *mtr* gene by TyrR protein and *trp* repressor', *Journal of Bacteriology*, 173: 4133–43.

Schreyer, R. and Bock, A. (1980) 'Phosphoglucose isomerase from *Escherichia coli* K10: Purification, properties and formation under aerobic and anaerobic conditions', *Archives of Microbiology*, 127: 289–98.

Seta, F.D., Boschi-Muller, S., Vignais, M.L., and Branlant, G. (1997) 'Characterization of *Escherichia coli* strains with *gapA* and *gapB* genes deleted', *Journal of Bacteriology*, 179: 5218–21.

Shimizu, K. (2004) 'Metabolic flux analysis based on ^{13}C labeling experiments and integration of the information with gene and protein expression patterns', *Advances in Biochemical Engineering/Biotechnology*, 91: 1–49.

Siddiquee, K.A.Z., Arauzo-Bravo, M., and Shimizu, K. (2004a) 'Metabolic flux analysis of *pykF* gene knockout *Escherichia coli* based on 13C-labeled experiment together with measurements of enzyme activities and intracellular metabolite concentrations', *Applied Microbiology and Biotechnology*, 63: 407–17.

Siddiquee, K.A.Z., Arauzo-Bravo, M., and Shimizu, K. (2004b) 'Effect of pyruvate kinase (*pykF* gene) knockout mutation on the control of gene expression and metabolic fluxes in *Escherichia coli*', *FEMS Microbiology Letters*, 235: 25–33.

Skinner, A.J. and Cooper, R.A. (1971) 'The regulation of ribose-5-phosphate isomerization in *Escherichia coli* K12', *FEBS Letters*, 12: 293–6.

Smith, M.W. and Neidhardt, F.C. (1983) 'Proteins induced by anaerobiosis in *Escherichia coli*', *Journal of Bacteriology*, 154: 336–43.

Somerville, R. (1992) 'The *trp* repressor, a ligand activated regulatory protein', *Progress in Nucleic Acids Research & Molecular Biology*, 42: 1–38.

Spencer, M.E. and Guest, J.R. (1985) 'Transcription analysis of the *sucAB*, *aceEF*, and *lpd* genes of *Escherichia coli*', *Molecular and General Genetics*, 200: 145–54.

Stokes, J.L. (1949) 'Fermentation of glucose by suspensions of *Escherichia coli*', *Journal of Bacteriology*, 57: 147–58.

Stols, L. and Donnelly, M.I. (1997) 'Production of succinic acid through over-expression of NAD^+-dependent malic enzyme in an *Escherichia coli* mutant', *Applied Environmental Microbiology*, 63: 2695–701.

Straus, D.B., Walter, W.A., and Gross, C.A. (1987) 'The heat shock response of *Escherichia coli* is regulated by changes in the concentration of σ^{32}', *Nature*, 329: 348–51.

Sugimoto, S. and Shiio, I. (1987) 'Regulation of 6-phosphogluconate dehydrogenase in *Brevibacterium flavum*', *Agriculture and Biological Chemistry*, 51: 1257–63.

Tarmy, E.M. and Kaplan, N.O. (1968a) 'Kinetics of *Escherichia coli* B D-lactate dehydrogenase and evidence for pyruvate-controlled change in conformation', *Journal of Biological Chemistry*, 243: 2587–96.

Tarmy, E.M. and Kaplan, N.O. (1968b) 'Chemical characterization of D-lactate dehydrogenase from *Escherichia coli* B', *Journal of Biological Chemistry*, 243: 2579–86.

Toya, Y., Ishii, N., Nakahigashi, K., Hirasawa, T., Soga, T. et al. (2010) '^{13}C-Metabolic flux analysis for batch culture of *Escherichia coli* and its *pyk* and *pgi* gene knockout mutants based on mass isotopomer distribution of intracellular metabolites', *Biotechnology Progress*, 26: 975–92.

Published by Woodhead Publishing Limited, 2013

Van de Walle, M. and Shiloach, J. (1998) 'Proposed mechanism of acetate accumulation in two recombinant *Escherichia coli* strains during high density fermentation', *Biotechnology and Bioengineering*, 57: 71–8.

Vemuri, G.N., Eiteman, M.A., and Altman, E. (2002) 'Effects of growth mode and pyruvate carboxylase on succinic acid production by metabolically engineered strains of *Escherichia coli*', *Applied Environmental Microbiology*, 68: 1715–27.

Wolf, J.R.E., Prather, D.M., and Shea, F.M. (1979) 'Growth-rate dependent alteration of 6-phosphogluconate dehydrogenase and glucose-6-phosphate dehydrogenase levels in *Escherichia coli* K-12', *Journal of Bacteriology*, 139: 1093–6.

Wolodko, W.T. and Bridger, W.A. (1987) 'Studies of the process of renaturation and assembly of *Escherichia coli* succinyl-CoA synthetase from its α and βa subunits', *Biochemistry and Cell Biology*, 65: 452–7.

Yang, C., Hua, Q., Baba, T., Mori, H., and Shimizu, K. (2003) 'Analysis of *E. coli* anaplerotic metabolism and its regulation mechanism from the metabolic responses to altered dilution rates and phosphoenolpyruvate carboxykinase knockout', *Biotechnology and Bioengineering*, 84: 129–44.

Yang, Y.T., San, K.Y., and Bennett, G.N. (1999) 'Redistribution of metabolic fluxes in *Escherichia coli* with fermentative lactate dehydrogenase over-expression and deletion', *Metabolic Engineering*, 1: 141–52.

Zhao, J., Baba, T., Mori, H., and Shimizu, K. (2004a) 'Effect of *zwf* gene knockout on the metabolism of *Escherichia coli* grown on glucose or acetate', *Metabolic Engineering*, 6: 164–74.

Zhao, J., Baba, T., Mori, H., and Shimizu, K. (2004b) 'Analysis of metabolic and physiological responses to *gnd* knockout in *E. coli* by using C-13 tracer experiment and enzyme activity measurement', *FEMS Microbiology Letters*, 220: 295–301.

Zhou, S., Causey, T.B., Hasona, A., Shanmugam, K.T., and Ingram, L.O. (2003) 'Production of optically pure D-lactic acid in mineral salts medium by metabolically engineered *Escherichia coli* W3110', *Applied Environmental Microbiology*, 69: 399–407.

Zhu, J. and Shimizu, K. (2004) 'The effect of *pfl* genes knockout on the metabolism for optically pure d-lactate production by *Escherichia coli*', *Applied Microbiology and Biotechnology*, 64: 367–75.

Zhu, J. and Shimizu, K. (2005) 'Effect of a single-gene knockout on the metabolic regulation in *E. coli* for d-lactate production under microaerobic conditions', *Metabolic Engineering*, 7: 104–15.

Zhu, T., Phalakornkule, C., Koepsel, R.R., Domach, M.M., and Ataai, M.M. (2001) 'Cell growth and by-product formation in pyruvate kinase mutant of *E. coli*', *Biotechnology Progress*, 17: 624–8.

Zurawski, G., Gunsalus, R.P., Brown, K.D., and Yanofsky, C. (1981) 'Structure and regulation of *aroH*, the structural gene for the tryptophan-repressible 3-deoxy-D-arabino-heptulosonic acid-7-phosphate synthetase of *Escherichia coli*', *Journal of Molecular Biology*, 145: 47–73.